Aalto University
School of Engineering

Kristian Martin

Demand response of heating and ventilation within educational office buildings

Master's Thesis
Aalto University
School of Engineering
Department of Energy Technology

Thesis submitted as a partial fulfillment of the requirements
for the degree of Master in Science in Technology

Espoo, 23.11.2017
Supervisor: Professor Risto Kosonen
Advisor: D.Sc. Juha Jokisalo

Aalto University
School of Engineering

Aalto University, P.O. BOX 11000, 00076 AALTO
www.aalto.fi

Abstract of master's thesis

Author Kristian Martin

Title of thesis Demand response of heating and ventilation within educational office buildings

Degree programme Energy and HVAC Technology

Major HVAC Technology **Code** K3008

Thesis supervisor Professor Risto Kosonen

Thesis advisor D.Sc. Juha Jokisalo

Date 17.11.2017 **Number of pages** 124 **Language** English

Demand response on the building level aids stabilization of the consumption profile in the district heating and electricity grid. A stable consumption reduces peak demand and need for high cost peak power plants like heat-only boilers and gas turbines. The main benefit achieved is less CO_2 emissions at the same time the producer and consumer benefit economically through cheaper production costs.

The main objective with this study was to simulate a detailed model of an educational office building floor to determine the monetary saving potential of demand response combined with dynamic hourly district heating and electricity prices. In addition, the difference in potential between centralized and decentralized control approaches was to be examined. The impact on indoor environmental comfort and heating flexibility of the building were areas of interest. The heating flexibility is a measure of the buildings ability to adapt the heating according to the dynamic price signals sent by the energy producer. Both CAV and VAV ventilation designs were included in the study. In addition, the monetary savings potential of contract-power limitation within district heating and its impact on thermal comfort were studied.

The impact of demand response was studied by control of space heating, adjustment of supply air temperature and airflow regulation. The research was conducted by dynamic energy simulations of an educational office building on the Aalto University campus area. The simulation software used was IDA Indoor Climate and Energy (version 4.7.1). Acceptable ranges of indoor environmental comfort parameters (temperature, PMV, CO_2) were chosen and rule based control algorithms were developed and implemented into the simulation program.

A centralized control approach of space heating did not show any significant potential in heat cost savings (1.5%) and the heating flexibility remained low (2.9%). The decentralized approach reached heat cost savings of 5% – 6% and heating flexibility of up to 15% when controlling both space heating and supply air temperature in CAV ventilation cases. All demand response control alternatives managed to maintain a good thermal comfort for over 90% of the occupied time. Occupancy did not affect neither cost savings, heating flexibility nor thermal comfort in any of the different simulation set-ups.
The contract power of the building could be cut by 35% without affecting the thermal comfort at all. This brought an annual cost saving of 6.1 €/m^2 – 26.9 €/m^2 (27.1% – 35%) depending on district heat provider. A peak demand cut by 43% had only minor impact on the thermal comfort and provided even greater annual cost savings. The main conclusions from the study are that demand response within heating is only beneficial with a decentralized control and that peak demand limiting within district heating have a big cost saving potential.

Keywords Demand response, district heating, ventilation, peak demand limiting, energy simulation, rule based control algorithm

Aalto-universitetet
Högskolan för
ingenjörsvetenskaper

Aalto-universitetet, PB 11000, 00076 AALTO
www.aalto.fi

Sammandrag av diplomarbetet

Författare Kristian Martin

Titel Efterfrågeflexibilitet inom uppvärmning och ventilation i pedagogiska kontorsbyggnader

Utbildningsprogram Energi och VVS-teknik

Huvud-/biämne VVS-teknik **Kod** K3008

Övervakare Professor Risto Kosonen

Handledare TkD Juha Jokisalo

Datum 17.11.2017 **Sidantal** 124 **Språk** Engelska

Efterfrågeflexibilitet inom fastigheter bistår till att stabilisera konsumtionsprofilen i fjärrvärme- och elektricitetsnätet. En stabil konsumtion förminskar efterfrågan av spetskraft och behovet av högkostnadskraftverk som oljebrännare och gasturbiner. Fördelen är ett minskat koldioxidutsläpp samtidigt som producent och konsument gagnas ekonomiskt av billigare produktionskostnader.

Ett av de primära målen med denna studie var att simulera en detaljerad modellvåning i en pedagogisk kontorsbyggnad för att fastställa den monetära besparingspotentialen hos efterfrågeflexibilitet kombinerad med dynamisk timbaserad prissättning av fjärrvärme och elektricitet. Därtill jämfördes potentialen mellan en centraliserad och decentraliserad reglerstrategi. Efterfrågeflexibilitetens inverkan på inomhusklimatet samt byggnadens uppvärmningsflexibilitet utgjorde områden av intresse. Uppvärmningsflexibiliteten är ett mått på byggnadens förmåga att anpassa uppvärmningen enligt de dynamiska prissignalerna som energiproducenten anger. Både konstant samt behovsstyrd ventilation inkluderades i studien. Därtill undersöktes besparingspotentialen vid begränsning av fjärrvärmeanslutningens toppeffekt.

Efterfrågeflexibilitetens inverkan studerades genom styrning av rumsuppvärmning, tilluftstemperatur samt reglering av luftflöden. Studien genomfördes med dynamiska energisimuleringar av en pedagogisk kontorsbyggnad belägen på Aalto Universitetets campus område. Simuleringsprogrammet som användes var IDA Indoor Climate and Energy (version 4.7.1). Acceptabla intervall för inomhusklimatets komfortparametrar (temperatur, PMV, CO_2) definierades och regelbaserade kontrollalgoritmer utvecklades samt implementerades i simuleringsprogrammet.

En centraliserad reglerstrategi inom uppvärmning gav inga signifikanta besparingar (1.5%) och uppvärmningsflexibiliteten förblev låg (2.9%). Den decentraliserade strategin gav kostnadsbesparingar uppemot 5% – 6% och en uppvärmningsflexibilitet på 15% vid styrning av både uppvärmning samt tilluftstemperatur. Alla regleralternativen rörande efterfrågeflexibilitet lyckades upprätthålla en god termisk komfort över 90% av den ockuperade tiden. Användningsgraden hade ingen inverkan på vare sig kostnadsbesparing, flexibilitet eller termisk komfort i något av fallen. Fjärrvärmeanslutningens toppeffekt kunde skäras ned med 35% utan att det inverkade på den termiska komforten. Detta gav en årlig kostnadsbesparing på 6.1 €/m^2 – 26.9 €/m^2 (27.1% – 35%) beroende på fjärrvärmeproducent. En nedskärning av toppeffekten med 43% hade endast smärre inverkan på den termiska komforten och tillförde ytterligare kostnadsbesparing. De primära slutsatserna från studien är att efterfrågeflexibilitet inom uppvärmning är endast fördelaktig med en decentraliserad reglerstrategi och att begränsning av toppeffekt inom fjärrvärme har en stor besparingspotential.

Nyckelord Efterfrågeflexibilitet, fjärrvärme, ventilation, begränsning av toppeffekt, energisimulering, regelbaserad kontroll algoritm

Preface

This master thesis has been carried out within the REINO project between April and November 2017. REINO is a Tekes-funded collaboration project between the Aalto University and different Finnish companies with aim to develop new business opportunities and concepts relating to optimal building energy use and IoT (internet of things).

I am truly grateful for getting the opportunity to do my master's thesis within the Aalto University's department of Mechanical Engineering's HVAC research group.

I would like to express my deepest gratitude to both my thesis advisor D.Sc. Juha Jokisalo and my thesis supervisor professor Risto Kosonen for bringing me a never-ending stream of constructive feedback and support during this process. Their help has been invaluable.

I direct my special thanks to my colleague in science Behrang Alimohammadisagvand for his advice and work input in implementing the rule based control algorithms into the simulation software. I also thank the rest of the work society over at Sähkömiehentie 4 for providing me with ideas, possibilities for discussion and a good work atmosphere.

Additionally, I want to thank all the people participating in the REINO project's steering group for interesting meetings and discussions. Special thanks are directed to Tekes, who made the financing of my thesis possible.

Finally, I want to thank my family and especially Veera for her support during the making of this thesis.

Espoo, 17th November 2017

Kristian Martin

Contents

1 Introduction

Due to urbanization and climate change, a need for increasing energy efficiency and reducing fossil fuel usage is present (Lombard-Pérez, et al., 2008). In EU, buildings account for 40 % and 36 % of the total energy consumption and CO_2 emissions respectively (European Commission, 2017). In 2015, heating of Finnish buildings accounted for 25 % of the end use energy. Additionally, they accounted for almost 50 % of the total electricity consumption (Statistics Finland, 2015).

The reduction of fossil fuel use within heat and electricity consumption can be achieved with twofold action by increasing energy efficiency or by introducing more renewable energy sources (RES) directly to buildings or to the electrical and thermal grid. Consumption fluctuations and especially high-peak periods are decreasing the efficiency of both the electrical and thermal grid since they are expensive to produce. The fluctuations can be prevented by cutting peaks or moving the time of energy usage. This would reduce the need to use expensive and high emission plants like oil and gas boilers (Kensby, et al., 2015), (Valor Partners Oy, 2015).

There has to be an incentive to realize intelligent energy consumption behavior among consumers. A dynamic tariff would represent the real-time cost of energy production. In this way, the consumers would be stimulated to manage their consumption towards the low-price periods which economically rewards both consumers and producers at the same time it rewards the whole society in form of decreased CO_2 emissions. Additionally, consumption according to supply makes it possible to increase the utilization of RES (i.e. wind and solar) in the electrical grid (Gelazanskas & Gamage, 2014).

Demand response (DR) is the term describing consumers reacting to the dynamic price of the energy grid. Since buildings are big energy consumers, there is potential within utilization of DR. For a building, DR interaction with the electrical grid can mean reduction in power usage during high price periods or scheduling the use of electricity towards low peak periods. In the case of thermal grid and buildings, heating can either be reduced or increased depending on the price trend. During low price periods, additional heat can be accumulated into the thermal mass of the building by increasing the room temperature. This passively stored heat can then be used during high price periods and the heating system can run on minimal power. Additionally, the use of active thermal energy storage e.g. hot water storage tank is possible.

From the building owner point of view, the potential with DR is cost reductions. For the energy producer, it means potential to minimize expensive and fossil fuel intensive heat and power generators. From the community perspective, the potential lies within reducing overall fossil fuel emissions and implementing RES, such as solar and wind into the electrical grid.

1.1 Research objective

The main objective with this thesis was to study the monetary savings potential of dynamic price tariff based demand response within heating and ventilation of educational and office buildings. Dynamic pricing is considered to be the most efficient pricing program to combine with DR (Borenstein, et al., 2002) and (Hu, et al., 2015).

There are many studies available on demand response, but they often tend to focus on electrical energy usage. According to Dréau & Heiselberg (2016), studies that focus on heating are usually conducted with a simplified model of the building, where the real thermodynamic behavior is not considered. The aim with this study was to conduct a detailed building model simulation with a dynamic simulation tool to provide realistic results on cost savings and thermal conditions.

A key objective in this study was to determine the difference in cost saving depending on whether a centralized or decentralized DR strategy is used. Centralized control refers to making adjustments on system level while decentralized control refers to making adjustments on room specific level.

Within heating DR, the room temperature can be increased during low price periods. The heat stored in the structures can then be used during high price periods. The prerequisite for this method is that the time-constant of the room or building has to be long enough. However, an increase in room temperature might not be favorable during warmer parts of the heating season due to risk of overheating the building. The effect of heat loading was included in this study.

The heating flexibility of the building is a term that ties together the realized building behavior with the district heat (DH) network. This concept was studied through the flexibility factor, which describes how well a building is able to cooperate with the dynamic price signals from the DH producer.

Airflows in non-residential buildings are normally large and there can be achieved substantial monetary savings by increasing CO_2 concentration set-point during high price periods. Therefore, the potential of this control strategy was examined in this study.

The district heat contract power of a building is based on the power demand during dimensioning outdoor temperature conditions. These cold outdoor temperature conditions occur quite rarely meaning there is potential in decreasing the contract power to gain monetary benefit. The potential of peak demand limiting was included in this study.

1.2 Structure of thesis

Chapter 2 presents the structure and the function of the current district heating and electricity markets in Finland. Additionally, the price components forming the final energy prices are briefly reviewed.

Chapter 3 gives an overview of the broad subject “Demand side management” and the different possible alternatives within the area. The specific concept “Demand response” and the practical elements within it such as control strategies and pricing programs are reviewed in more detail.

Chapter 4 deals with demand response within buildings regarding heating and ventilation system. Some results from former studies about heating demand response are briefly reviewed. Favorable outdoor temperature ranges are discussed and additionally the concept of thermal mass and heating

flexibility is presented. For demand response within ventilation systems, the control of supply air temperature and airflow is discussed.

Chapter 5 presents the methodology of the study. Acceptable ranges for indoor environment comfort are reviewed and the applied dynamic energy prices and simulation software presented. In addition, the simulated case study building and its structure properties, technical systems, internal heat gains and profiles are presented. Finally, the demand response control algorithms used in the simulations and the actual simulation cases and their characteristics are presented.

Chapter 6 deals with the simulation results starting by presenting relevant energy and cost information for the non-DR-controlled reference cases. Next, analysis of values regarding two control parameters used in the algorithms (marginal value and limiting outdoor temperature) for determination of the optimal starting point for the simulations is presented. The results of the actual demand response case simulations are presented and analyzed in terms of energy consumption, cost and flexibility factor. Additionally, the indoor environmental comfort such as room air temperature and CO2 durations of the rooms is analyzed. Finally impact on thermal comfort and cost saving potential for peak demand limiting of district heating is presented.

Chapter 7 summarizes the main results and conclusions of the study.

2 Energy markets and pricing

The main difference between the current electricity and DH markets is that the electricity price is formed in an open market based on supply and demand, whereas district heating price is based on bilateral contracts between suppliers and consumers.

There is already a market available if wanting to utilize real time price based demand response for electricity, but for district heating this is not yet established in Finland. However, the topic is being regularly discussed and there are examples of DH-open market experiments in Stockholm and Copenhagen (Pöyry Management Consulting, 2016).

The DR possibilities in this thesis are studied on the assumption that dynamical pricing is available for both electricity and DH. The actual price data is presented in chapter 5.1.5. In the following sub-chapters, the market and price structure of electricity and district heating is presented.

2.1 Electricity market

The electricity market in Finland faced a big change in 1995 when the production and selling of electricity were released from trade restrictions into a free and open market. For consumers this meant the possibility to buy electricity from whichever producer they want instead of being obligated to buy from the local energy company. Additionally, Finland joined into the Swedish and Norwegian electricity marketplace Nord Pool in 1998 (Partanen, et al., 2015) & (Nord Pool, 2017a). Nord Pool is a company governing a market place for wholesale electrical energy and was founded in 1991 by Sweden and Norway, but it has been expanding to other countries after that including Finland, Denmark and Baltic countries. The company owners are the transmission system operators (TSO) of the countries involved (Partanen, et al., 2015). Additionally, the German and UK markets are partly included in the activities provided by Nord Pool due to the transmission cables connecting different parts of Europe (Nord Pool, 2017b). Nord Pool makes it easier to identify areas lacking capacity by determining electricity price based on supply and demand (Nord Pool, 2017c).

The structure and connection of the parties forming the current electricity market in the Nordic countries is shown in Figure 1. All the electricity generated by producers is the so-called wholesale electricity and it can be sold either through the electric stock market (Nord Pool) or via over-the-counter markets (OTC-markets). In the OTC-market electricity is sold by producers directly to large energy consumers e.g. factories or retailers through bilateral contracts. The retailers are mostly comprised of local and regional electricity companies, who then sell it to the end consumers (Partanen, et al., 2015).

Figure 1. Electricity market structure and connections between parties (Partanen, et al., 2015).

Nord Pool has two market channels for electricity trading: Day-ahead market (Elspot) and intraday market (Elbas). In the Elspot market, the hourly wholesale electrical prices for the upcoming day (hours 0 – 23) are released every afternoon at 12.42 central European time (CET) or later. The spot price is calculated by an algorithm from the 24 hours forward hourly-based offers made by the producers and retailers. Hence at 12.00 CET the spot prices for the upcoming 12 hours are known (12 – 23) and at around 13.00 CET the upcoming 36 hours' prices are known (Nord Pool, 2017d) & (Partanen, et al., 2015).

Elbas works as an after-sales market for Elspot and makes it possible to trade electricity continuously up to one hour ahead the actual time of the usage. This is needed to secure the balance between production and consumption in the network, since there are time periods when some power plants might have a temporary outage or when windmills generate more wind power than needed etc. The importance of the Elbas market is increasing especially due to the increment in installed wind power in the grid (Nord Pool, 2017b).

2.1.1 Electricity pricing

The end-users' electricity price consists of three components: electrical energy price, transfer price and taxes which all are marked and priced separately in the energy bill. The taxes are not going to be discussed further in this thesis.

Transfer price

The transfer price is defined locally by the grid operator at a particular region and it is of the same magnitude for every same-class customer within that region. In other words, every small customer e.g. detached houses pay the same price for transfer and the bigger consumers are paying a different price according to which consumption class they are identified with. Since the local distributor has monopoly on the distribution and its transfer price, the Energy agency is supervising the business activity to prevent unjustified price levels. For smaller consumers the transfer price is consisting of a basic monthly or annual charge and a separate charge per kWh of transferred electricity. For bigger customers there can additionally be an annual power charge depending on peak usage. The basic and the energy charge are meant to compensate for costs related to the management and development of the grid operations. The structure and the cost components constituting the transfer price is visualized in Figure. 2.

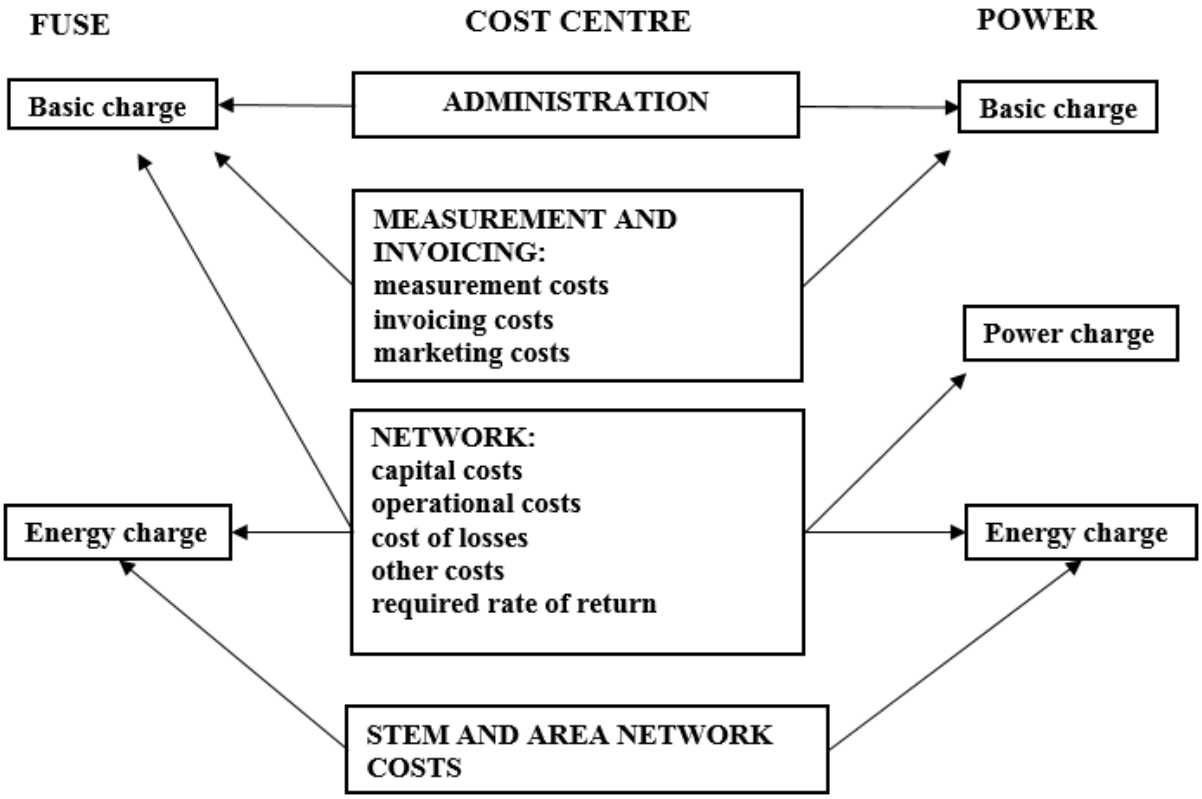

Figure. 2 Cost structure of electricity transfer price (Partanen, et al., 2015).

Energy price

The electric energy price can be categorized as fixed-term static price or hourly spot price. The static price is an agreement between the retailer and the end customer where the period of agreement can vary from a couple of months to one year or more. The spot price is determined by the electricity whole sale market on top of which a regional adjustment is made (Partanen, et al., 2015). The regional adjustment (e.g. Nord Pool Finland spot price) accounts for the areas physical transmission limitations (Nord Pool, 2017e).

The available hydropower has impact on the electrical price and especially Norway's water resources are strongly affecting the spot price. The reason is that during rainy years, the need for expensive condensing power plants is short term, which keeps the price level down. Additionally, if the generation of base load facilities (CHP or nuclear) are enough, the electricity price stays lower than if condensing or peak power plants have to be used. Since electricity usage naturally is higher during winter, also the price is higher. The price variation is shown in Figure 3.

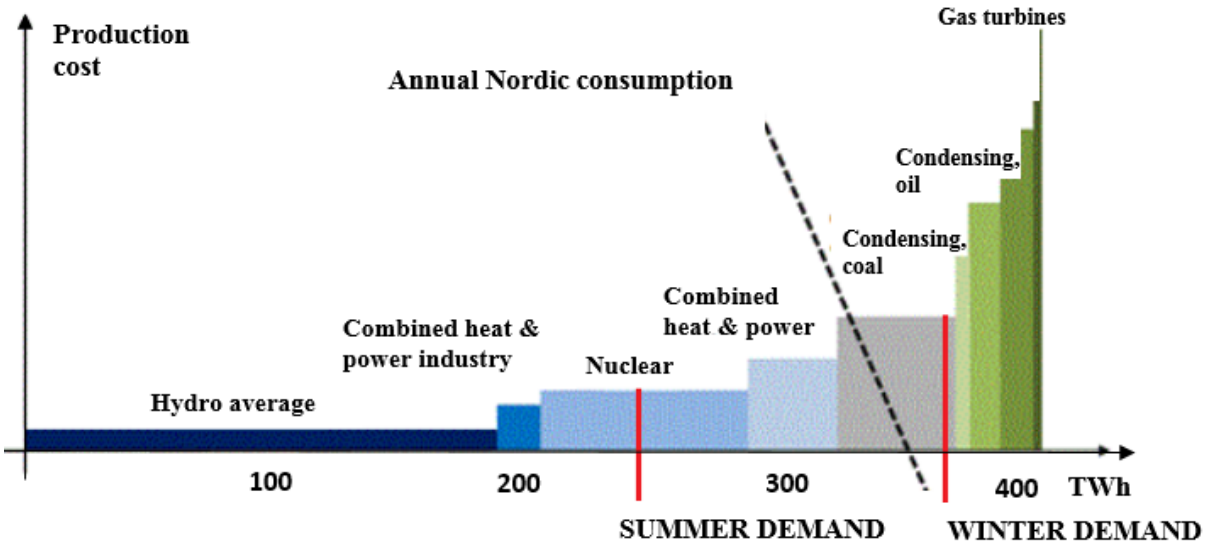

Figure 3. Electricity price structure (Nord Pool, 2017f) & (Partanen, et al., 2015).

Among smaller consumers in Finland fixed-period static prices are more common while spot price based contracts are popular in Norway and Sweden (Partanen, et al., 2015).

2.2 District heating market

District heating is the most common heating source in Finland with a total market share of 45 % and over 90 % in bigger cities. Most of the heat (70 – 75 %) is produced by CHP plants, industry waste heat or biogas burning on the waste tips. During colder time periods the peak load is handled by oil or gas boilers. The main fuels used are natural gas, coal and peat but also wood chips and biogas are used (Sarvaranta, et al., 2012). Additionally, 5 power plants in Finland are at the moment producing electricity and heat from waste combustion (Helsingin Sanomat, 2017).

The normal market structure today is that one producer owns the local distribution network, and both sells and distributes the heat to its customers. However, it is also possible for big industries to sell their waste heat to the DH-company by a bilateral contract agreement. There has been discussion in Finland whether the operation of the DH-network should be corporatized into an own business. This would reduce the monopoly status of the local producer, but it has not yet been seen as profitable (Sarvaranta, et al., 2012).

The DH-business can be divided into four parts: heat production, selling, distribution and consumption. The role structure and responsibilities can be seen in Figure 4.

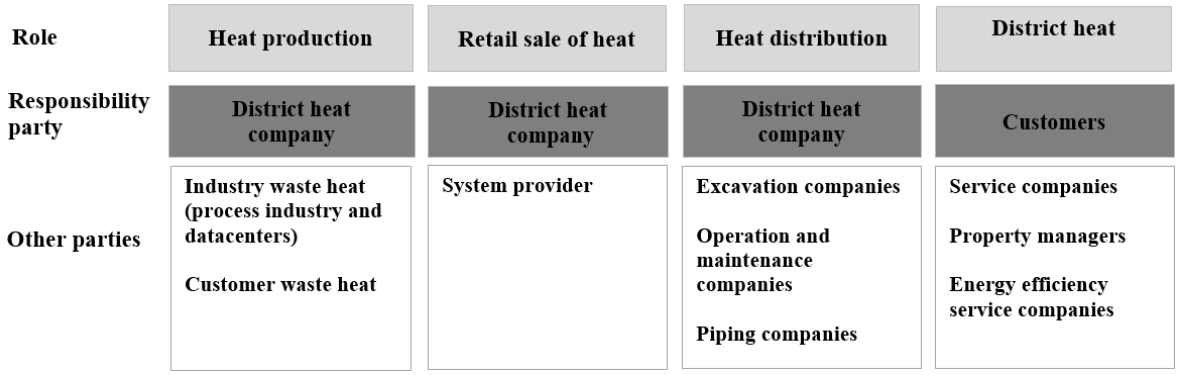

Figure 4 Role structure and responsibilities within DH-system (Valor Partners Oy, 2015)

Unlike the whole-sale electricity market the DH market can be said to be a closed business where the producer independently can choose the price of the heat. However, the competition authority oversees the operation to prevent abuse of the monopoly status in form of overpricing (Manninen, 2014).

There have been several discussions regarding whether to transform the DH market into a dynamic price based open market. Then small consumers could also be producers (prosumers) by transferring waste heat from solar collectors and heat pumps to the network. Pöyry Management Consulting (2016) investigated different possible business models for open DH-markets. The report presented different alternatives that could work in different networks. The report concluded that new business models could support efficient heat production both economically and environmentally and additionally enforce the future market position of DH.

There is an example from Sweden where the local DH-company has tested partly open DH-network which allows third party producers to feed their waste heat into the DH-network. The price of the heat is defined according to the actual demand at that time. In Copenhagen, the optimization of the DH-network is conducted by a separate operator who trade heat from separate producers on an hourly basis (Pöyry Management Consulting, 2016).

2.2.1 District heating pricing

The main component affecting the DH price is the structure and costs of the actual plant entity providing the heat. The fuel type used has significant influence on the DH-price and this is varying between DH-producers which makes the price vary between regions in Finland. Investments, maintenance, plant age and administrative costs are also affecting the price (Sarvaranta, et al., 2012).

The DH-price is divided into three parts: connection charge, basic charge (or power charge) and energy charge. The connection charge is a one-time payment which accounts for the connection installation between the customer and the DH network. The power charge is based on max flow requirement of the facility at peak load and it is meant to cover fixed-costs of the network operation. Heat companies calculate the power charge in different ways which complicates the price comparison (Sarvaranta, et al., 2012).

The energy charge (€/MWh) is paid according to energy usage. Since static pricing is the program in use, the DH companies account for the average annual production cost which also covers use of peak power plants (Sarvaranta, et al., 2012).

3 Demand side management

Demand side management (DSM) is not a new concept and it was introduced already in the 1960's and 1970's in Europe, New Zealand and then USA. For a long time, it has only been related to the electrical grid and the management of its load profile. Gellings (1985) defines the concept as *"Demand side management is the planning and implementation of those electric utility activities designed to influence customer uses of electricity in ways that will produce desired changes in the utility's load shape"*.

The earliest forms of DSM aimed at shifting electricity use partly to night-time by introducing day and night tariffs (valley filling and load shifting). This was followed by peak clipping, which means that the utility could control the power distributed whenever necessary (e.g. direct load control of electric water heaters). It is stated by Palensky and Dietrich (2011) that while DSM has traditionally been coordinated and implemented by the utilities (i.e. direct load control), it might change in the future and become more user managed.

The reason for why utilities wanted to maintain a stable load curve with minimum high-peaks were that during those peak times the hydro, coal and nuclear power plants managing the base load were not enough and oil and gas boilers had to be used to provide sufficient power. Since the oil price was rising heavily during the 70's, these high peaks were very expensive for the utilities (Gellings, 1985).

The reliable operation of the electrical or thermal grid means that supply and demand should be at the same magnitude all the time. This is a difficult task to uphold, since the consumption is varying a lot and high peaks can occur. Additionally, RES in the electrical grid have varying production and makes it even more challenging.

Figure 5 presents a load duration curve for a typical district heating network in Finland. Most of the time, the heat is produced by efficient CHP facilities, but during high peak periods (around 1000 hours/year), heat is produced by oil boilers. The oil boiler usage is expensive, it releases a lot of CO_2 and additionally does the start-up and shut-down of peak facilities reduce the efficiency of the whole network (Valor Partners Oy, 2015). Figure 6 shows the load duration curve for the Finnish electricity grid during 2011-2014, the characteristic is similar to the DH-duration profile.

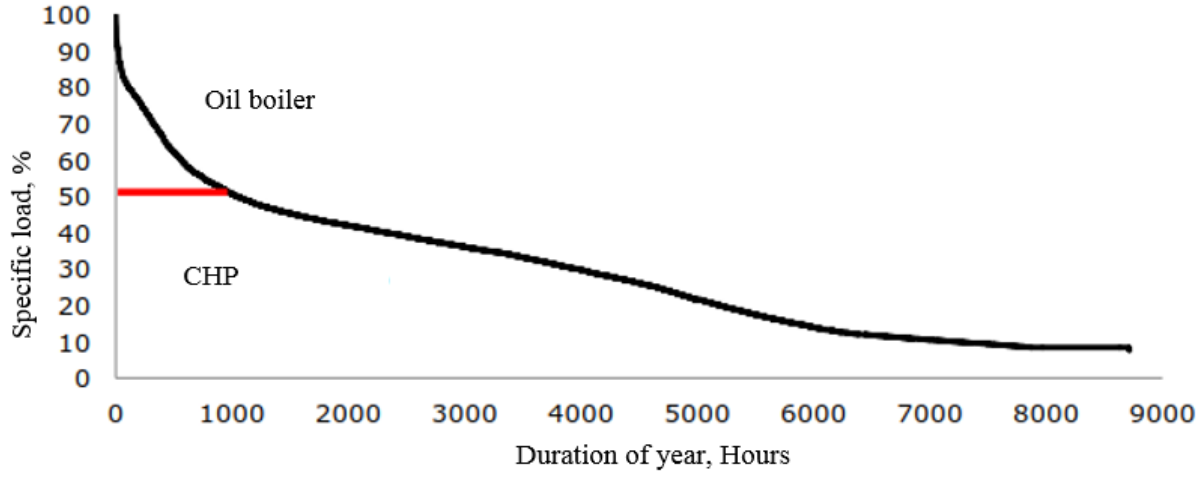

Figure 5. Duration curve for medium DH-system in Finland, 2011 (Valor Partners Oy, 2015).

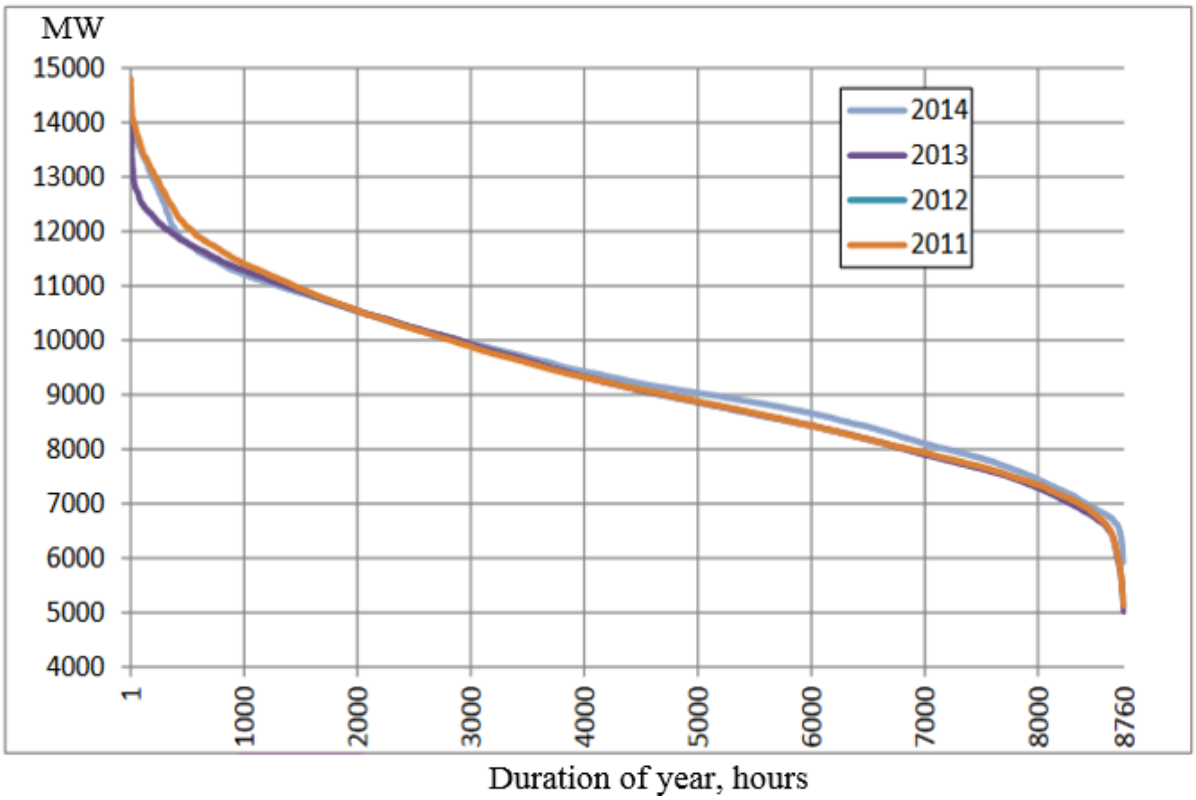

Figure 6. Duration curve for electrical power in Finnish grid (Energy authority, 2015).

Another aspect of the electrical grid is that the peak demand sets the dimensioning criteria for the generation assets. This reduces the load factor (ratio of actual power usage to max capacity) and drives the electricity prices upwards (Strbac, 2008). Tiptipakorn and Lee (2007) conclude that price signals or dynamic pricing is needed to motivate consumers to adapt according to the energy available and increase system efficiency. The same thing is stated by Schuler (2004), who suggests "*to let the consumers into the game"* to motivate change in energy usage behavior.

Energy efficient performance of the electrical and thermal grid includes maximizing CHP utility operation at nominal power (higher load factor) and minimizing start-ups of peak power plants (Valor Partners Oy, 2015). Additionally, increasing the amount of RES in the electrical grid and introducing RES into the thermal grid would decrease CO_2 emissions (Lund, et al., 2014).

Demand side management (DSM) may provide ways to support the fore mentioned aspects. At the building level, electrical DSM can be implemented by e.g. using household appliances during low price periods. In the thermal grid, it could involve storing excess heat either to the thermal mass of a building or an active thermal water storage for use during high price periods (Shan, et al., 2016).

For the energy producer, DSM is referring to some kind of incentive price mechanisms which will motivate the consumers to shape their consumption according to the need of the producer. For the consumer, it means the adaptation of energy usage to minimize costs. The common benefit for both stakeholders is reduced costs and CO_2 emissions (Gelazanskas & Gamage, 2014).

3.1 Concepts

DSM consists of several different concepts. Figure 7 presents the concepts usually related to DSM in the literature e.g. (Gellings, 1985), (Kreith & Goswami, 2016) (Wang & Yan, 2014) & (Gelazanskas & Gamage, 2014). The methods can be considered applicable both to electrical and thermal energy.

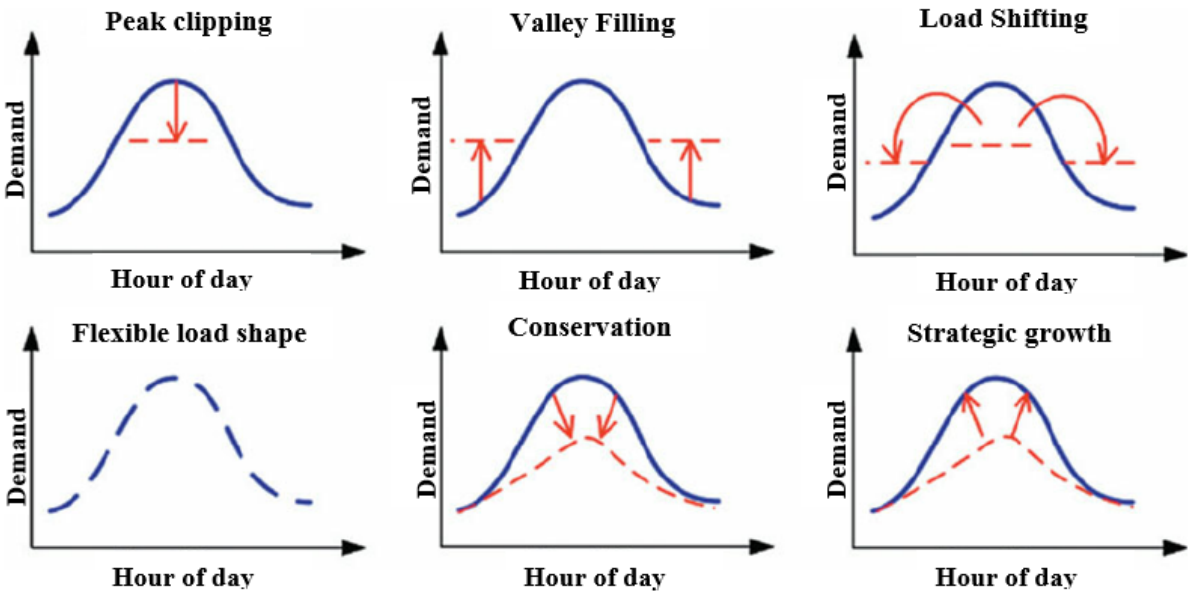

Figure 7. Overview of DSM concept (Wang & Yan, 2014).

Peak clipping is the reduction in peak demand. It can be realized by incentive based strategies, where the consumer adjusts the load during high or low peak periods. Alternatively, energy companies can handle it by directly regulating the energy transferred to a customer. Peak clipping is usually divided into demand limiting and demand shedding, which is explained by Shan et al (2016) as: *"demand limiting flattens the load curve, when the load is about to exceed a predetermined value, while demand shedding, limits the load curve during grid critical peak periods"*. Demand shedding is controlled according to grid conditions while demand limiting is controlled according to building load conditions.

Valley filling and load shifting are closely related and aims to shift part of the high-peak loads to off-peak periods to save cost, but not necessarily energy. If heat (DH or electricity) is to be shifted, the energy can be stored in e.g. water tanks or passively in the structures of the building.

Flexible load shape gives the energy company the opportunity to adjust the power distributed according to their needs. Variation in power distribution means variation in the conditions at the consumer and is therefore motivated by incentive payments.

Conservation refers to cutting total energy use by retrofitting measures in buildings or by using energy efficient appliances. The motivating instance can be the government, utility companies or grid regulators that offer different kinds of incentive refund programs for the end-user who invests in energy efficient technologies (Pierluigi, 2014).

Strategic growth refers to the overall growth of energy consumption. Kreith and Goswami (2016) explains that an increasing share of electrical processes in particularly the industry sector may decrease the use of fossil energy, which may give a better overall energy efficiency.

DSM consists of a sub-set called "Demand response" (DR) to which peak clipping, valley filling, load shifting and flexible load shape belong. DR will be discussed more detailed in the following chapter.

3.2 Demand response

Even though the overarching goals with demand response is monetary savings, the occupant satisfaction should not be undermined. The indoor conditions should preferably not be sacrificed, and all changes have to be acceptable and not cause health risks (Motegi, et al., 2007). The monetary savings from DR could easily be annihilated if the indoor thermal comfort or air quality is reduced too much. The relation between indoor temperature and performance of workers have been focus for many studies over the years and its effect has been scientifically proved many times (Wargocki & Wyon, 2017), (Seppänen, et al., 2005), (Wargocki, et al., 2000).

Depending on control strategy used, the DR can be considered centralized or decentralized. If it is possible to control the indoor temperature of each zone individually in the building a decentralized DR-strategy could be used. Otherwise, the DR can be done on a centralized basis by e.g. altering the inlet water temperature of the whole radiator network (Motegi, et al., 2007).

3.2.1 Control strategies

Shan et al. (2016) presents DR-control strategies for different types of buildings. In commercial buildings: HVAC-systems, lighting and onsite renewable energy production are considered important when wanting to utilize DR. The HVAC-systems consume a significant share of the buildings total energy. The systems are usually connected to a central building automation system (BAS) which makes the control flexible. Onsite RES production cannot be treated as a direct way of DR due to its dynamic characteristics, but it is possible to combine it with a storage system for later use.

The DR-strategies can be divided into two concepts: peak limiting and demand shifting. The DR-strategies are further linked to control strategies, which indicate what parameters are going to be controlled in the building. Figure 8 gives an overview and insight of how the DR-concept can be categorized from the perspective of a building. The actual implementation of DR is done by choosing the most applicable DR-control strategy.

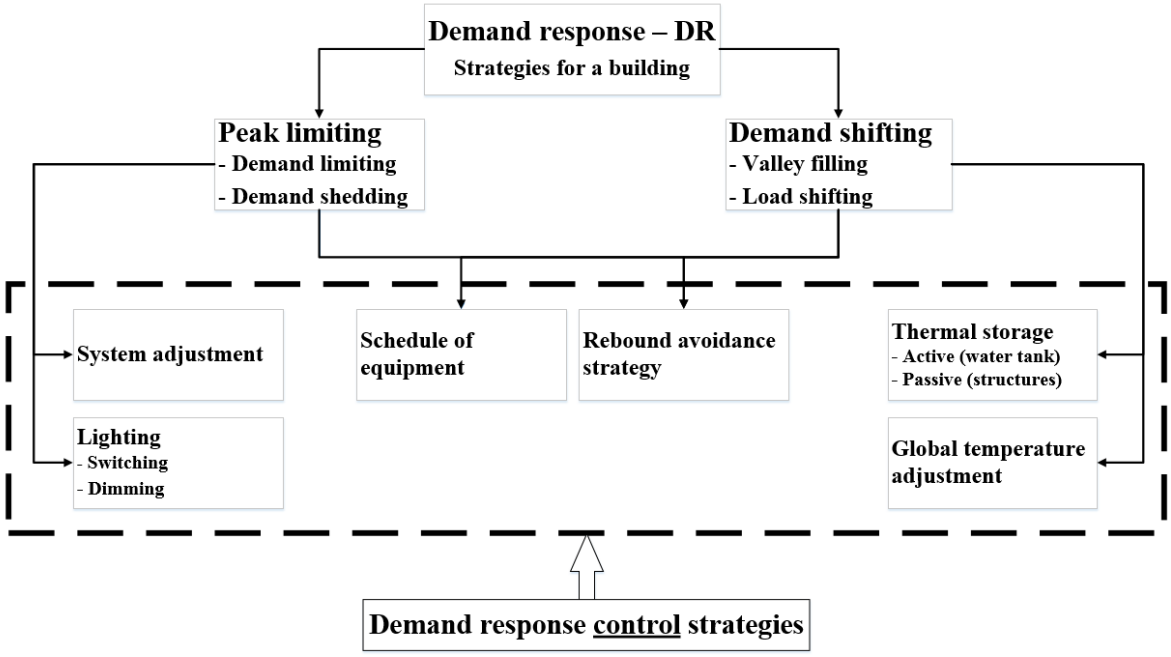

Figure 8. The DSM concept from the perspective of a building.

Global temperature adjustment (GTA) and thermal storage (TS)

The GTA control strategy is based on temperature set-point adjustments and seems to be the most common control strategy in the literature. Depending on the situation the indoor temperature set-point can be adjusted up or down to either charge or discharge heat into the structures of the building. The thermal mass of the building slows down room temperature variations when adjusting the temperature set-point. This preserves the thermal comfort a while even when the heating system is off. The GTA method can also be used for precooling or preheating to increase the thermal energy bound in the structures and extend the period of time the heating/cooling system can be turned off (Shan, et al., 2016).

Thermal storage is closely related to the GTA method which is based on the fact that structures or water tanks can provide the thermal energy needed for a while when the heat generation system is off.

System adjustment (SA)

The main idea is to limit energy usage e.g. in the centralized system by adjusting the temperature of inlet water in the heating/cooling network or the ventilation supply air. It should be considered that such adjustment would make the room unit control valves or dampers to open up and increase the total fluid flow resulting in higher pumping or fan operation costs (Motegi, et al., 2007). Typically, the pumping costs constitute only a small fraction of the total cost while the fan operation cost constitutes a great part.

The main alternatives for SA and its practical measures are presented in Figure 9 (Shan, et al., 2016).

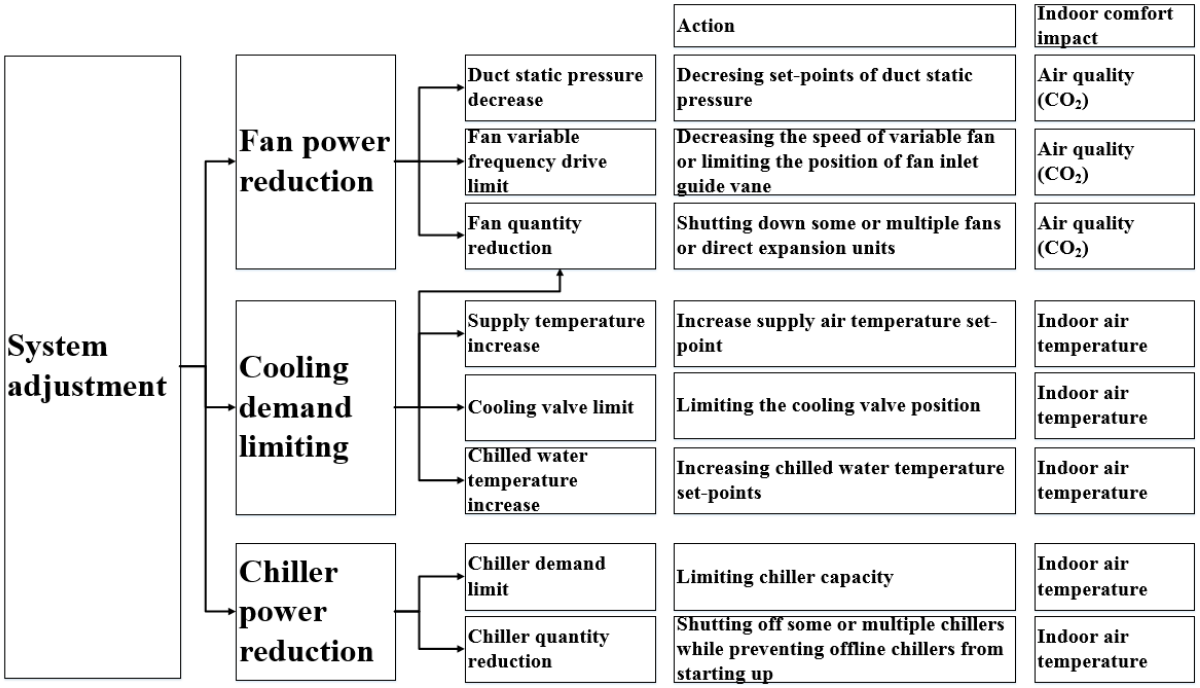

Figure 9. Alternatives of system adjustment, practical measures and their impacts.

Schedule of equipment

By choosing the schedule of equipment, the time of energy consumption can be altered. This time period can be fit to coincide with on or off-peak periods.

Rebound avoidance strategy

Rebound is the phenomena which might occur after a DR period when the system returns to ordinary operating conditions. After a heating power limiting sequence, the heating system would need additional power to achieve the normal indoor temperature. This rebound effect could also occur during early mornings when the air handling units (AHU) are starting up or the indoor temperature is retrieved from night time set-back mode (Shan, et al., 2016).

Strategies to minimize the rebound effect are among others:

- Slow recovery, which recovers the altered temperature set-points gradually in small steps
- Sequential equipment recovery avoids starting all appliances (e.g. AHU:s) at the same time
- Extended DR control period simply extends the control period until the power demand has reached lower levels, for instance non-occupied hours.

Figure 10 shows the rebound effect, where the blue base line shows the power demand if no DR is utilized and the red line shows the power demand during DR.

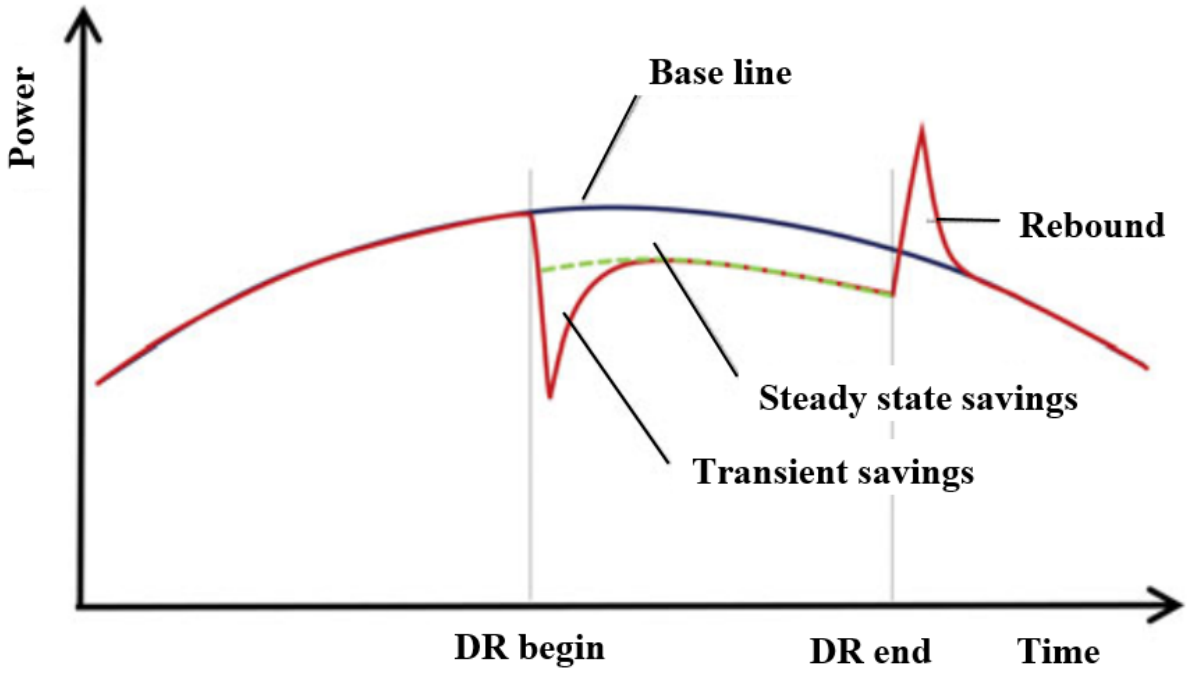

Figure 10. The rebound effect (Shan, et al., 2016).

Lighting

Lighting is usually the second most power consuming category in a commercial facility after the HVAC-systems and therefore it has great potential to control lighting within DR. Other benefits are that the lighting level can be reduced more or less instantly which also reduces cooling demand. Additionally, there is no rebound effect connected to lighting adjustment (Shan, et al., 2016).

3.2.2 Pricing programs

Demand response can be divided into two main categories: incentive based program (IBP) and price based program (PBP).

In IBP, users are paid for agreeing to that their power supply can be reduced during times of need. The IBP are also known as event-based, system-led, emergency-based or stability-based DR-programs. A program of this type motivates the end-users to reduce their energy consumption when the grid stability and reliability needs it. IBP: s are usually classified to be either production-based or market-based programs. In a production-based program the utilities, or the user, reduces power usage according to defined agreement. In a market-based program the consumers can participate in load-reduction bidding systems (Shan, et al., 2016) & (Gelazanskas & Gamage, 2014).

The price based programs are aiming to reflect the actual energy price according to current situation at the supplier. The cornerstone in PBP is dynamic pricing and the consumers are motivated to adapt their consumption according to high and low prices (Shan, et al., 2016).

The main difference between IBP and PBP is that IBP gives economic benefit from an on beforehand specified agreement, while the PBP gives benefit if the end-user is reacting to actual market prices. Hence in IBP, the user has to reduce power upon agreement, but in PBP the user can reduce power if he wants to.

The structure and classification of different DR-programs are presented in Figure 11 and a brief description of the programs is given in Table 1 (Shan, et al., 2016).

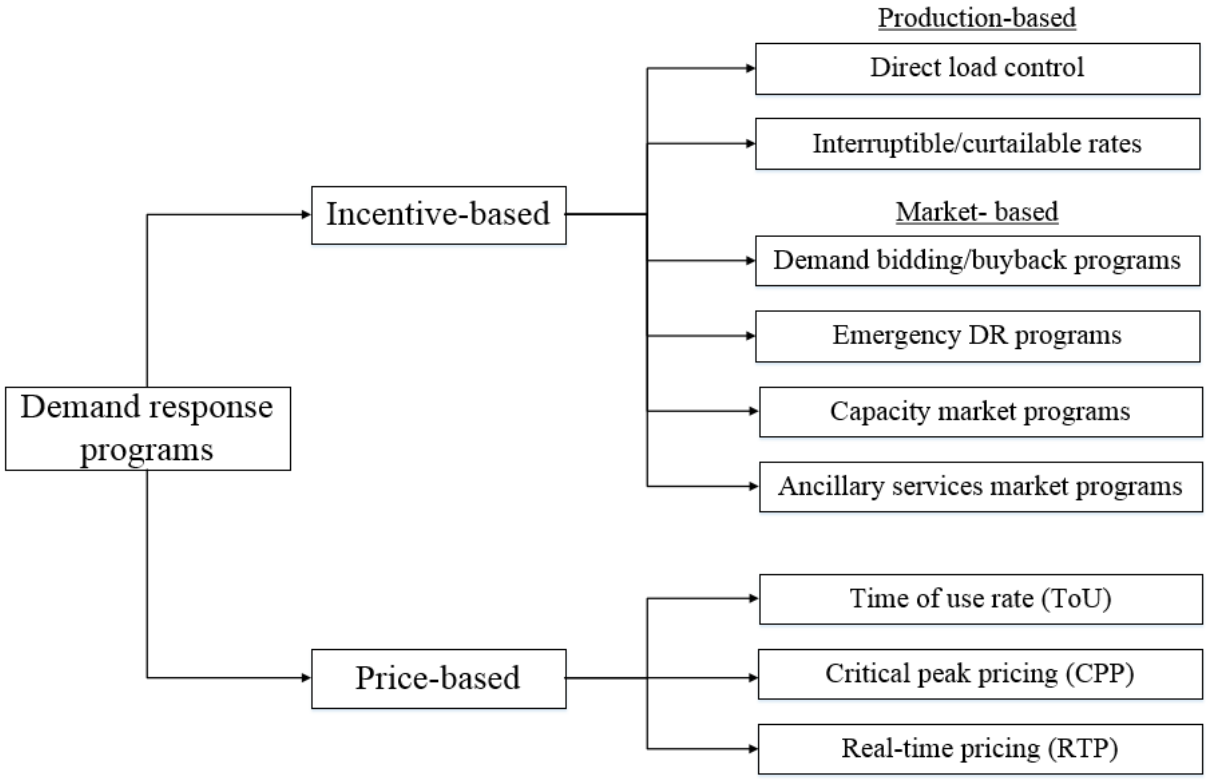

Figure 11. Categorization of DR programs (Shan, et al., 2016).

Table 1. DR-programs explained (Shan, et al., 2016).

	INCENTIVE-BASED DR PROGRAMS	INCENTIVE MECHANISM DESCRIPTION
CLASSICAL PROGRAMS	Direct load control	Usually based on previous agreements, the utilities have the ability and authority to remotely shut down the specific end-use equipment on a short notice to achieve the desired load reduction
	Interruptible/ curtailable rates	Participants are required to reduce their load to predefined values. Otherwise, penalties would be charged according to agreed terms
MARKET-BASED PROGRAMS	Demand bidding/buyback programs	Participants bid for specific load redcutions in the electricity wholesale market. In case of failing to curtail the specified amount of load, the customers have to face penalties
	Emergency DR programs	Participants are provided with incentive payments for reducing load during DR periods
	Capacity market programs	Participants typically receive day-ahead notice of events. They may receive payments in the programs, or penalties for failing to curtail when required to do so.
	Ancillary services market programs	Participants bid for load reduction in markets. If the bids are accepted, they will receive economic benefits both for being standby and for curtailing load upon needed.
	PRICE-BASED DR-PROGRAMS	**PRICE MECHANISM DESCRIPTION**
	Time of use (ToU)	The price is varying according to the particular time period, but during one time period, the price is static (e.g. day and night electricity). Prices are usually agreed upon one year ahead
	Critical peak pricing (CPP)	It is a variant of ToU, but the time periods when it is enabled are usually only a few hours or days per year. CPP can also be used additionally to ToU. The notice time of CPP is less than for ToU. A special variant is extreme CPP, when the price of energy can be very high for up to 24 hours. The notification time of extreme CPP can be as little as 1 day on beforehand
	Real-time pricing (RTP)	The most pure form of dynamic pricing, where the prices can be determined on an hourly basis and foretold to the consumers one day on beforehand. RTP is considered to be the most developed DR-program, since it demands two-way communication between the supplier and the consumer. Without these signals the pricing would be almost impossible.

Borenstein et al. (2002) and Hu et al. (2015) conclude in their studies that real time pricing is the most efficient DR-program. However, while the greatest reward potential can be achieved by RTP, it also has the biggest risk exposure due to high price uncertainty. Time of use programs is the opposite with low reward potential and low risk exposure due to static prices within pre-defined time periods. Critical peak pricing programs fall somewhere in between the fore mentioned schemes (Figure 12).

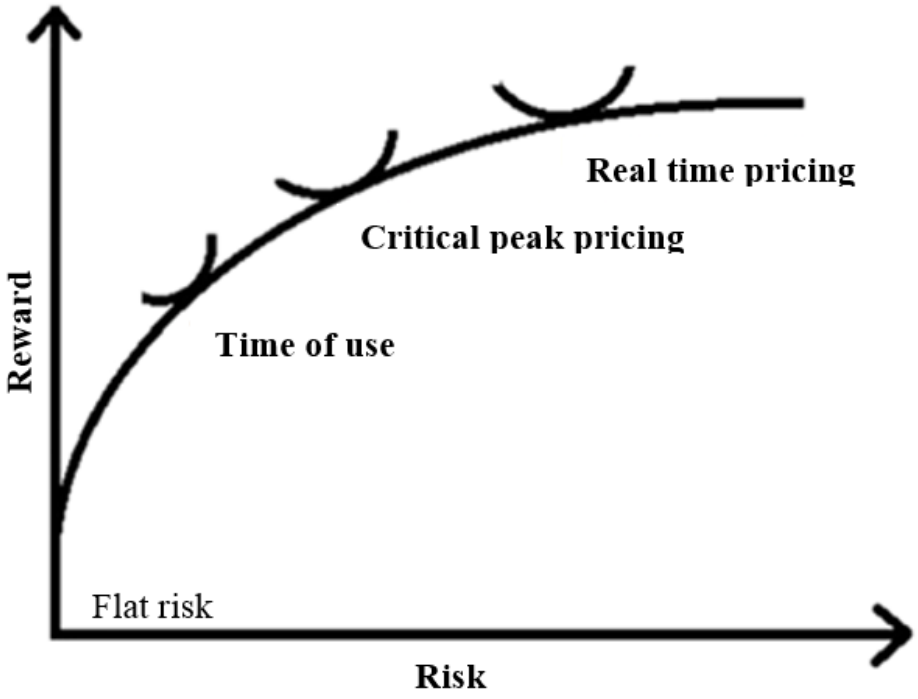

Figure 12. Risks and reward of price based DR (Hu, et al., 2015).

4 Demand response within buildings

4.1 Heating

DR in the thermal grid has been studied by simulations and measurements in case buildings but it is not implemented in practice as in the electrical grid. The fundamental goals are the same as for the electrical grid. A stable load curve which favors the operation of CHP-plants and reduce the need of expensive peak power boilers. Kärkkäinen et al. (2003) conducted field measurements for three case buildings to study the potential of DR within DH. The obtained data were used to calculate and simulate the impact on the whole regional DH-network in Jyväskylä when 160 buildings of same type were using DR. Syri et al. (2015) presented an example for an open district heating market with a dynamic price tariff in the Espoo region in Finland. The authors concluded that dynamic pricing and DR could give monetary savings to both producer and consumer.

Kärkkäinen et al. (1999) have studied the potential of DH DR in Finnish public buildings where the needed heating power could be cut on an average by 40 %.

Kensby et al. (2015) studied the possibility for residential buildings to act as heat storages for the DH-network by utilizing DR. The results showed a more stable daily load profile and a decreased peak power demand.

Jokinen (2013) showed the impact of thermal mass and insulation in buildings. The heat storage potential of district heated Helsinki residential buildings of different age were simulated. The results show that buildings from 1940 – 2003 had the greatest potential in cutting heat power since the heat demand is big as well as their thermal mass. Buildings built after 2003 had lower heat demand because of better insulation, which prolonged the possible time of heating shut-down.

Wernstedt & Johansson (2008) included 350 apartments in 14 houses in a DSM experiment. The heating was cut off from the warmest apartments while heat was provided to the colder apartments. The heating power need and energy was cut by 11% and 7 % respectively without reducing thermal comfort too much. During the DR-control period the apartments measured room temperatures ranged from 21 – 22 °C.

Dréau and Heiselberg (2016) and Alimohammadisagvand (2015, 2016a, 2016b, 2017) studied the potential of the GTA method combined with thermal storage within residential houses. Some of the studies have shown annual monetary savings around 0.2 % – 14.5 % depending on DR-control algorithm and building type. The best results have been obtained by predictive algorithms which are making control decisions based on future price information.

4.1.1 Favorable outdoor temperature ranges

It is usually assumed in Finland that the building does not need any heating during spring and autumn days when the daily average outdoor temperature exceeds 10 and 12 °C respectively (Finnish Meteorological institute, 2017). The dimensioning outdoor temperature for heating in Southern Finland (zone I) is -26 °C according to the Finnish building code D3 (2012). From the demand response point of view, the temperature range of -10 to +10 °C is the most interesting since it constitutes a great part of the year. Additionally, the heating system has much capacity to utilize if needed e.g. during temperature recovery. As can be seen from Figure 13, the outdoor temperature stays almost 60% of the year (218 days) in the range of (-10) to +10 °C.

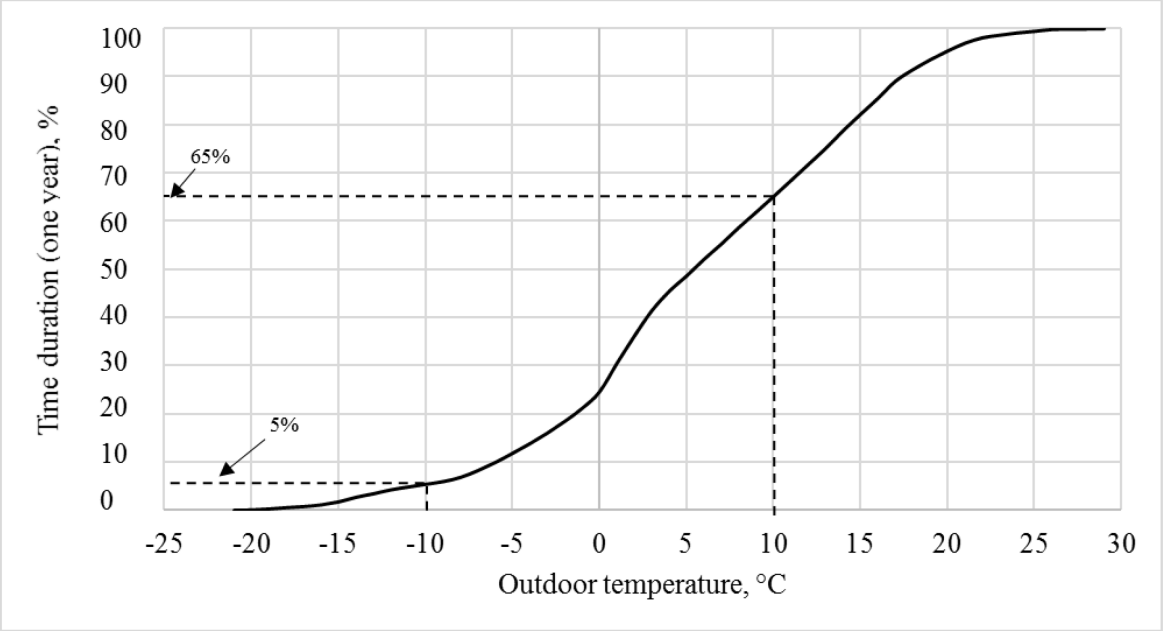

Figure 13. Outdoor temperature duration in Helsinki-Vantaa test reference year (Finnish Meteorological institute, 2012).

Valor Partners Oy (2015) stated that the biggest potential of DR within DH is periods during the spring and autumn. In other words, periods when there is big difference between the 24-hour moving average outdoor temperature and the daily high and low peak temperatures. Figure 14, Figure 15, Figure 16 and Figure 17 show the plot of the actual and the 24-hour moving average temperature for different times of the Finnish test reference year 2012 (Finnish Meteorological institute, 2012). It can be seen that during spring and autumn months the daily low and high peaks are constantly out of phase with the moving average outdoor temperature. However, Figure 18 shows that the biggest differences between daily average outdoor temperature and maximum peak temperatures are actually occurring during winter months. This suggests DR-potential also during December to February, but the potential decreases due to longer periods of colder weather when buildings cannot dispense heat power for long periods.

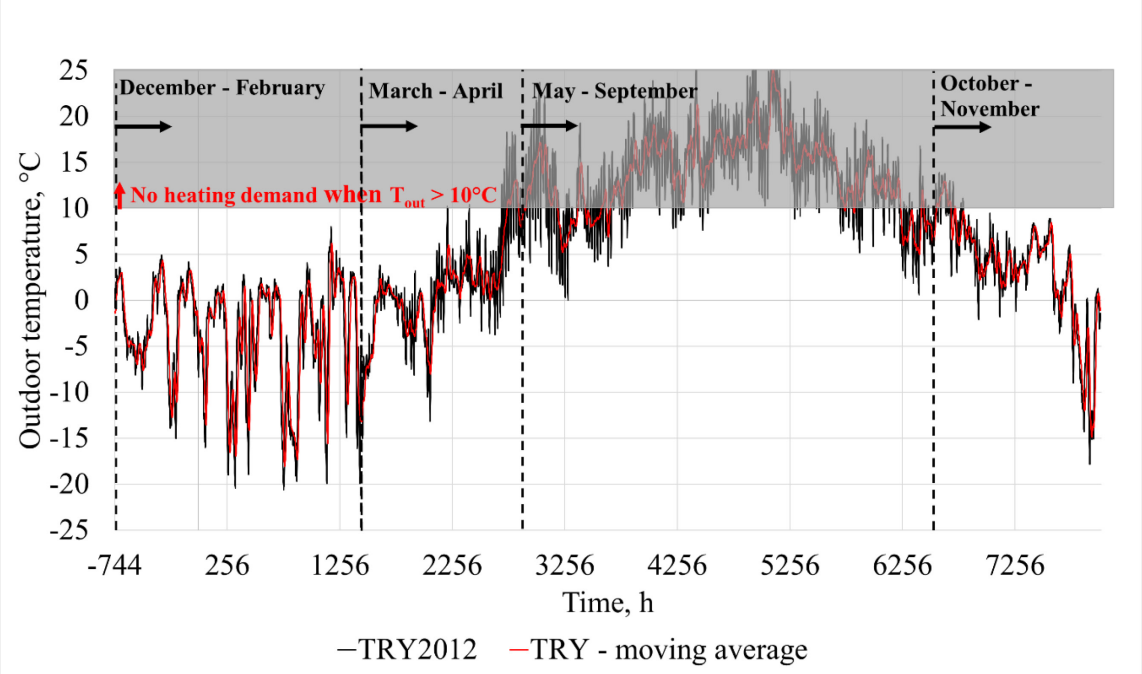

Figure 14. Outdoor temperature vs. 24 hour moving average outdoor temperature.

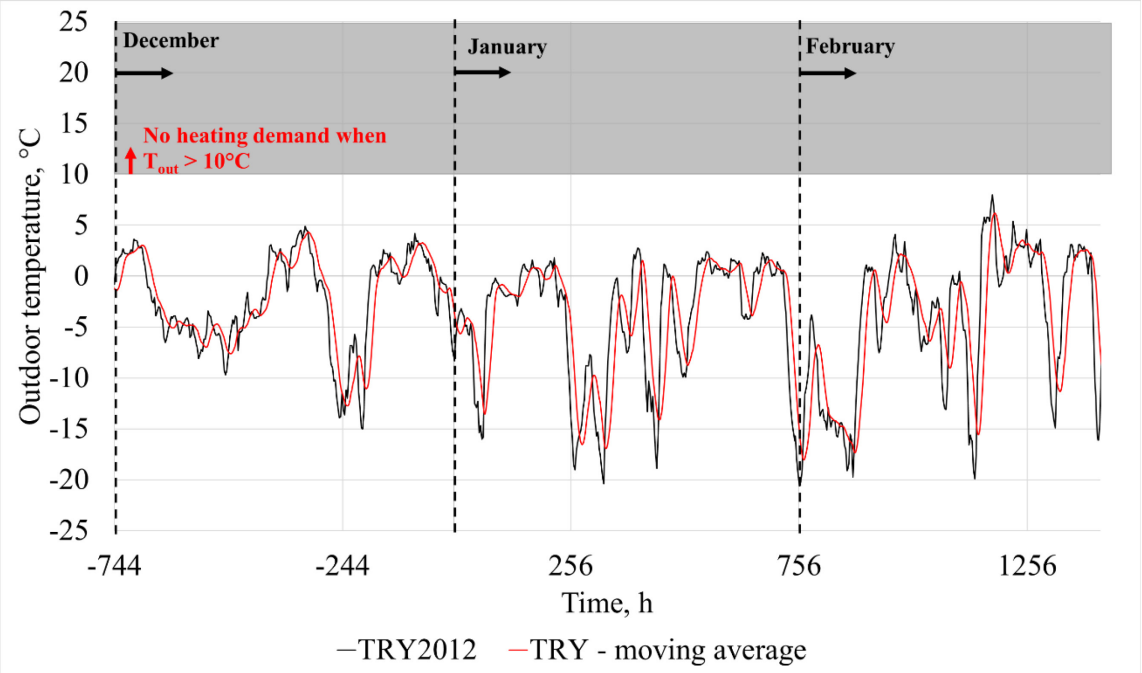

Figure 15. Outdoor temperature vs. 24 hour moving average outdoor temperature during winter months.

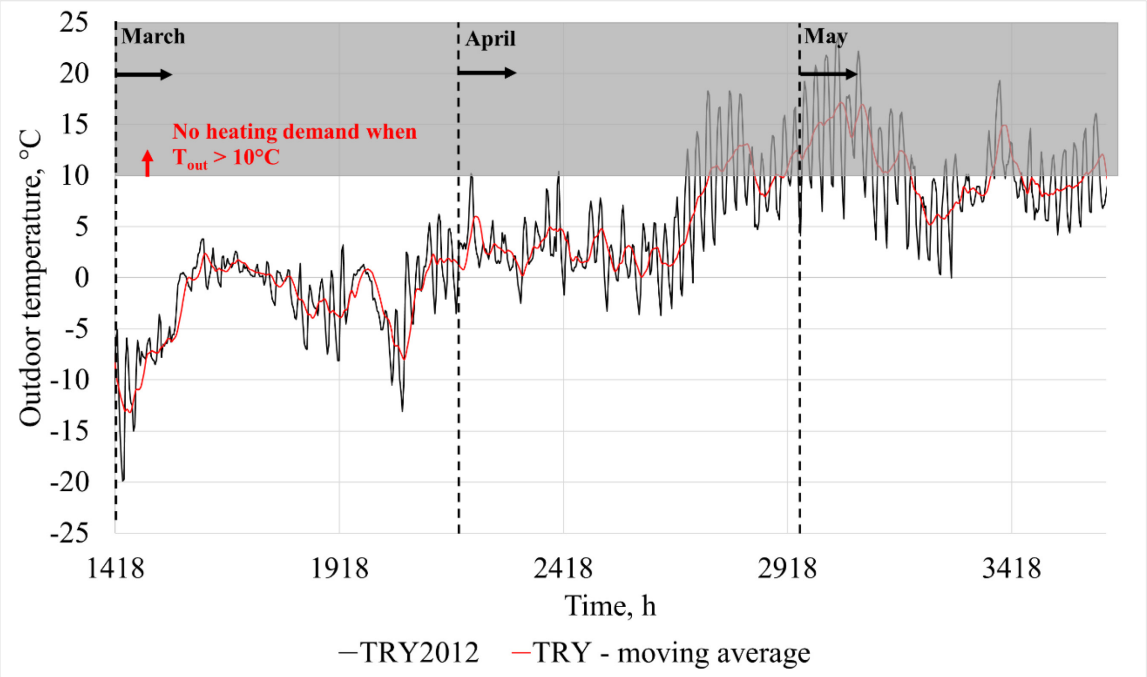

Figure 16. Outdoor temperature vs. 24 hour moving average outdoor temperature during spring months.

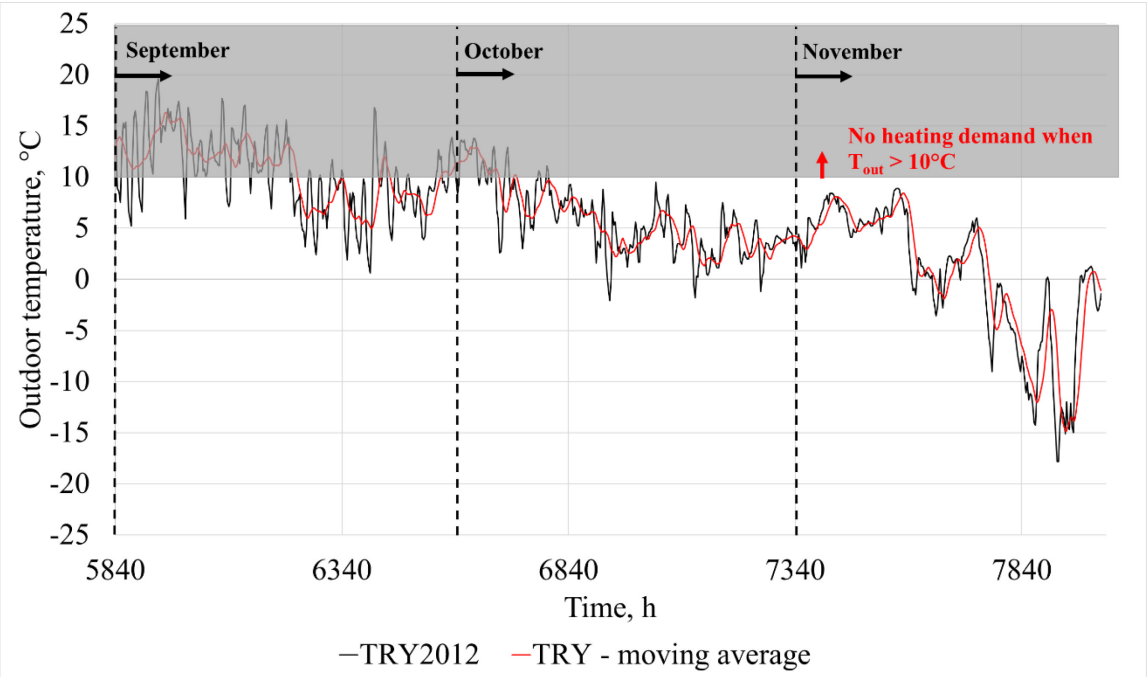

Figure 17. Outdoor temperature vs. 24 hour moving average outdoor temperature during autumn months.

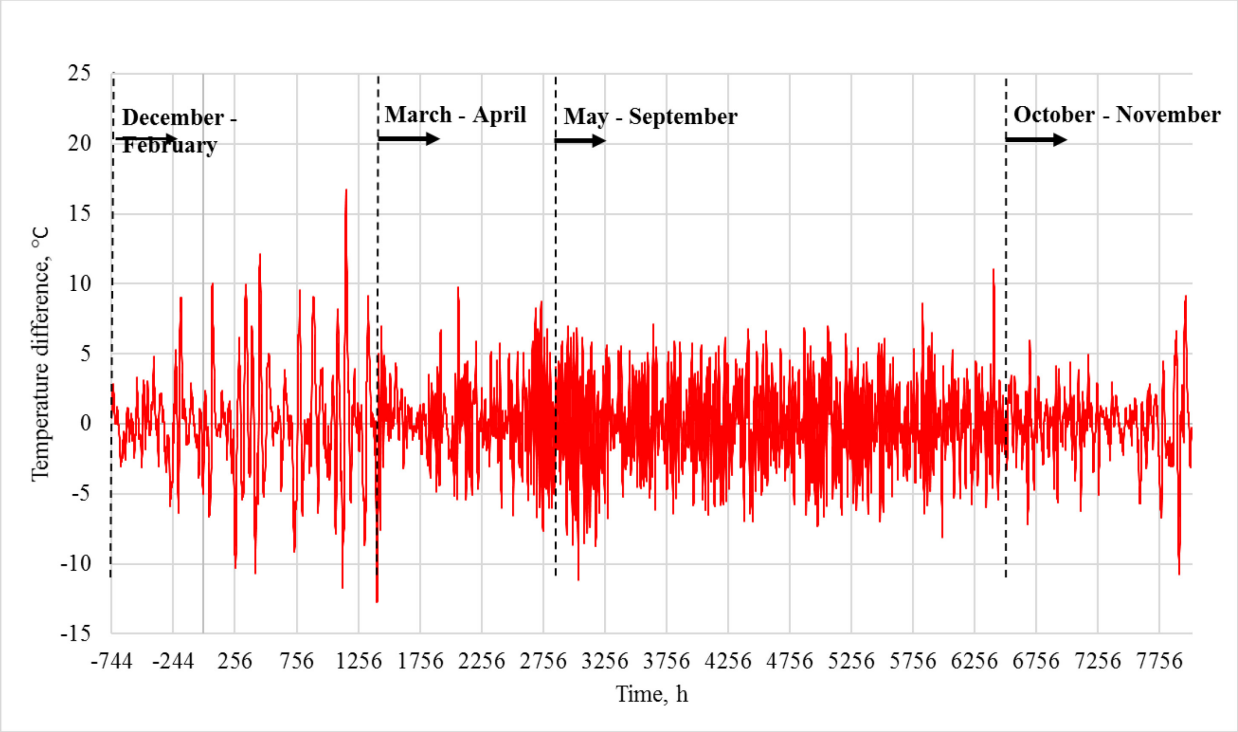

Figure 18. Difference between 24 hour moving average outdoor temperature and maximum peak temperature.

4.1.2 Thermal mass and heating flexibility

Heat can be stored in buildings either actively through water tanks or passively into the structures. The heat storing capacity of a building can be examined by the heat capacity or time constant of a building. The heat capacity describes the amount of energy needed to change the temperature of a structure. Hence, in a light-weight building the temperature will drop faster than in a massive-weight structure if the insulation level is kept the same. A massive-weight building is an advantage, since the room temperature is not fluctuating too much during the heating or cooling season. A negative factor is the slow controllability of a heavy-weight building since it reacts slowly to changes of the heating or cooling system (Jokinen, 2013).

The time constant describes how long it takes for the indoor temperature to drop 36.8 % of the maximum possible temperature drop after the heating has been shut-down. The time constant for a room or a building and the actual cool down time to a certain temperature are calculated according to equation (1) and (2) (Seppänen, 1995).

$$\tau = \frac{C_t}{G_t} \tag{1}$$

$$t = -\tau \ln \frac{T - T_{out}}{T_0 - T_{out}} \tag{2}$$

Where τ is the time constant [s], C_t is the total heat capacity of indoor air and structures [J/K], G_t is the total conductance of the room [W/K], t is the cooling time [s], T is the final temperature [°C], T_{out} is the outdoor temperature [°C] and T_0 is the initial room temperature [°C].

The thermal mass of a building is important when wanting to modulate the heating use of a building. Modulation refers to either increasing heat usage (loading) when the heat is cheap or decreasing heat use (conservation) when it is expensive. When a DH-heated building is modulating, it is responding to the signals given by the energy producer (Dréau & Heiselberg, 2016).

The heating-flexibility of a building, in other words how well a building is able to respond to the will of the energy producer, is linked to its thermal mass. A massive well insulated building manages without heating, maintain thermal comfort for a longer time period than a light-weight less insulated building. Hence, thermal mass increases flexibility and the ability to maximize heating usage during low-price periods and thereby high thermal mass buildings are better suited for DR.

Figure 19 show the difference in cooling time for a massive well insulated building and a normal light-weight building.

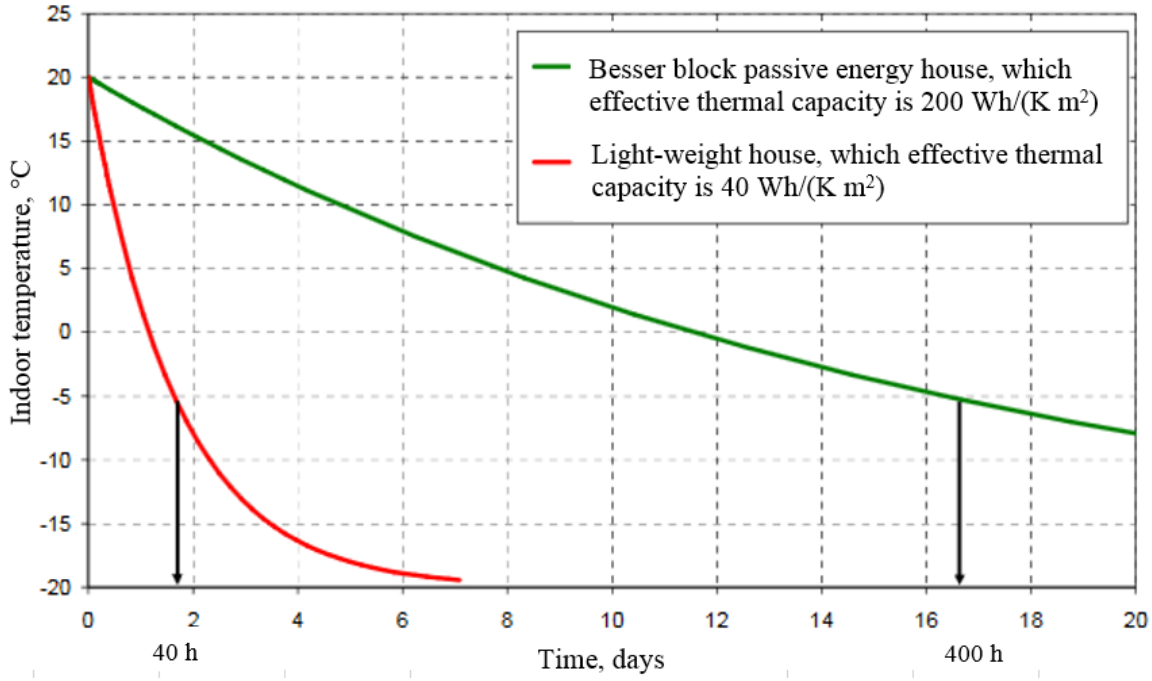

Figure 19. Indoor air cooling time depending on building type (Saari & Laine, 2009).

The index flexibility factor indicates the successfulness of the building's ability to modulate according to the dynamic price signals of the energy producer. Hence if the building is able to use heat only during low price periods, when the demand in the DH grid is low, the buildings have a high flexibility factor (Dréau & Heiselberg, 2016).

The flexibility factor is the ratio of the difference between heating energy bought at low and high price times and the sum of these energy amounts. The hourly low and high price limits were defined by analyzing the historical prices of the two recent weeks, according to the following:

Low price < 1st quartile of 2-week historical prices

High price > 3rd quartile of 2-week historical prices

The time period of defining the price quartiles should match the time period used by the control algorithm. In other words, if the heating system is controlled by an algorithm dealing with e.g. 24 hours future price information, the 1st and 3rd quartiles should be defined based on the same time interval.

The flexibility factor was calculated according to equation (3).

$$Flexibility\ factor = \frac{\int_{low\ price\ time} q_{heating} \cdot dt - \int_{high\ price\ time} q_{heating} \cdot dt}{\int_{low\ price\ time} q_{heating} \cdot dt + \int_{high\ price\ time} q_{heating} \cdot dt} \quad (3)$$

Where $q_{heating}$ is the heating power [W] and t is the time [s].

Additionally, during medium price periods (between 1st and 3rd quartile) the building would use heat according to its need.

Dréau and Heiselberg (2016) calculated the flexibility factors from heating modulation simulations of a typical Danish house built in the 80's and a state of the art passive house. The simulations were done for both radiators and under floor heating (UFH). The calculated flexibility factors considered distributed space heating energy and were in the range of 38 % – 97 % (Table 2). As can be seen from the results, a building with high thermal mass was achieving higher flexibility factors. However, also the heating distribution system played a role. The impact on temperature, thermal comfort and energy use depending on heating distribution system has also been studied by Hasan et al. (2009). UFH systems utilize thermal mass of the floor structure more efficiently than a radiator system and will therefore emit heat for a longer time period after shut-down.

Table 2. Flexibility factor results of old and new buildings with radiator and under floor heating systems (Dréau & Heiselberg, 2016).

		CONSERVATION			**LOADING + CONSERVATION**		
		Duration			Duration		
		4 hours	12 hours	24 hours	4 hours	6 hours	1 + 24 hours
80'S HOUSE	Radiator	38 %	-	-	63 %	69 %	-
	UFH	51 %	-	-	73 %	80 %	-
PASSIVE HOUSE	Radiator	-	69 %	92 %	-	-	95 %
	UFH	-	81 %	96 %	-	-	97 %

Thermal mass affects the outcome of the flexibility factor but additionally, climatic conditions are also having impact, which makes it difficult to use as a comparison in between buildings at different locations.

Dréau and Heiselberg (2016) did use two weeks of historical price data to determine the low and high price limits (LP and HP-limit), but if this time period is shrunk to one week or one day, the value of flexibility factor will be different. There seem to be room for discussion regarding the length of this period, but by choosing a shorter period like one day, the flexibility factor describes

how well the building can cooperate with the thermal grid on a daily level instead of on a two-week level. Since price peaks over two weeks are more likely to have greater variations, the quartiles defining high and low price would be located further apart than for a case where 24 hours is used as a base. A shorter time period results in that the conservation and loading takes place more often. Hence, the building would more rapidly adapt according to daily fluctuations in the grid. In a two-week scenario, the hourly heat price is likely to often be classified as a medium price type which results in the building uses heat according to need without modulation.

Figure 20 presents two types of LP and HP-limits, depending on analyzing two weeks or one day of historical price data. The data input for calculation of the first 48 hours are based on the last 48 hours of the same year. The LP-limit is seldom passed when based on two weeks of data, but the HP-limit is exceeded more often. The dynamic prices are presented in chapter 5.1.5.

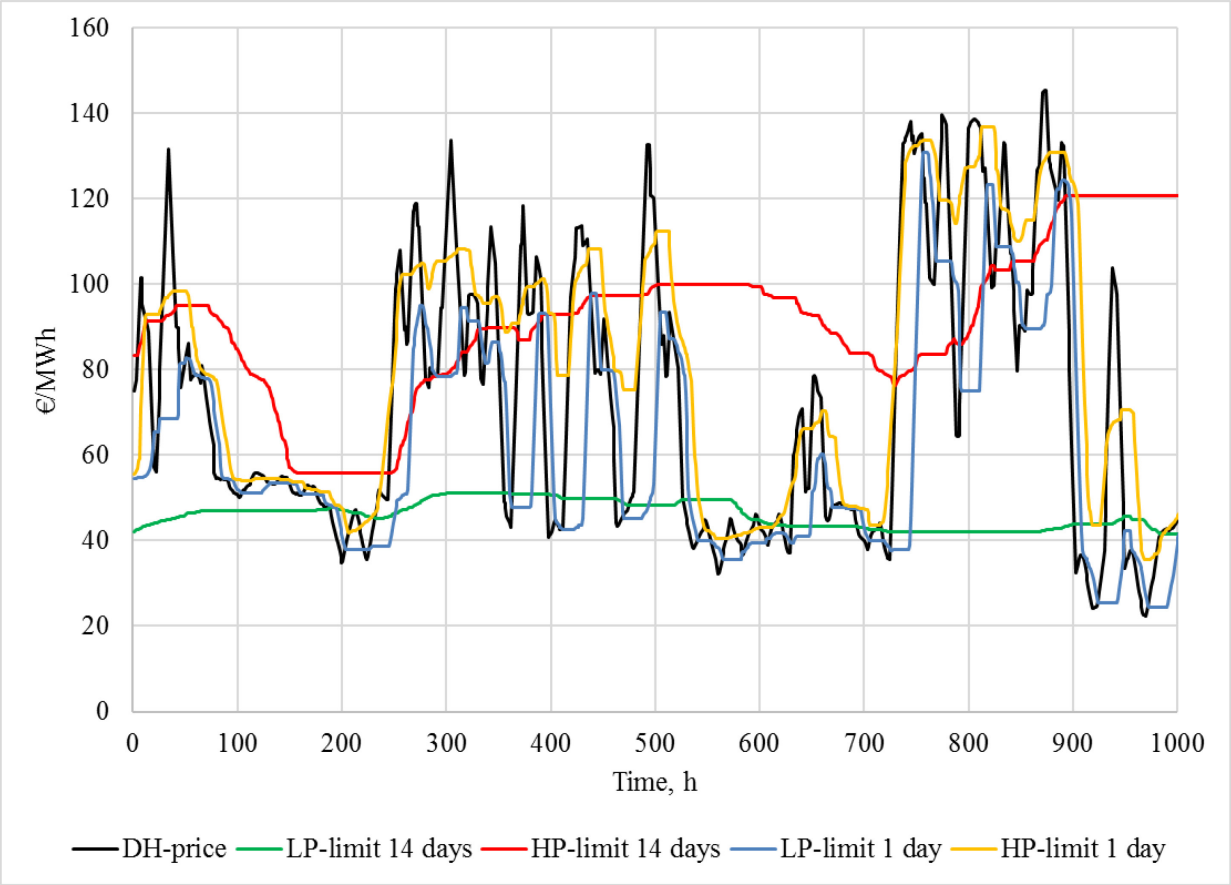

Figure 20. Low and high price limits respective to time period of determination.

If all consumers in a district heating network would be using DR, the limit price ranges would not differ much from each other regardless of time period. The reason is that during widely adopted DR, the load curve can be assumed to be stable, which results in a stable district heating price due to no or low need of peak power heat boilers. Based on this thought it is proposed that when a DH-distributor is offering DR-programs, the limit price ranges for the initial customers should be determined on a daily basis (historical or future). This would enhance the flexibility factor for the consumers which could then be rewarded by an additional incentive payment at the end of the year from the distributor. When more consumers join the DR program with the same conditions, the DH network load curve will start to stabilize. As a result, the price limits will be moving quite

close to each other and the flexibility factor would decrease resulting in decreasing incentive payments at the end of the year. For the distributor, this would pay off as stable network load curve and enhanced efficiency of the power plants. For the consumer, the overall DH-price would stay on an overall lower level without huge fluctuations, resulting in less need to modulate heat load, which in turn gives a more stable indoor thermal comfort.

The situation might change if and when, renewable energy sources are introduced also to the thermal grid, as predicted by Lund et al. (2014). Such a scenario would probably cause more down peaks making heat loading attractive. This is however only speculations about a possible future scenario. One thing though seems clear and that is: buildings using DR should be rewarded by an additional incentive payment from the distributor, which correlates to the magnitude of their yearly flexibility factor, which should be calculated on a daily level.

4.2 Ventilation

4.2.1 Supply air temperature

During cooling season in ventilation cooled zones, the supply air temperature has to be low enough to cool down the room to its set-point temperature. In a fully mixed ventilation system, the air temperature can be 14 – 18°C. With displacement ventilation, the supply air temperature should be higher (around 18°C). In a constant-air-volume (CAV) system the supply air temperature may be determined by the room with the highest cooling demand which may result in overcooling in other rooms and there is a need for re-heating coils in the branch ducts. In Variable-air-volume (VAV) systems, the supply air temperature is generally kept constant, since the cooling control is applied through airflow adjustment. However, supply air temperature compensation according to exhaust or outdoor air temperature may be applied. The extract air temperature is a good indicator of the average room air temperature and if this gets warmer than a set value, the supply air temperature can be decreased to provide cooling to the room (Swegon, 2014). According to Engdahl and Johansson (2004) the control strategy is related to optimization of total energy use of the ventilation and cooling system. The optimized supply air temperature depends on internal heat load, specific fan power, chiller COP and outdoor air enthalpy.

During DR-control of both space heating and ventilation, there may be situations when ventilation is cooling and heating system is heating at the same time. To avoid this conflict control, the supply air temperature could be adjusted based on space heating control. Table 3 presents the envelope and ventilation heat losses and fractions of total heat loss for a typical office room with a supply airflow of 60 l/s (close to 2 l/(s m^2). As can be seen, the cooling impact of the ventilation is increasing rapidly with increasing indoor air temperature.

Table 3. Distribution of heat losses in a room depending on outdoor and indoor temperature with supply airflow 60 l/s.

T_{out} [°C]			**-10**		**-5**		**0**	
T_{in} [°C]	T_{supply} [°C]	$Q_{ventilation}$ [W]	$Q_{Envelope}$ [W]	$Q_{ventilation}$ share	$Q_{Envelope}$ [W]	$Q_{ventilation}$ share	$Q_{Envelope}$ [W]	$Q_{ventilation}$ share
20	20	0.0	653	0 %	544	0 %	435	0 %
21	20	72.4	675	10 %	566	11 %	457	14 %
23	20	217.1	719	23 %	610	26 %	501	30 %
24.5	20	325.6	751	30 %	642	34 %	533	38 %

Likewise, in a situation where the indoor temperature set-point is reduced, the supply air temperature should also be reduced. However, the importance is not of the same magnitude here since if the supply air is providing some heat to the room, the space heating can be turned off even longer.

4.2.2 Airflow control through CO_2 set-point adjustment

In a VAV system the airflow is adjusted according to need. The combined indicators of need are usually occupancy sensors, indoor air temperature and CO_2 concentration of the indoor air. If one of these crosses a set-point level, the airflow is either increased or decreased according to situation (California energy commission, 2003).

The VAV system can itself be either working on a zonal or room specific level. In a zonal system the airflow is adjusted according to the need of the worst room or based on average conditions. In a room specific system, the airflow can be independently regulated according to the need of every individual. Airflows in commercial and office buildings are quite high and therefore VAV systems are recommendable to avoid excess energy usage in the AHU during unoccupied periods. Nowadays, the Finnish building code D2 (2012) specifies that VAV should be used in rooms with variation in occupancy or pollution.

In a VAV system, DR-control of airflow can be utilized by allowing a higher CO_2 concentration during high price periods of either electricity or heat. This would result in energy and monetary savings regarding both electricity and heat or cooling. When this scheme is used, air quality should always fulfill the minimum demand that health based ventilation demand set.

According to the affinity laws the power and airflow are connected through a cubic ratio and there is high electricity savings potential with decreasing airflow. When VAV systems are designed with a constant static pressure in the duct, the actual power reduction will be less than calculated by ideal affinity laws. However, the difference is decreasing with decreasing static pressure set-point, which implies that the pressure sensor should be situated in the most difficult duct branch and not near the fan.

The ideal affinity laws and the modified affinity laws which account for a static pressure set-point are presented in equations 4 – 5 and 6 – 8 respectively (Vaillencourt, 2005).

$$\left(\frac{N_1}{N_2}\right)^2 = \left(\frac{Q_1}{Q_2}\right)^2 = \frac{\Delta p_1}{\Delta p_2} \tag{4}$$

$$\left(\frac{N_1}{N_2}\right)^3 = \left(\frac{Q_1}{Q_2}\right)^3 = \frac{P_1}{P_2} \tag{5}$$

$$\frac{N_2}{N_1} = \frac{Q_2}{Q_1} = \left(1 - \sqrt{\frac{\Delta p_{min}}{\Delta p_{design}}}\right) \cdot \left(\frac{Q_2}{Q_1}\right) + \sqrt{\frac{\Delta p_{min}}{\Delta p_{design}}} \tag{6}$$

$$\frac{\Delta p_2}{\Delta p_1} = \left[\left(1 - \sqrt{\frac{\Delta p\ min}{\Delta p_{design}}}\right) \cdot \left(\frac{Q_2}{Q_1}\right) + \sqrt{\frac{\Delta p\ min}{\Delta p_{design}}}\right]^2 \quad (7)$$

$$\frac{P_2}{P_1} = \left[\left(1 - \sqrt{\frac{\Delta p\ min}{\Delta p_{design}}}\right) \cdot \left(\frac{Q_2}{Q_1}\right) + \sqrt{\frac{\Delta p\ min}{\Delta p_{design}}}\right]^3 \quad (8)$$

Where N is the shaft-speed of the fan [rpm], Q is the volumetric airflow rate [m^3/s], Δp is the total pressure rise of the fan [Pa], P is the fan power [W] Δp_{min} is the static pressure set-point [Pa] and Δp_{design} is the total pressure rise of the fan at nominal flow [Pa].

Table 4 presents how the reduction of airflow affects the needed electrical power for two type of system designs where p_s is the static pressure set-point and $P_{relative}$ is the relative fan power. The system without static pressure set-point could be a CAV system and the system with static pressure set-point could be a VAV system. Figure 21 shows a flow-power plot of the two system designs.

Table 4. Effect of flow reduction on fan power demand.

	Without minimum p_s requirement			**With minimum p_s = 180 Pa**		
Q [m^3/s]	Δp [Pa]	P [W]	$P_{relative}$ %	Δp [Pa]	P [W]	$P_{relative}$ %
1000	700	700	100 %	700	700	100 %
800	448	358	51 %	569	513	73 %
600	252	151	22 %	451	362	52 %

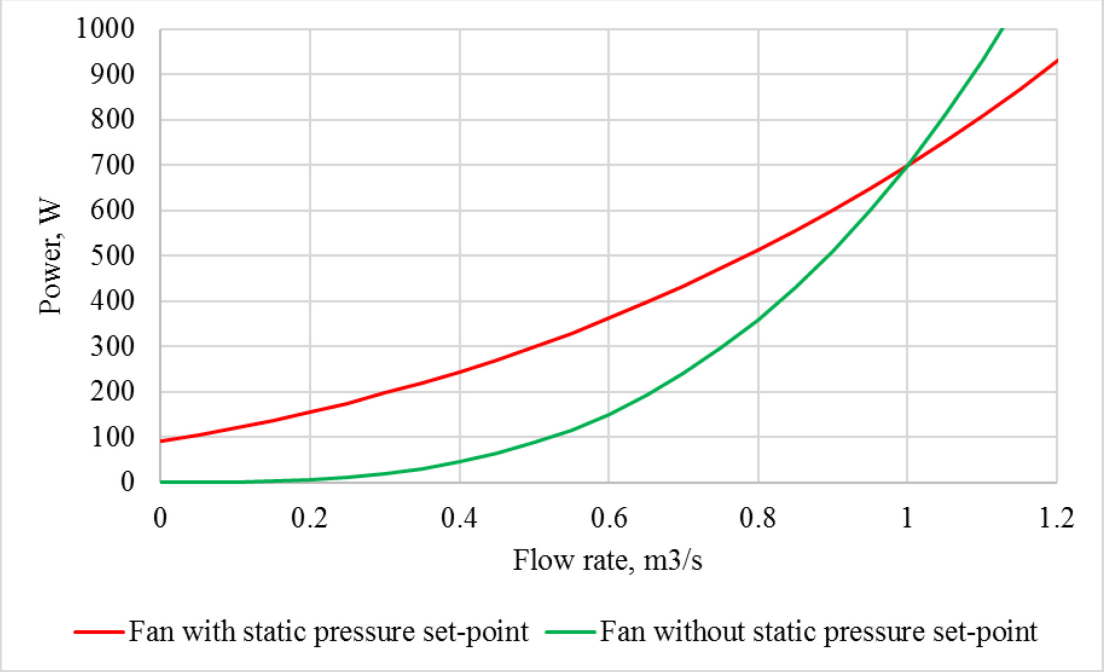

Figure 21. Fan power as a function of airflow rate depending on static pressure set-point.

5 Demand response simulations in an educational office building

The topic and its potential were approached by investigating both decentralized and centralized DR. Cost saving potential was believed to be higher for the decentralized approach since level of control is higher.

The research was conducted by building model simulations based on an educational office building on the Aalto University campus in Otaniemi, Espoo. Both the centralized and decentralized approaches were applied to a single building floor with a floor area of 580 m^2.

The DR control of room temperature was realized by adjustment of mass flow rate to water radiators (equipped with electronic control valves) or inlet water temperature and supply air temperature. Additionally, the room specific airflow was controlled in some cases. Night time set-back modes for both SH, heating of supply air and demand based ventilation were included in the simulations to study the energy savings potential and the effect on thermal conditions.

The DR control was executed by different rule based control algorithms. The control algorithms decision-making was based on the incoming control signal from the dynamic price information, the outdoor air temperature, the indoor air temperature and the CO_2 concentration in the room air. The control signal was defined according to two different approaches and will be further presented in chapter 5.3.1. The dynamic price data was obtained from Rinne (2017) and is presented in chapter 5.1.5.

5.1 Methodology

5.1.1 Temperature ranges

The temperature range was decided based on the newest classification of indoor environment by The Finnish society of indoor air quality (FiSIAQ, 2017). Heating DR has most potential during spring and autumn and therefore the outdoor temperature range of 0 – 7.5 °C and its corresponding indoor operative temperature was considered when choosing the temperature range for the cases (Figure 22). The Finnish indoor environment classification defines the indoor operative temperature set-point based on the 24-hour moving average temperature instead of the actual outdoor temperature. The reason is here as well the great variations during spring and autumn, which would complicate the governing of the indoor environment.

The indoor temperature was allowed to vary within the range 20 – 24.5 °C. Additionally, the chosen temperature ranges are fulfilling the design recommendations for operative temperature within offices, given in the indoor environmental standard SFS-EN 15251 (2007), class II (20 – 26 °C).

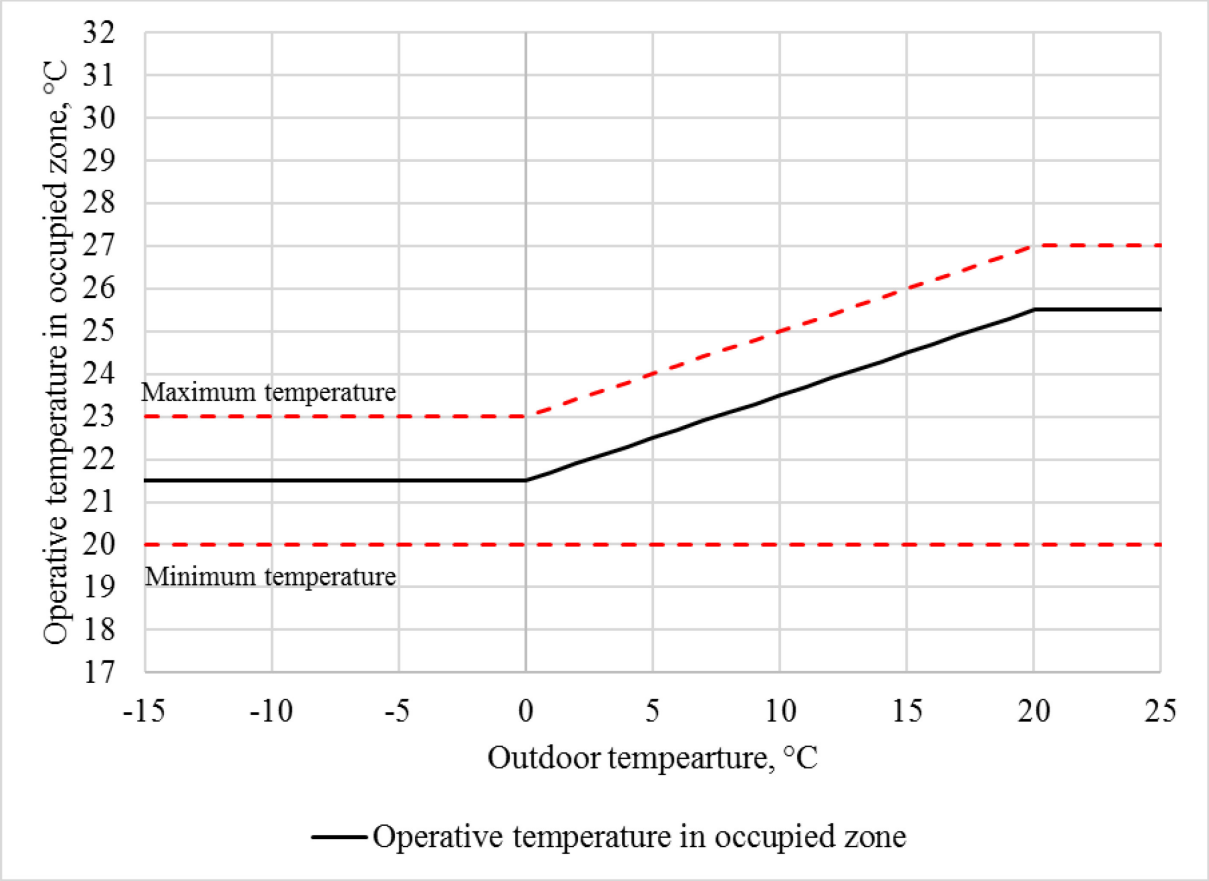

Figure 22. Indoor environment classification S2.

As an addition can be mentioned that The Finnish building code D2 (2012) does not include a binding directive regarding the relative time interval the design indoor temperature should be fulfilled per year. However voluntary indoor environment classification S2 defines, that the set operative temperature should be fulfilled for at least 90 % of the year.

For the supply air temperature of ventilation there are no laws or regulations available and it is up to the system designer to choose a supply air temperature suiting the specific system. Kärkkäinen et al. (2003) suggest that adjustments done to supply air temperature should be small (1 – 2 °C) since even small changes are easily sensed by the occupants. For this study the minimum, normal and maximum supply air temperature set-points were chosen to be 17, 20 and 22°C respectively.

5.1.2 Thermal comfort

When evaluating the thermal comfort of the indoor environment, Fanger's predicted mean vote (PMV) and predicted percentage of dissatisfied (PPD) values are often used. The models are based on heat-balance equations of humans and empirical studies. The PMV model has 6 input parameters: room air temperature, mean radiant temperature, room air velocity, relative humidity, metabolic rate and clothing insulation. The result of PMV calculation is a number ranging from -3 (cold) to 3 (hot), where zero represents thermal neutrality and it is considered the optimal value. The PPD value is proportional to the PMV value (Figure 23) (Fanger, 1970).

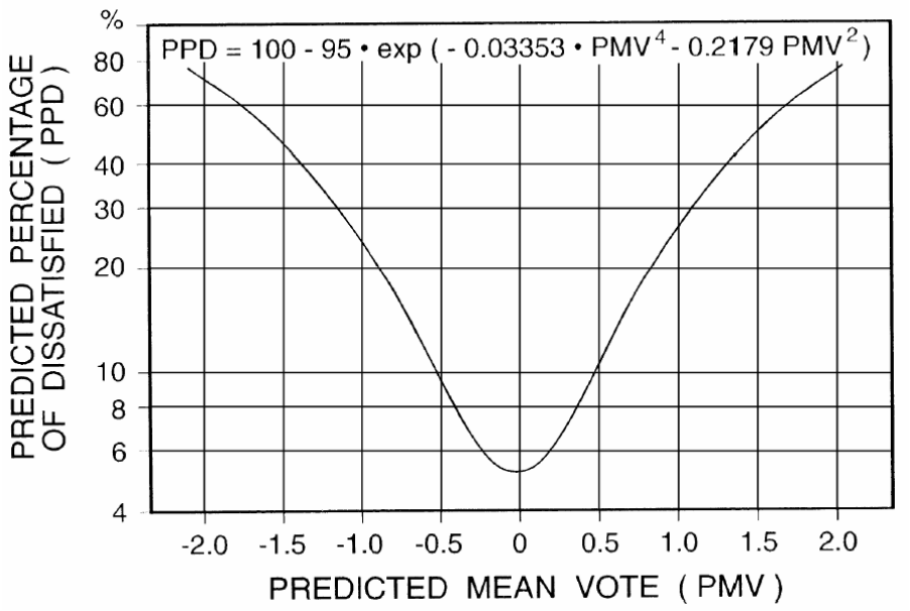

Figure 23. Predicted mean vote and predicted percentage of dissatisfied.

According to the ASHRAE standard 55-2013 (2013) the PMV value should be within the range of -0.5 to 0.5, which correlates to a PPD value of about 12%. The same standard states that the PPD cannot be higher than 20 % for the building to meet the requirements of indoor thermal comfort and this is the limit value chosen for this study. Since the PPD value don't specify whether the indoor conditions were sensed hot or cold it is recommendable to also consider the PMV value.

5.1.3 Building occupancy, indoor air CO_2-concentration and airflow rate

Occupancy

According to studies, there is huge variation of the occupancy ratio within office buildings. Manicca et al. (1999) reported an average occupancy rate of 46 % and Page et al. (2008) reported a typical range of 35 – 40 %. However, Baumann & McClintock (1993) reported occupancy rates of 75 – 30 %.

In this study two different schemes were chosen: 40 % and 70 % occupancy. These schemes can be thought to represent two different types of offices: the low occupancy rate is likely to represent a consult or sales office where the workers often are away in meetings while the latter one is thought to represent an office of administration where workers often are present for the whole day.

CO_2 concentration

An indoor air CO_2 concentration of > 20 000 PPM cause deepened breathing, 100 000 PPM can cause unconsciousness and 250 000 PPM can cause death (Satish, et al., 2012). The Finnish society of indoor air quality (FiSIAQ, 2008) defines three indoor climate categories: S1 (individual indoor climate), S2 (good indoor climate) and S3 (satisfying indoor climate) with the corresponding CO2-concentrations of < 750, < 900 and < 1200 PPM respectively. The CO_2-concentration of category S3 is according to the limit value allowed by Finnish building code D2 (2012).

Higher CO_2-concentrations in indoor air has been related to lower human performance in sense of reaction time and neurologic symptoms (Mendell & Heath, 2005). This is confirmed by Satish et al. (2012) which expose humans in an office like chamber to CO_2-concentrations of 600, 1000 and 2500 PPM and have them to do computer based decision-making tests and fill in questionnaires regarding perceived air quality and health symptoms. Additionally, Seppänen et al. (1999) report many studies are supporting the reduction of sick building symptoms with reducing CO_2-concentration below 800 PPM. It is important to note that CO_2 concentrations due to normal human activity in a room is not a contaminant itself, but instead it is an indicator of the amount of human generated bioeffluents in the air. This makes the CO_2 concentration a suitable parameter of use in ventilation flow control during occupied times (Xu, et al., 2009).

A sedentary office worker has a metabolic heat rate of 55 – 70 W/(m^2 skin area) and an average male person has a skin area of 1.8 m^2. These values were chosen for this study and sums up to a metabolic heat production of 126 W per person, which is equal to 1.2 MET (1 MET = 58.15 W/m^2 skin area) (ISO 8996:2004, 2004). The CO_2 concentration in a room at steady-state can be calculated according to equation 3 – 6 (Alanne, 2016), (ISO 8996:2004, 2004).

$$C_{CO_2} = q_v \cdot C_{sup} + \frac{q_{CO_2} \cdot persons}{q_v} \tag{9}$$

$$q_{CO_2} = (RQ)q_{O_2} = \frac{M}{e} \tag{10}$$

$$q_{O_2} = \frac{M}{(RQ)e} \tag{11}$$

$$e(T) = e_0 \frac{T_0}{T} \tag{12}$$

Where C_{CO2} is the CO_2 concentration in room air [PPM], C_{sup} is the CO_2 concentration in supply air [PPM], q_v is the supply air rate [l/s], q_{CO2} is the CO_2 emission per person [l/(h person)], q_{O2} is the oxygen consumption per person [l/(h person)], (RQ) is the unitless ratio of CO_2 emission and oxygen consumption (e.g. 0.83 at rest and 1.0 at heavy work), M is the metabolic heat production [W/person], e is the energy equivalen (ratio of metabolic energy consumption and oxygen consumption) [Wh/l], e_0 is the energy equivalent at reference temperature T_0 (5.8 Wh/l), T_0 is the reference temperature (273 K) and T is the actual temperature [K].

In this study CO_2 set-points of 800 and 1200 PPM were chosen. The lower set-point is used outside of DR-control and the higher set-point is used during DR-control. The lower set-point is based on the calculated average CO_2 concentration in the studied building during design conditions (see chapter 5.4, Table 18).

5.1.4 Night time set-back mode

Cost saving may be achieved by decreasing the room air temperature during night time when the building is unoccupied. This is not a form of demand response, but it is an easy way to save heating energy and costs. However, the recovery of the minimum indoor temperature has to be achieved before the occupants arrive in the morning. The colder it is outdoors, the longer time or more heating power will be demanded for the recovery.

During dimensioning heat load conditions, the building uses in theory 100% of its available heat power. This means that outside of dimensioning heat load conditions, the building would have additional heat power to use for recovery of the indoor temperature. However, the heat output of

radiators is normally controlled by adjusting the inlet water temperature according to outdoor temperature. Therefore, it is not by normal means possible to achieve 100 % heating power during outdoor air temperatures below the design conditions. Figure 24 presents the inlet water temperature as a function of outdoor air temperature and the corresponding relative heat output of a radiator. The relative heat output is calculated according to Stephan's method (Stephan, 1986).

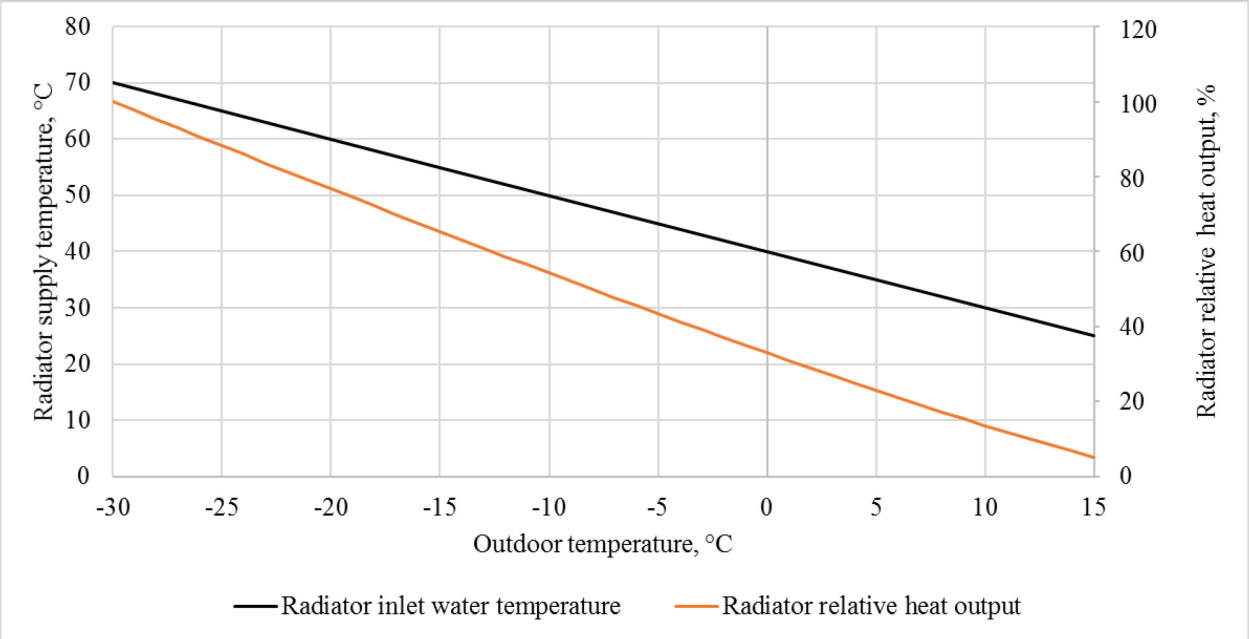

Figure 24. Water radiator inlet temperature and relative heating power as a function of outdoor air temperature.

In this study three night time set-back simulations were done at constant outdoor temperature of -26, -20 and -15 °C to determine the time period of temperature recovery from night time set-back (18°C) to normal indoor air temperature (21°C). Even in the coldest case (-26 °C), the indoor air temperature was almost totally recovered in half an hour. The fast recovery can be explained by a relatively high airflow rate (about 2 l/(s m^2) and a supply air temperature of 20°C. Figure 25 presents the results from the simulation where the black dashed line is the space heating set-point and the other curves represent the temperature behavior of the rooms in the 4^{th} floor of the building.

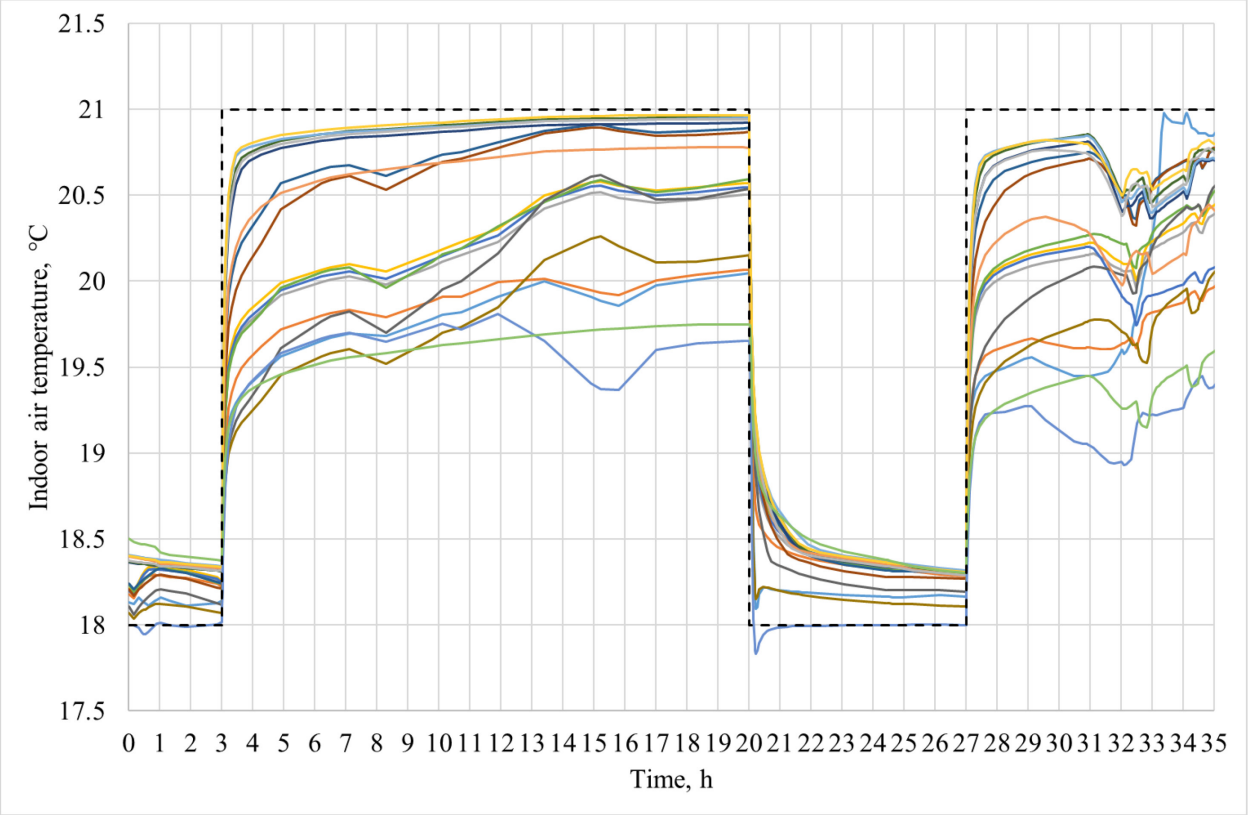

Figure 25. Indoor air temperature recovery time after night time set-back during a constant outdoor temperature of -26°C.

During night time set-back mode, it is also possible to decrease the supply air temperature of ventilation and additionally decrease the ventilation airflow to a minimum level equaling 0.15 l/(s m^2) (National Building Code of Finland D2, 2012). The chosen set-points during night time set-back and unoccupied periods for this study is presented in Table 5.

Table 5. Set-points during night time set-back and unoccupied time periods.

NIGHT TIME SET-BACK (8PM-6AM)		
Parameter	Value / description	Comment
Indoor air temperature	18°C	
Ventilation supply air temperature	18°C	
UNOCCUPIED TIME PERIODS (16PM-8AM)		
Ventilation airflow	0.15 l/(s m^2)	For VAV cases
OCCUPIED TIME PERIODS (8AM-16PM)		
Indoor air temperature	21°C or 20-24.5°C	Depending on simulation case
Ventilation supply air temperature	17°C, 20°C, 22°C or according to compensation curve (Figure 29)	Depending on simulation case
CO_2 concentration	800 - 1200 PPM	Depending on simulation case

5.1.5 Dynamic price data

The generation of dynamic price data was done by Rinne (2017) and is based on the weather data from the Finnish test reference year 2012 (Finnish Meteorological institute, 2012). The dynamic tariffs are in the form of hourly prices for district heating and electricity. The DH price is representative for a typical DH producer in Finland and contains both energy and transfer costs. The wholesale electricity price is taken from Nordpool and electricity tax and a dynamic transfer cost is added to it. Additionally, the value-added tax (VAT) 24% is added to form the final prices.

Figure 26 presents the hourly district heat price. The prices are quite stable during April to middle of November with an average value of 40.5 €/MWh and a standard deviation of 7.7 €/MWh. From end of November to end of March the corresponding values are 68 and 29.7 €/MWh.

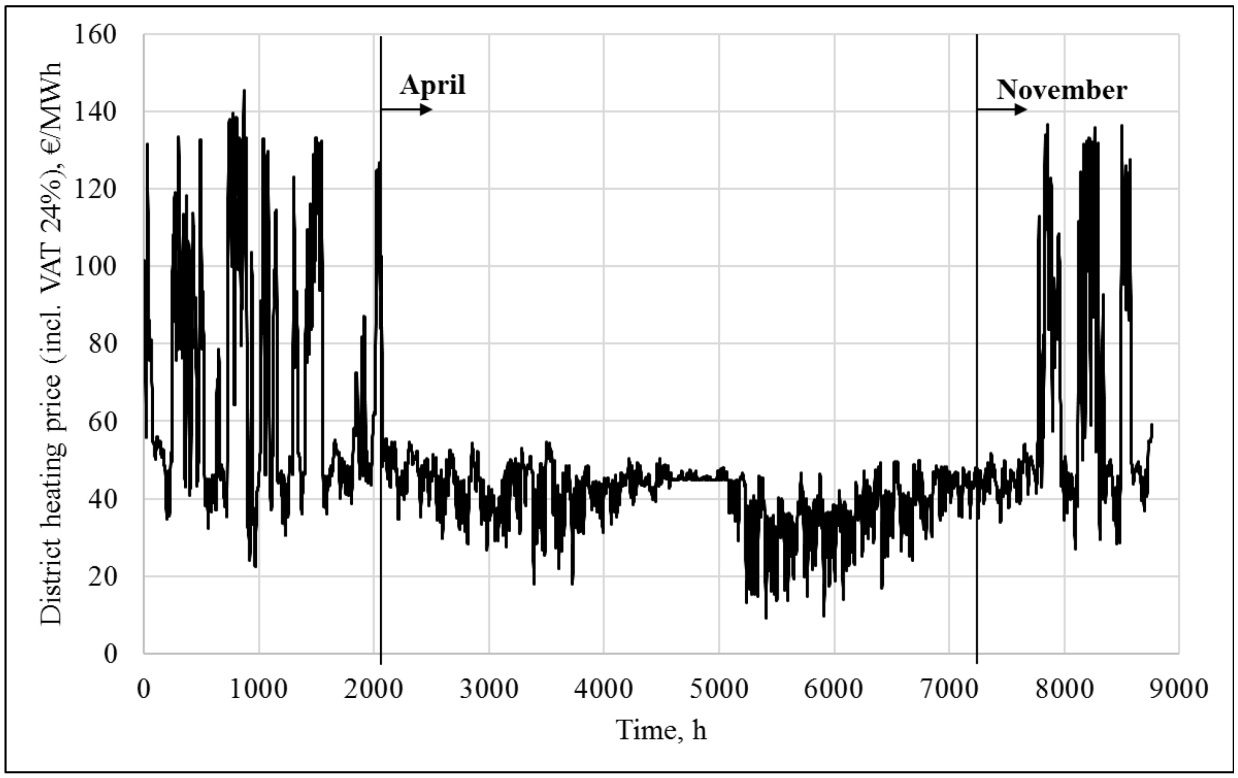

Figure 26. Hourly spot price for district heating 2012 (including VAT 24%).

Figure 27 presents the hourly electricity price. The price is more stable than the district heating price, but most of the high peak prices are still taking place during winter months. During April to the middle of November the average price is 118.1 €/MWh, with a standard deviation of 36.9 €/MWh. Between the end of November to the end of March the corresponding values are 152 and 54.3 €/MWh.

The price fluctuations are according to expectation, since energy consumption is normally higher during colder periods of the year.

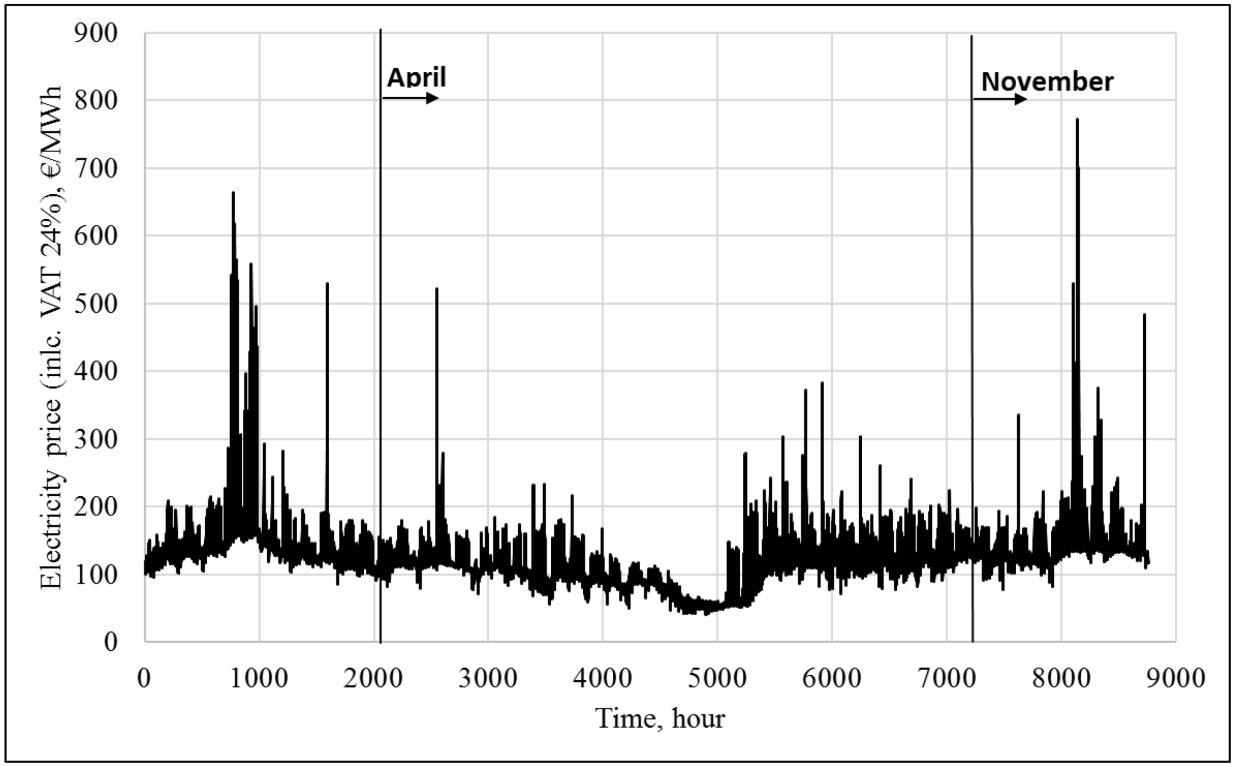

Figure 27. Hourly spot prices for electricity 2012 (including VAT 24%).

5.1.6 Flexibility factor

The flexibility factor was presented in chapter 4.1.2 and was used in this study to indicate how well the building could interact with the dynamic price signals from the energy producer. It was calculated for space heating, air handling unit and total delivered district heating. During the heating season the air handling unit will often demand heating even when the supply air temperature is reduced. Hence it is reasonable to assume a lower flexibility factor based on the total delivered DH energy than solely based on delivered space heating energy.

As mentioned in chapter 4.1.2, price classification regarding the flexibility factor is based upon the same time period and price information as the DR-control algorithm uses for decision-making. In this study the time period included either 2 weeks of historical hourly prices or 24 future hourly prices depending on control signal definition (algorithms and control signal definitions are explained in detail in chapter 5.3).

The flexibility factor was additionally calculated for electricity in the simulations regarding DR control of ventilation airflow rate.

5.1.7 Simulation software

The simulations done in this study were conducted by the IDA Indoor Climate and Energy 4.7.1 (IDA-ICE) building simulation software. The dynamic multi-zone simulation software IDA-ICE provides a simulation environment in which the characteristics of a building and its technical systems can be modelled and studied. IDA-ICE supports calculation of different heat and mass transfer processes within a building and enables the study of energy consumption, indoor air quality and thermal comfort. Additionally, it is possible to create own detailed models of different components and utilize self-built macros for the control of the technical systems in the building.

The software is detailed and utilizes variable time steps during simulations and it fulfils the European standard prEN 13791 (Kropf & Zweifel, 2001). IDA-ICE is a well-known software within building simulation and it has been validated many times in several studies (IEA, 1999), (Acherman & Zweifel, 2003), (EQUA Simulation Ab, 2010). Due to the fore-mentioned reasons the program was selected as simulation software in this study.

Since thermal comfort was one parameter of interest, the advanced zone option *"model fidelity"* was chosen to be *"climate"*. This takes temperature gradients into consideration during calculations and provides a higher accuracy to the end result. The outdoor air CO_2 concentration was set to 400 PPM and the time step for output data was set to 1 hour.

5.2 Description of the case study building

The educational and office building at Otakaari 4 was completed in 1966 (Aalto university, 2017), and has been renovated a couple of times over the years. The outer walls and the upper slab are of original construction, but the windows have been changed to more energy efficient ones.

Only the fourth floor of the building was modelled. The modelling was done according to design documents and estimated occupancy pattern. The heating power of the radiators in the room are modelled according to the design data, the same applies to the airflows. Regarding the physical building model only one thing will be altered, namely the ventilation design.

Figure 28 presents an overview of the 4th floor model and its room layout.

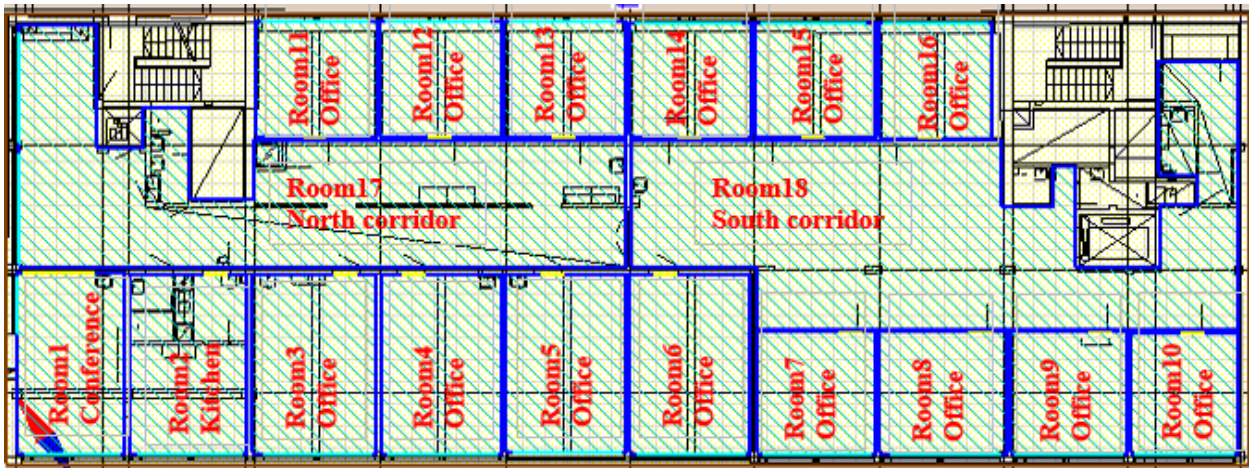

Figure 28. Layout of Otakaari 4, 4th floor building model.

5.2.1 Building structures

The original structure drawings were not available, but instead drawings from a nearby building built in the same time and style was used as input data for the envelope structures. The evaluation of the building infiltration air rate was done according to the study of Vinha et al. (2009), where they conclude an air leakage rate (n_{50}) of 0.7 at 50 Pa pressure difference is typical for high-rise apartment buildings built out of concrete by on-the-spot concrete casting, which is the case for Otakaari 4. However, since we cannot be sure of the magnitude of leakage air, a more conservative air leakage rate of 1.6 was used in the simulations, which is the average air leakage rate for high-rise apartment buildings built out of concrete-elements.

The essential thermal bridge losses were set according to recommendations in Finnish building code D5 (2012).

The general IDA-ICE input data and building model characteristics are summarized in Table 6, Table 7 and Table 8.

Table 6. General building model information.

Location	**Espoo, Finland (Helsinki, Finland used in IDA-ICE)**	
Climate	Helsinki-Vantaa reference year 2012	
Wind profile	Urban	
Heated net floor area	586	m^2
Volume	2102	m^3
Envelope area	947	m^2
Window/envelope	11.5 %	

Table 7. Building model U-values and distribution of conduction heat losses.

Building envelope	**Area**	**U-value**	**Conduction**	
	[m2]	[W/(m2 K)]	[W/K]	Fraction, %
Walls above ground	252	0.38	97	24
Roof	586	0.30	176	43
Windows	109	1.10	120	29
Thermal bridges			17	4
Total	947	0.43	409	100

Table 8. Structures and properties of Otakaari 4 building model.

Structure	Description	
External wall	Brick 130 mm Air gap 20 mm Heavy insulation 100 mm Concrete 160 mm Render 10 mm	
Roof	Gravel: 50 mm Mineral wool: 20 mm Polyamidic sheet: 0.2 mm Light-weight concrete: 30 mm Light-gravel: 235 mm Polyamidic sheet: 0.2 mm Concrete: 250 mm	
Internal wall	Concrete 160 - 260 mm	
Internal floor	Concrete 150 mm	
Windows, South-west (58.7 m^2)	Window type: MS2E (two-frame and three-glazing structure, opened inwards, argon filled, one solar protection glazing Glazing U-value: 1 W/m2 K g-value: 0.38 T-value: 0.32 Tvis: 0.65 Internal/external emissivity: 0.84 Fraction frame of the total window area: 10% Frame U-value: 2 W/m2 K	
Windows, North-west & North-east (15.5 & 34.8 m^2)	MS2E (two-frame and three-glazing structure, opened inwards, argon filled, one low-e glazing Glazing U-value: 1 W/m2 K g-value: 0.59 T-value: 0.5 Tvis: 0.75 Internal/external emissivity: 0.84 Fraction frame of the total window area: 10% Frame U-value: 2 W/m2 K	
THERMAL BRIDGES & INFILTRATION AIR		
Structure part	**Conductance** [W/(m K)]	**Comment**
External wall / external wall	0.06	Per meter joint
External window perimeter	0.04	Per meter joint
Roof / external wall	0.08	Per meter joint
Air leakage rate n_{50}	1.6	ACH, (Vinha, et al., 2009)

5.2.2 Heating and cooling systems

District heating is used for the buildings space heating and AHU heating coils. The zone and AHU cooling is handled by a liquid cooled chiller. The main characteristics of the heating and cooling system can be found in Table 9. The efficiency of the DH-substation was set to 97 %, which is considered a normal value for substations in bigger buildings (National building code of Finland, D5, 2012).

Table 9. Otakaari 4 heating and cooling systems.

	Description	**Comment**
Heating system	District heating	[1)]Heating power = 251 (SH) + 530 kW (AHU) Efficiency of sub-station = 97%
Type of heat distribution system	Hydronic radiator heating	
Inlet/outlet temperatures of heating distribution system	70/40°C	Dimensioning temperatures at T_{out} = -26°C
Room temperature set-point	21°C	
Cooling system	Liquid cooled chiller	[1)]Cooling power = 251 kW, SEER = 3.64 (Chiller Oy, 2017)
Inlet/outlet temperatures of cooling distribution system	9-14°C	Both AHU and zone cooling
1) The 4th floor share of available zone heating and AHU heating power in the DH-substation is calculated to be 17.4 kW and 40 kW respectively, based on square meter ratio *The 4th floor share of cooling power would be 19 kW*		

The radiator dimensions and heat powers (Table 10) were modelled according to heating design documents, where the nominal power is achieved at an inlet water, return water and indoor air temperature of 70°C, 40°C and 20°C respectively.

Domestic hot water consumption is neglected in this study.

Table 10. Main features of radiators in Otakaari 4 building model

Zone	$Q_{tot.}$ [W]	Radiator amount	Dimension [mm]
Room1 - Conference	1540	3	300x1400 / 300x1600 / 300x1600
Room2 -Kitchen	1140	2	300x1600
Room3 – Office	1140	2	300x1600
Room4 – Office	1140	2	300x1600
Room5 – Office	1140	2	300x1600
Room6 – Office	1140	2	300x1600
Room7 – Office	1140	2	300x1600
Room8 – Office	1140	2	300x1600
Room9 – Office	900	2	300x1600
Room10 – Office	1030	2	300x1200 / 300x1600
Room11 – Office	1150	2	300x1200 / 300x1600
Room12 – Office	1220	2	300x1600
Room13 – Office	1220	2	300x1600
Room14 – Office	980	2	300x1600
Room15 – Office	1180	2	300x1600
Room16 – Office	1180	2	300x1600
Room17 - North hallway/corridor	2920	4	600x1600
Room18 - South hallway/corridor	2110	3	600x1100 + 600x1600

Supply air and inlet water temperature curve modifications

During initial simulations with aim to examine the behavior of the building it was discovered that 75 % of the heating demand in zones was supplied by the ventilation. The building uses supply air temperature compensation according to measured exhaust air temperature. This means that during lower exhaust air temperatures, the supply air temperature is increased and vice versa. The temperature level and slope used in the curve were high and steep, which resulted in a constantly high supply air temperature, minimizing the radiator impact during heating season and minimizing the ventilation cooling during cooling season.

Annual heating demand covered only to a small share by radiator heating would most likely have had a negative impact on the final DR-simulation results, which are governed by space heating algorithms (see chapter 5.3). Due to the fore-mentioned reasons the original supply air temperature curve was modified according to more common industry standards.

After the supply air temperature modification, the share of annual heating obtained from ventilation was reduced to 50 %, giving more room for the radiators. Additionally, the ventilation cooling ability was utilized more wisely during the cooling season. However, after modifying the supply air temperature curve, the indoor air temperature could not be maintained at 21 °C during certain parts of the year. In order to correct this, the original inlet water temperature curve of the heating system was also modified.

The original and modified temperature curves regarding supply air and inlet water are shown in Figure 29 and Figure 30.

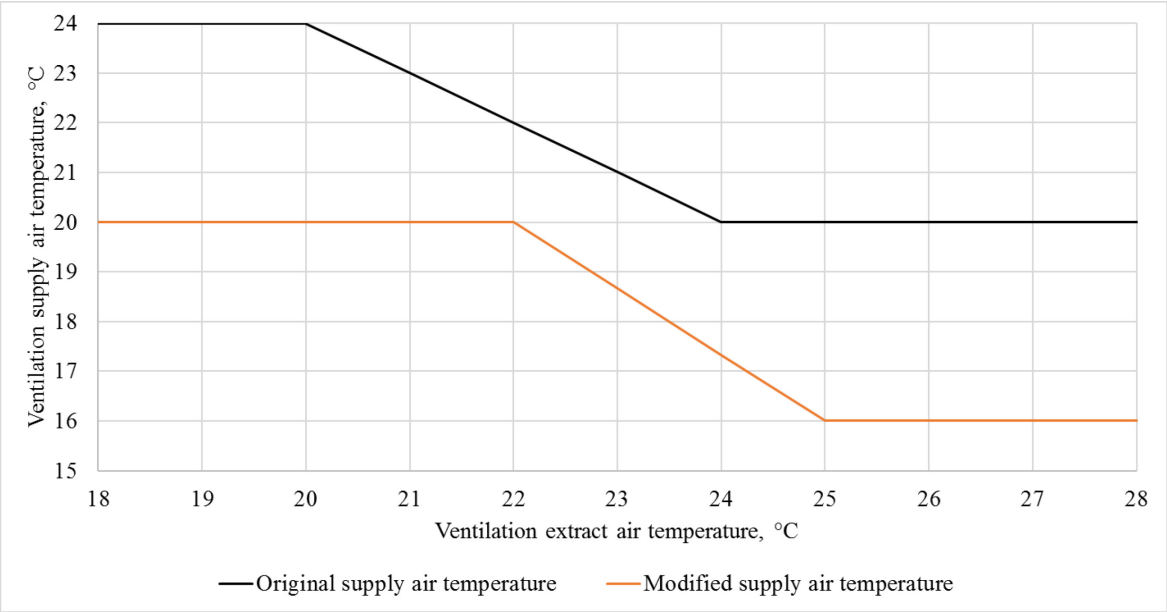

Figure 29. Otakaari 4 supply air temperature curves.

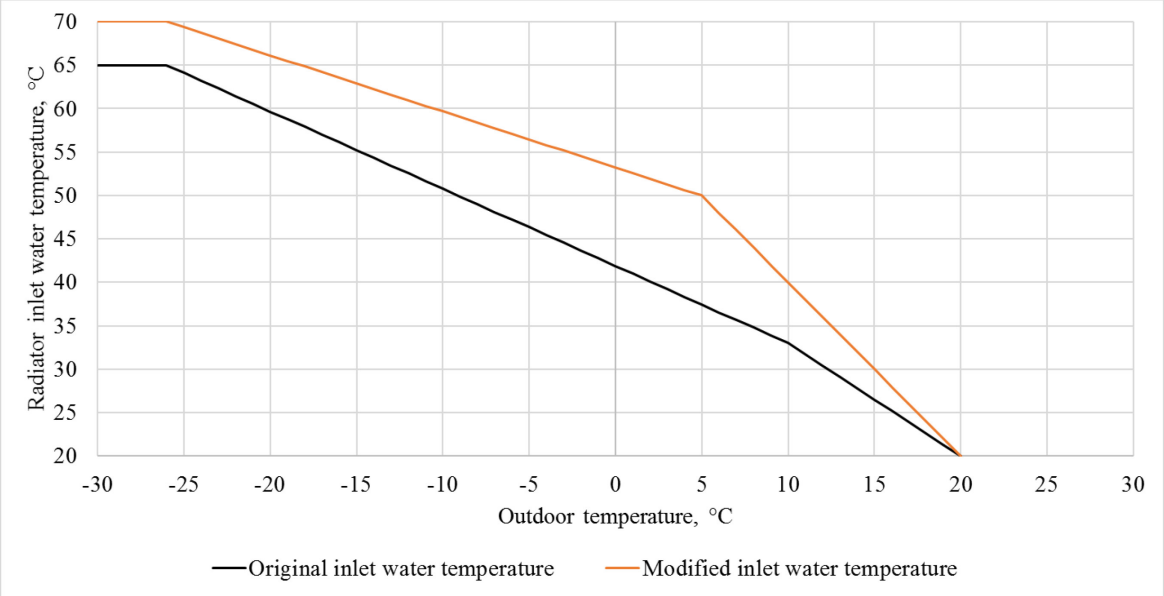

Figure 30. Otakaari 4 inlet water heating temperature curves.

5.2.3 Ventilation system

The ventilation system design is mechanical supply and extract ventilation with VAV in lecture halls and conference rooms and CAV in other types of zones. There are several AHU:s serving the building. AHU 302 and 303 are both partly serving the 4th floor and they are controlled according to the measured static duct pressure. The building model only concerned the 4th floor and the rest of the building was assumed to behave in the same way.

The ventilation system and airflows were modelled according to design drawings with the exception that AHU 303 was assumed to be handling the whole floor. The effect of this simplification is negligible since the two AHU:s have the same technical components and temperature set-points. The main characteristics of the ventilation system are presented in Table 11.

Table 11. Main characteristics of building model ventilation system.

	Description / Value	**Comment**
Mechanical supply/exhaust ventilation	TK/PK303	CAV, supply air temperature compensation according to extract air
Operation schedule	00:00-24:00	Same operation schedule throughout the year
Supply airflow	6.4 m^3/s	4^{th} floor share = 1.15 m^3/s
Supply fan pressure rise	1013 Pa	At nominal airflow
Supply duct static pressure set-point	700 Pa	
Supply fan efficiency	67 %	At nominal airflow
Exhaust airflow	5.7 m^3/s	4^{th} floor share = 1.15 m^3/s
Exhaust fan pressure rise	701 Pa	At nominal airflow
Exhaust duct static pressure set-point	500 Pa	
Exhaust fan motor efficiency	58 %	At nominal airflow
Heat recovery, $\eta_{temperature}$	72.6 %	Regenerating heat-recovery
SFP-value of AHU	2.55 $kW/(m^3/s)$	At nominal airflow

The AHU in the building utilize night purging ventilation when necessary and available. The schedule of night purge mode is from 00:00 – 05:30 every day. In the building model this characteristic was omitted, since an AHU equipped with both night purging and supply air temperature compensation was not available as default model in IDA. Additionally, night purging ventilation would not have affected the end results very much, since the cooling season was not a matter of interest in this study.

Partial load operation of AHU

During the simulations, two different design alternatives were considered: CAV and VAV. Within CAV systems it is not possible to adjust the airflow, since there are no CO_2 sensors or electronic airflow dampers available. Within a room specific VAV-system the CO_2-concentration and indoor air temperature is normally kept within a design limit range and depending on the amount of people present the air flow might be lowered without changing the intended design indoor air condition. During CAV ventilation and design conditions with 100% occupancy the average CO_2 concentration in the zones is near to 800 PPM. This CO_2 concentration was chosen as set-point for the VAV system.

The reason for studying both CAV and VAV systems, was to find out the DR potential by actual design and the maximum potential if able to control both heating system and ventilation airflows

Partial load operation needs a lower total pressure rise of the fan than during design conditions, which results in lower power usage influenced both from a decrease in flow and pressure rise.

The pressure rise values for partial load were thought to be used in IDA as input values for a more realistic simulation of AHU electricity consumption. However, this could not be implemented in practice and instead the power at partial load was calculated according to equation 8 in chapter 4.2.2 (see Figure 31).

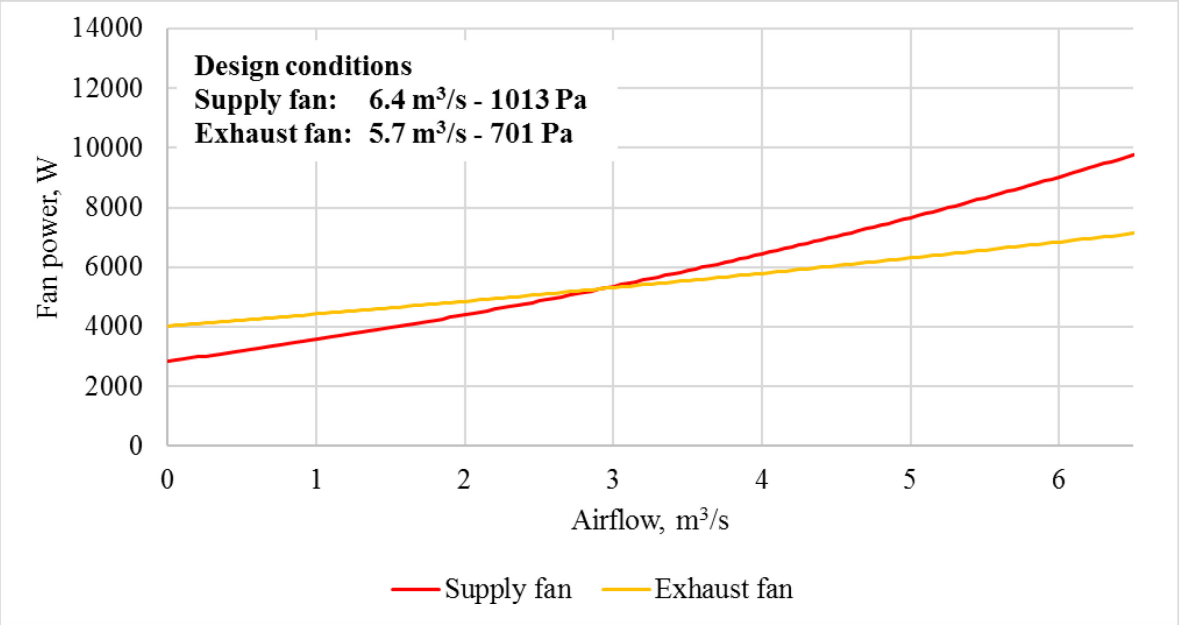

Figure 31. Power usage of AHU 303 fans at partial load conditions.

Since the simulated floor is only part of the AHU total serving area, the actual power used by the 4th floor was scaled according to ratio of 4th floor airflow and AHU airflow. This was done for both supply and return fan respectively according to equation 13 (continuation on equation 8) and 14.

$$P_{partial\ 4th} = P_{fan\ nom.} \cdot \left[\left(1 - \sqrt{\frac{\Delta p_{\ min}}{\Delta p_{design}}}\right) \cdot \left(\frac{Q_{fan\ partial}}{Q_{\ fan\ nom.}}\right) + \sqrt{\frac{\Delta p_{\ min}}{\Delta p_{design}}}\right]^3 \cdot \frac{Q_{4th\ nom.}}{Q_{fan\ nom.}} \quad (13)$$

$$Q_{fan\ partial} = \frac{Q_{4th\ partial}}{Q_{4th\ nom.}} \cdot Q_{fan\ nom.} \quad (14)$$

Where $P_{partial\ 4th}$ is the fan partial load power share of the 4th floor [W], $P_{fan\ nom.}$ is the nominal fan power [W], Δp_{min} is the static pressure set-point [Pa], Δp_{design} is the total pressure rise of fan at nominal flow [Pa], $Q_{fan\ partial}$ is the partial airflow of the fan [m³/s], $Q_{fan\ nom.}$ is the nominal airflow of the fan [m³/s], $Q_{4th\ partial}$ is the partial airflow of the 4th floow [m³/s] and $Q_{4th\ nom.}$ is the nominal airflow of the 4th floor [m³/s].

5.2.4 Internal heat gains and profiles

The maximum number of occupants (i.e. 100% occupancy) in the 4th the floor was determined by calculating the number of workstations in the rooms. As explained in chapter 5.1.3, occupancy cases of 70 % and 40 % were chosen and the distribution of persons in the rooms was conducted in an equal manner. The heat gain from the occupants was chosen according to

1.2 MET and a clothing of 0.75 ±0.25 clo, which is in line with the recommendations in the Finnish building code D3 (2012). The lighting heat gain was determined by checking the actual lamps installed in the rooms and calculating an average value out of a sample. The equipment heat load was based on the assumption that every occupant has one computer and one screen in use. The normal power consumption for a Fujitsu esprimo E9900 E-star5 table computer and Fujitsu B23-T LED display has been used (Fujitsu, 2011) and (Fujitsu, 2014).

The internal heat gains for different occupancy cases and their schedules are presented in Table 12.

Table 12. Occupancy schemes and heat gains.

Internal heat gain	**Description**			**Comment**	**Occupied hours**
Lighting	7.5 W/m^2			Measured value	**08 - 16**
Equipment	50 W/occupant			Equals a laptop and screen	**08 - 16**
Occupancy	100 %	70 %	40 %		
Room	Persons				
1 Conference	4	4	4	126 W/person	**09-11, 12-13, 14-16**
2 Kitchen	0	0	0		**Unoccupied**
3 Office	4	3	2	126 W/person	**08 - 16**
4 Office	4	3	2	126 W/person	**08 - 16**
5 Office	1	1	1	126 W/person	**08 - 16**
6 Office	4	3	2	126 W/person	**08 - 16**
7 Office	3	2	2	126 W/person	**08 - 16**
8 Office	3	2	0	126 W/person	**08 - 16**
9 Office	3	2	1	126 W/person	**08 - 16**
10 Office	2	2	1	126 W/person	**08 - 16**
11 Office	2	1	0	126 W/person	**08 - 16**
12 Office	2	1	1	126 W/person	**08 - 16**
13 Office	2	1	0	126 W/person	**08 - 16**
14 Office	2	1	1	126 W/person	**08 - 16**
15 Office	2	1	0	126 W/person	**08 - 16**
16 Office	2	2	1	126 W/person	**08 - 16**
17 Corridor	0	0	0		**Unoccupied**
18 Corridor	0	0	0		**Unoccupied**

5.3 Rule based control algorithms

The control algorithms used for the demand response cases are presented in this chapter. Chapter 5.3.2, 5.3.3 and 5.3.4 deals with the decentralized approach and chapter 5.3.5 with the centralized approach. The control algorithms were implemented into the IDA-ICE program. The decision making within the algorithms is based on indoor air temperature, outdoor 24 hour moving average temperature, CO_2 concentration in rooms and the price trend of the district heat and electricity. The principle of the process is visualized in Figure 32.

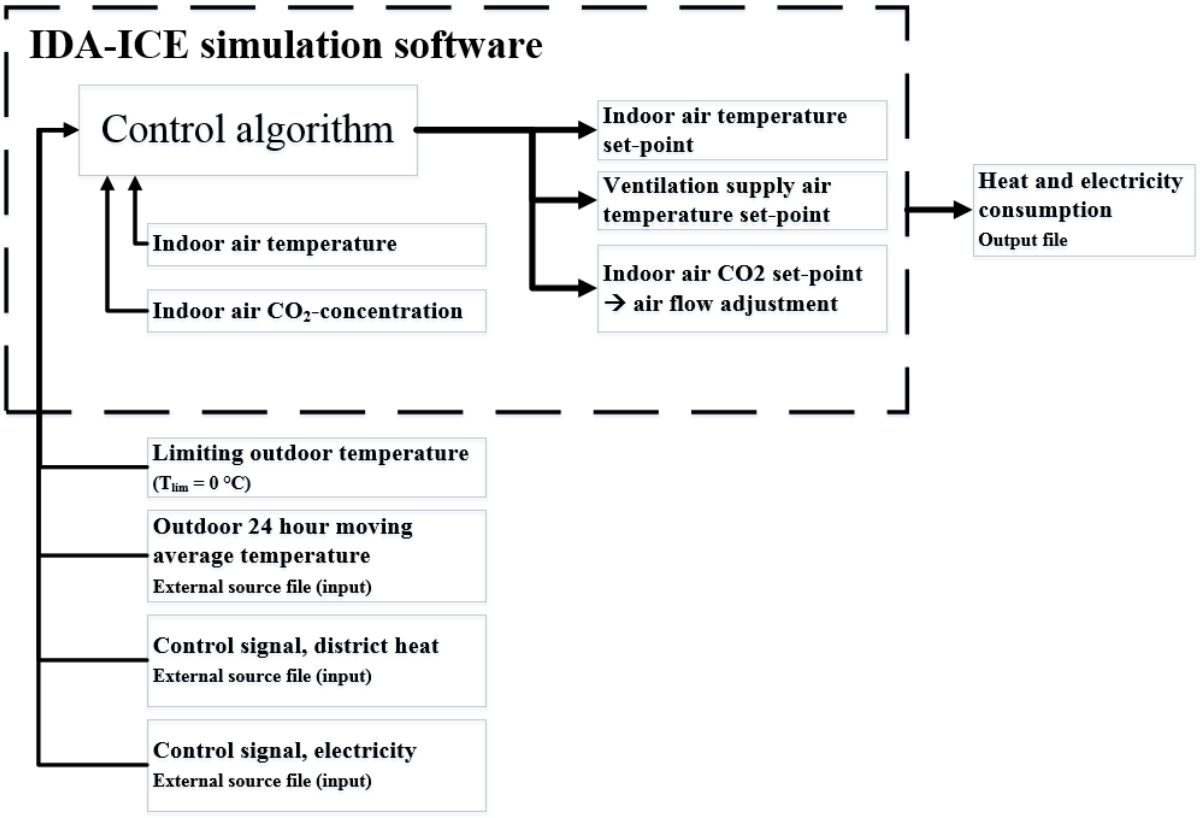

Figure 32. Simulation process principle.

The abbreviations and notations used within the algorithms are presented in Table 13. The algorithms are presented as visual flowcharts in chapter 5.3.2 – 5.3.4.

Table 13. Abbreviations and notations used in control algorithm flowcharts.

Abbreviation	Value	Unit	Description
$T_{avr, 24\ out}$	-	°C	24 hour moving average outdoor temperature
$T_{lim, out}$	0	°C	Limiting outdoor temperature for when DR-control is allowed to increase the indoor air temperature or supply air temperature above normal level
$T_{SH, set}$	-		Set-point of room air temperature
$T_{SH, max}$	24.5	°C	Maximum allowed room air temperature
$T_{SH, min}$	20	°C	Minimum allowed room air temperature
$T_{SH, norm}$	21	°C	Normal room air temperature
$T_{SH, night}$	18	°C	Night time room air temperature
$T_{any\ room}$	-	°C	Measured maximum/minimum temperature within all zones
$T_{in.}$	-	°C	Water radiator inlet temperature
$T_{norm.}$	-	°C	Water radiator inlet temperature according to temperature curve
$T_{AHU, set}$	-	°C	Set-point of AHU supply air temperature

*(Continuation of **Table** 13)*

$T_{AHU, max}$	22	°C	Maximum allowed supply air temperature of AHU
$T_{AHU, min}$	19	°C	Minimum allowed supply air temperature of AHU
$T_{AHU, med.}$	20	°C	Medium supply air temperature of AHU
$T_{AHU, norm}$	-	°C	AHU supply air temperature according to exhaust air temperature compensated curve
$T_{AHU, night}$	18	°C	Night time supply air temperature of AHU
$C_{CO2, set}$	-		Set-point of indoor air CO2 concentration
$C_{CO2, design}$	800	PPM	Design CO2 concentration in indoor air
$C_{CO2, max}$	1200	PPM	Maximum allowed CO2 concentration in indoor air
$Q_{v, max}$	-	l/s	Maximum available airflow of zone
$Q_{v, min}$	-	l/s	Minimum allowed airflow of zone (0.15 l/(s m^2)

5.3.1 Control signal

The control signal determining the price trend of district heat and electricity was generated according to two methods: the Behrang-Sirén method (Alimohammadisagvand, et al., 2017) and the Dréau-Heiselberg method (Dréau & Heiselberg, 2016).

Behrang-Sirén method

In this study it was assumed that we know the future electricity and district heat prices for a moving 24 hours forward. Based on this price information a control signal was generated, which describes the price trend. The price trend can be increasing, decreasing or flat and is characterized by the values: +1, -1 or 0 respectively. The generation of the control signal was done in Excel according to the moving average method presented by Alimohammadisagvand et al. (2017).

The control signal was calculated based on: hourly energy price (HEP), average of future hourly energy prices from hour p to hour q ($HEP^{+p,+q}{}_{avr}$), marginal down value (negative), marginal up value (positive). Equation 15 presents the pseudo code of the control signal used. Since this study assumed future price information to be available for 24 hour forward, the second condition for CS=+1 was set to $HEP^{+6,+24}{}_{avr}$ instead of the original $HEP^{+6,+30}{}_{avr}$.

$$IF \begin{Bmatrix} HEP < HEP_{avr}^{+1,+24} + marginal\ value_{down} \\ OR \\ HEP_{avr}^{+6,+12} < HEP_{avr}^{+6,+24} + marginal\ value_{up} \end{Bmatrix} THEN\ CS = +1 \quad (15)$$

$$ELSEIF\ HEP > HEP_{avr}^{+1,+24}\ THEN\ CS = -1$$
$$ELSE\ CS = 0$$
$$END\ IF$$

The price trend is always classified as decreasing if the HEP is higher than the moving 24-hour average price. For the price trend to be classified as increasing the HEP has to be lower than the sum of the 24-hour moving average price and the marginal down value. Hence by choosing a small marginal value the HEP will more often be classified as cheap and the price trend as increasing.

The magnitude of the marginal values are parameters of free choice. In this study they will be determined through simulation to find the optimal value giving most monetary saving (see chapter 6.2).

Dréau-Heiselberg method

The Dréau-Heiselberg approach of determining low and high energy prices regarding the flexibility factor was presented in chapter 4.1.2. The same approach was used for generation of the control signal. The price classification was done based on two weeks of historical hourly price data. Table 14 presents the price classifications and their corresponding control signals depending on strategy (loading + conservation or conservation only).

Table 14. Price classification based on 2 weeks of historical price data and the corresponding control signal output values of the Dréau-Heiselberg method.

	Control signal (heating)	
Price classification	**Loading & conservation**	**Conservation only**
Low price	1	0
Medium price	0	0
High price	-1	-1

5.3.2 Space heating

It was assumed that the room air temperature should not be increased if the outdoor 24 hour moving average temperature ($T_{avr, 24\ out}$) is over 0°C ($T_{lim, out}$), since that could cause overheating from solar radiation during warmer periods of the year.

Figure 33 presents the first control algorithm which controls the space heating system via room air temperature set-points. The algorithm determines the future price trend of district heating from the control signal. If the trend is increasing (CS=+1) and the $T_{avr, 24\ out} < T_{lim, out}$ (0 °C), the control system loads additional heat into the structures by setting $T_{SH,set}$ to $T_{SH, max}$. If the trend is decreasing (CS=-1) the control system goes into conservation mode by setting $T_{SH,set}$ to $T_{SH, min}$. Finally, if the price trend is flat (CS=0) the building is heated as normally by setting $T_{SH,set}$ to $T_{SH, norm}$.

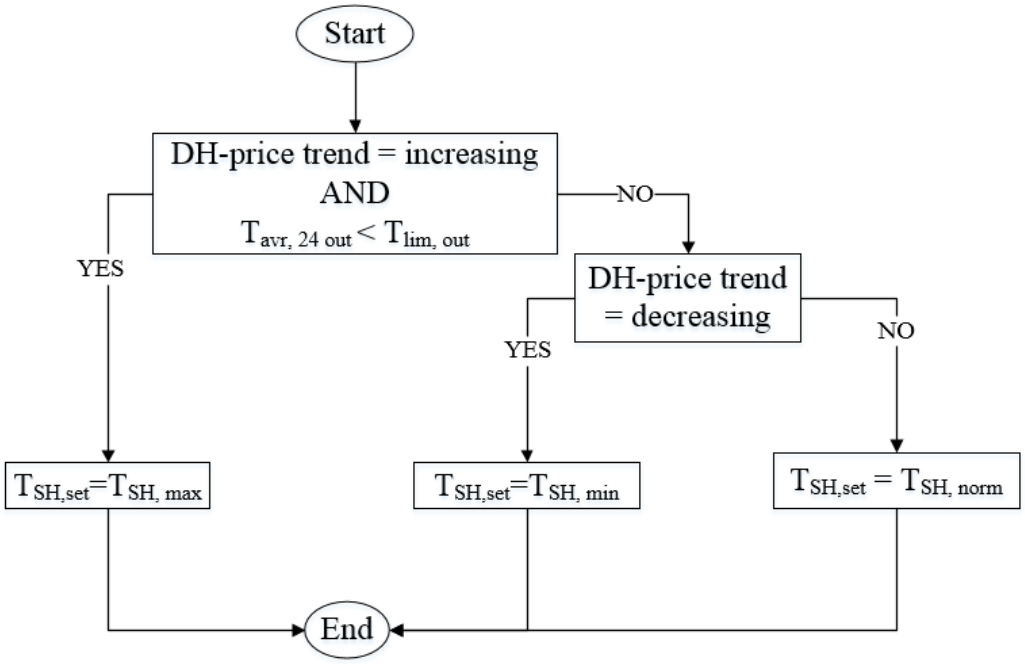

Figure 33. Control algorithm A1 for space heating.

Figure 34 presents algorithm A2, which additionally to DR-controlled space heating also includes night time set-back mode (green box) during holidays, weekends and night time (8 PM – 6 AM).

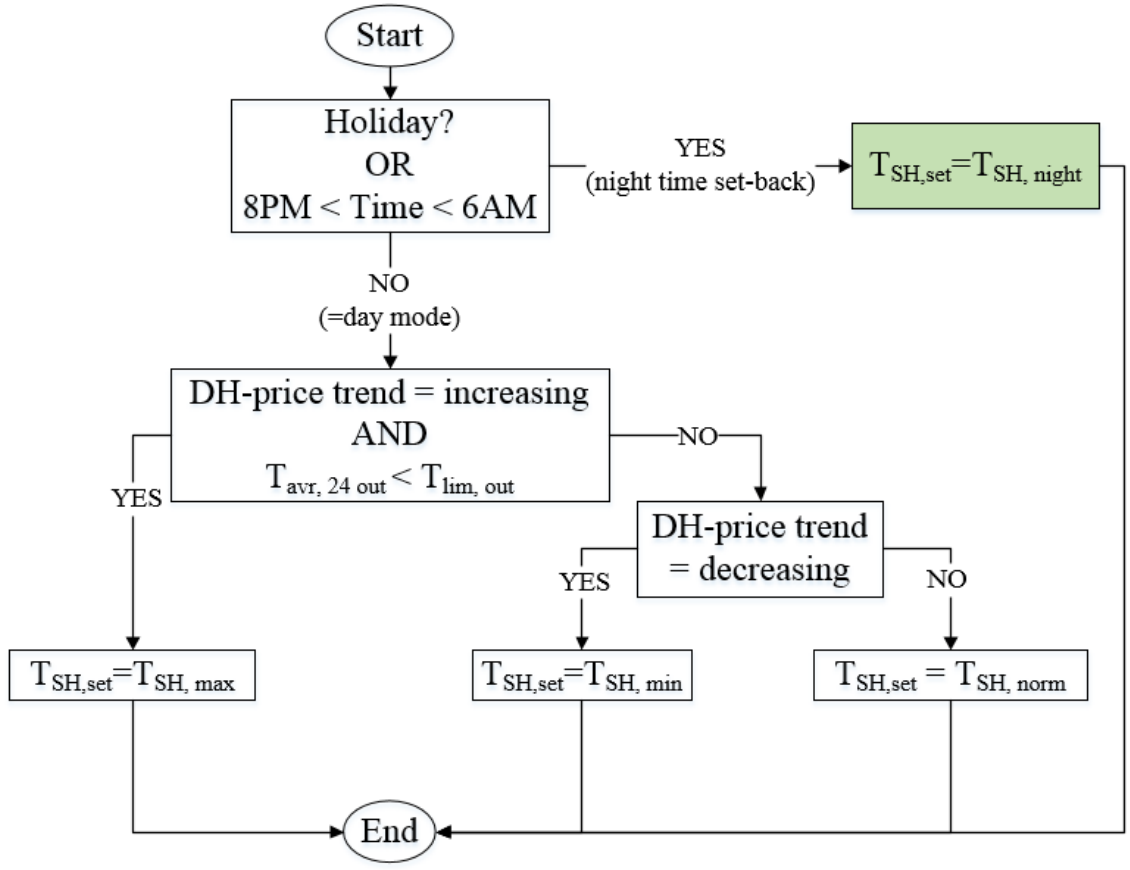

Figure 34. Control algorithm A2 for space heating and night time set-back mode.

5.3.3 Supply air temperature and space heating

Figure 35 presents algorithm B1 which controls the supply air temperature of the ventilation. As for the room air temperature set-point, it is assumed that the supply air temperature should not be increased if $T_{avr,\ 24\ out} > T_{lim,\ out}$ (0 °C). Instead the supply air temperature set-point is defined according to the normal exhaust temperature compensated curve (Figure 29) to prevent additional cooling when needed. Otherwise the control algorithm is working according to the same principle as algorithm A1.

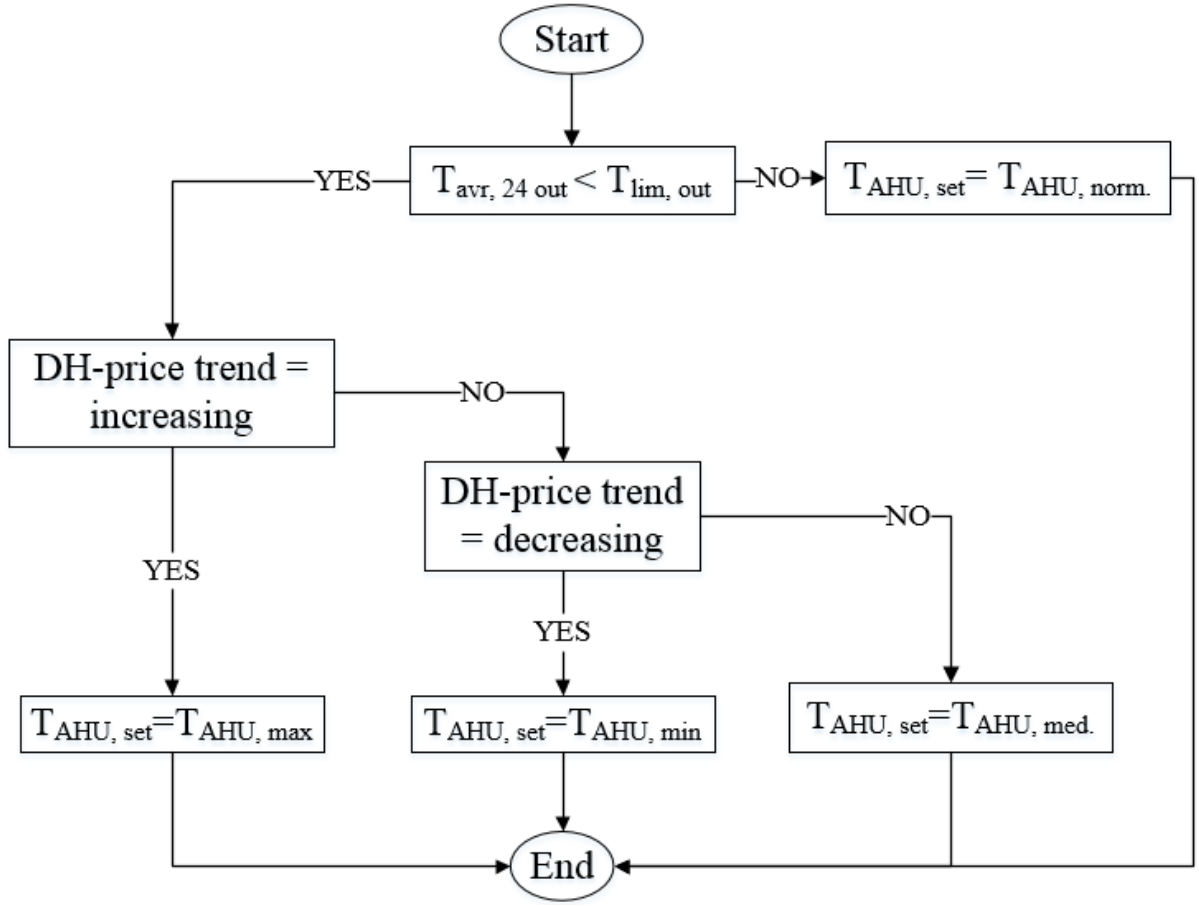

Figure 35. Control algorithm B1 for supply air temperature.

Figure 36 presents algorithm B2 which in addition to supply air temperature also controls space heating (green boxes). When $T_{avr,\ 24\ out} > T_{lim,\ out}$ (0 °C), the supply air temperature is defined according to the normal curve (Figure 29) but room air temperature set-points are either $T_{SH,norm.}$ or $T_{SH,\ min.}$ depending on price trend.

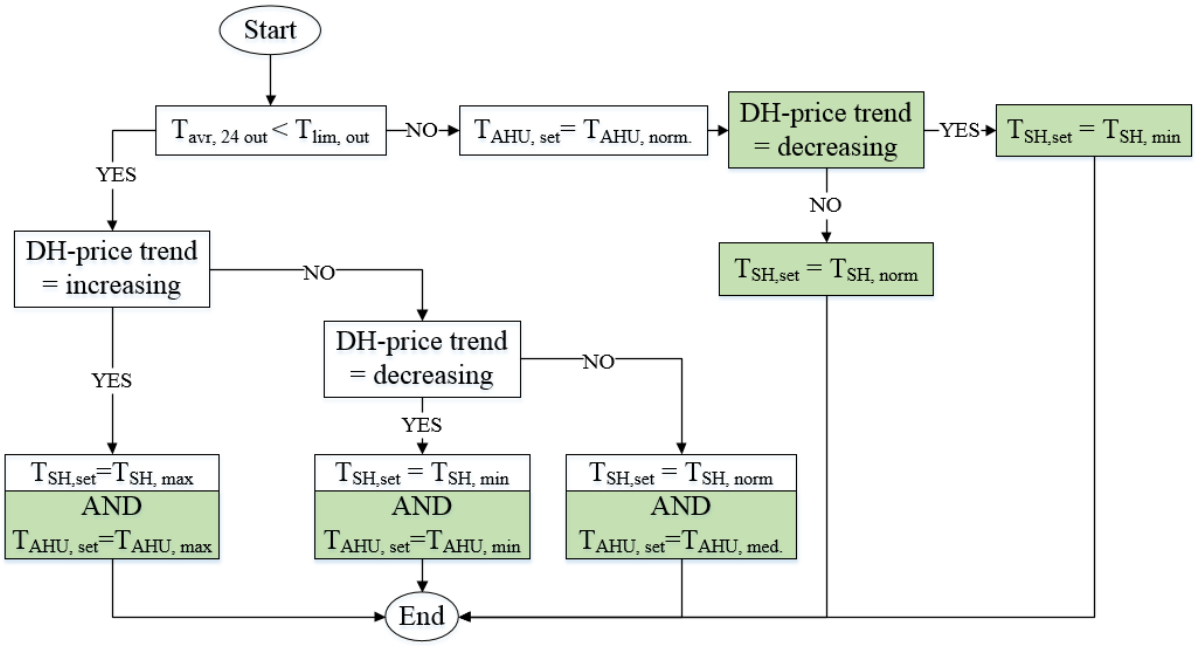

Figure 36. Control algorithm B2 for supply air temperature and space heating.

Figure 37 presents algorithm B3 which in addition to DR-controlled space heating and supply air temperature includes night time set-back mode (green boxes).

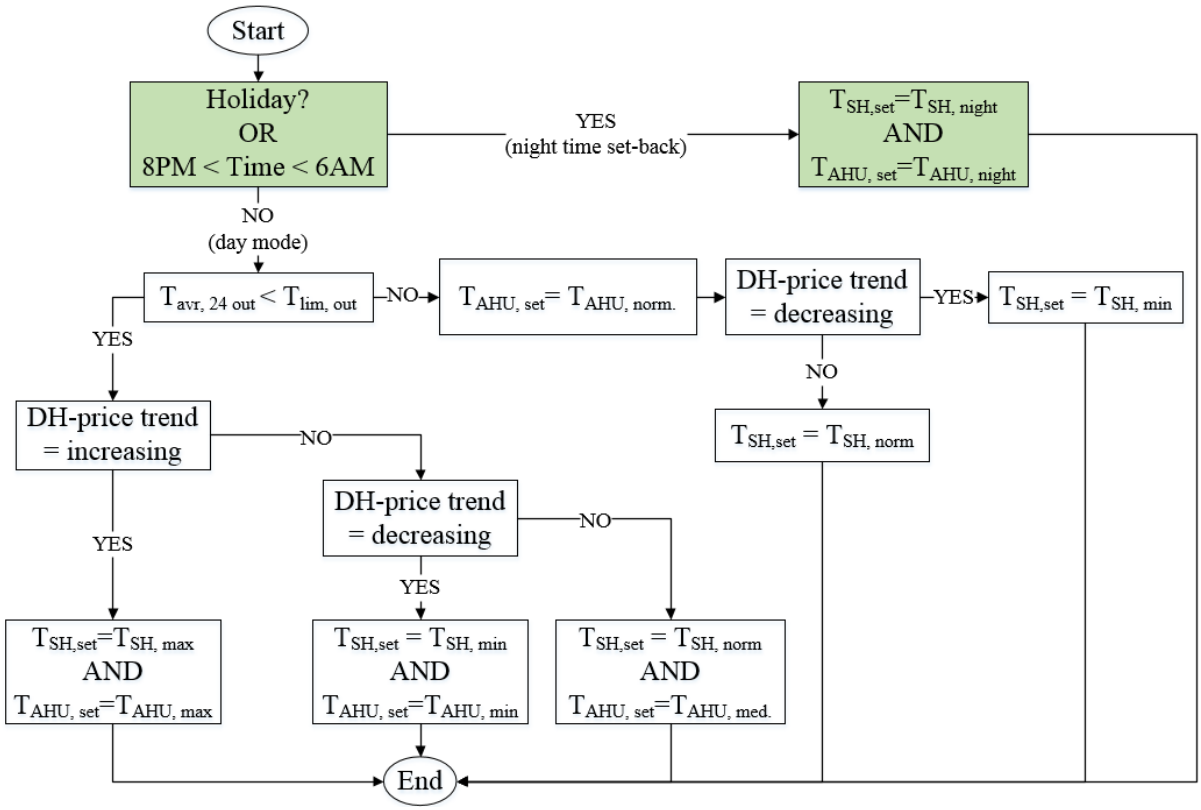

Figure 37. Control algorithm B3 for supply air temperature, space heating and night time set-back mode.

5.3.4 Ventilation, supply air temperature and space heating

The following algorithms were constructed for a building with VAV ventilation.

Figure 38 presents algorithm C1 which controls the ventilation airflow by adjusting the CO_2 set-point of the zones according to price trend of either district heating or electricity. The CO_2 set-point can only be increased if the future price trend is decreasing (CS=-1). In all other cases the CO_2 set-point is according to design value.

However, if the room temperature exceeds the cooling set-point of 24.5°C and $T_{avr,\ 24\ out} > T_{lim.}$ (0°C), the airflow is increased to maximum regardless of control signal. This is done to prevent too high room air temperatures during warmer periods of the year.

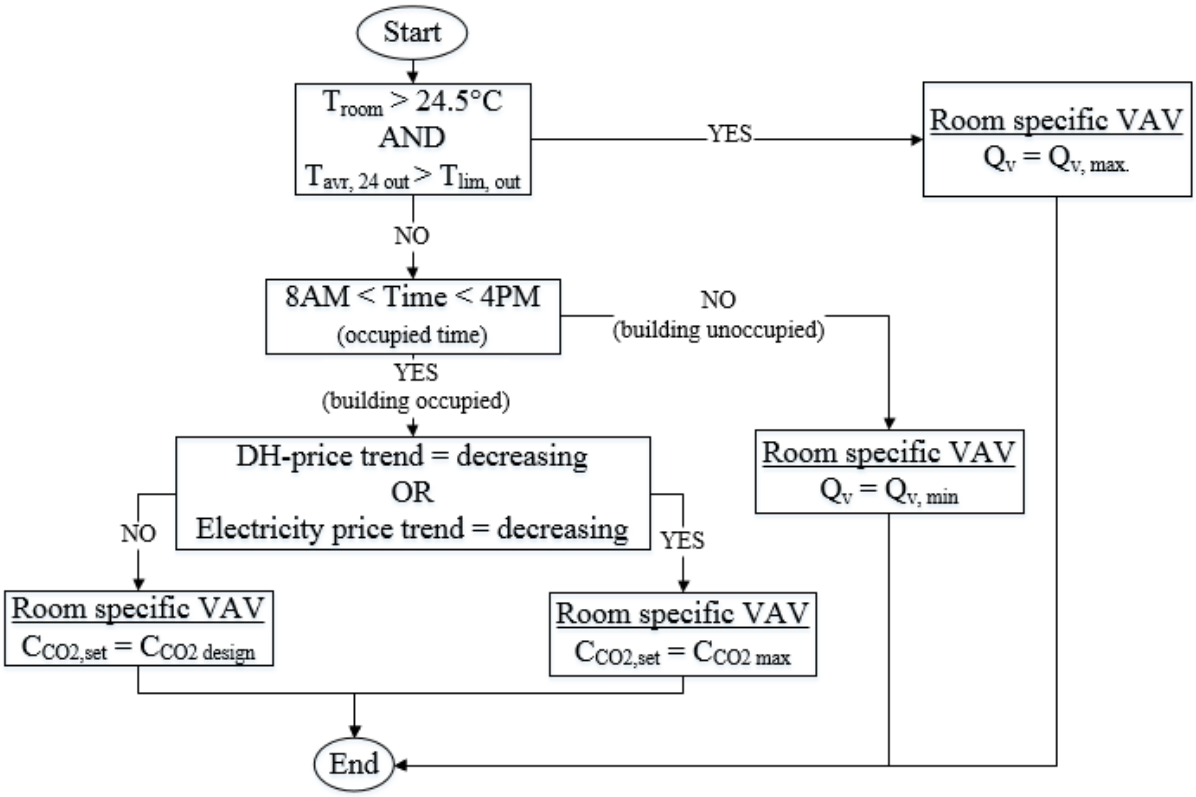

Figure 38. Control algorithm C1 for ventilation airflow.

Figure 39 presents algorithm C2 which controls both airflow and space heating (green boxes).

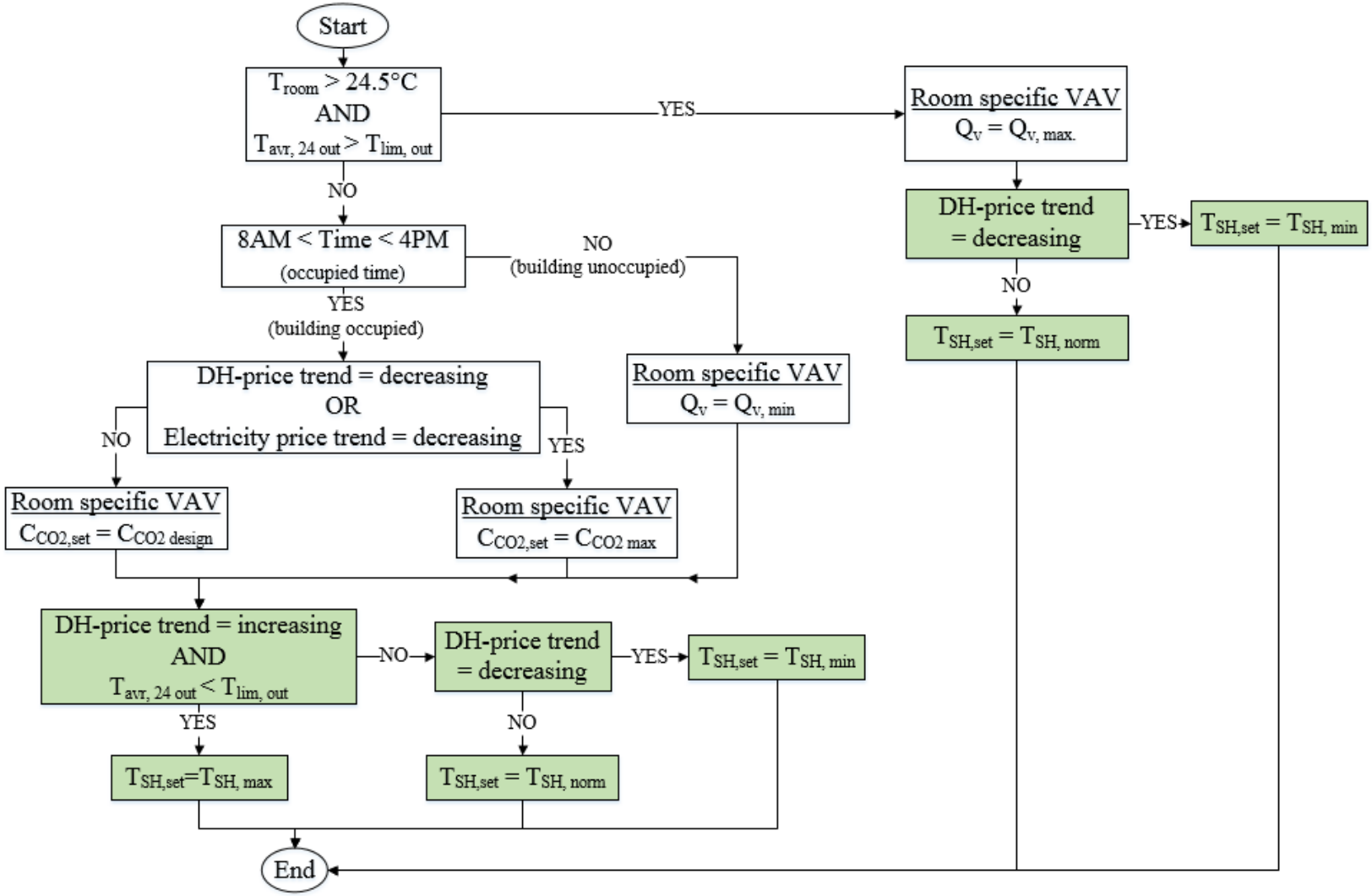

Figure 39. Algorithm C2 for ventilation airflow and space heating.

Figure 40 present algorithm C3 which controls airflow, space heating and supply air temperature (green boxes).

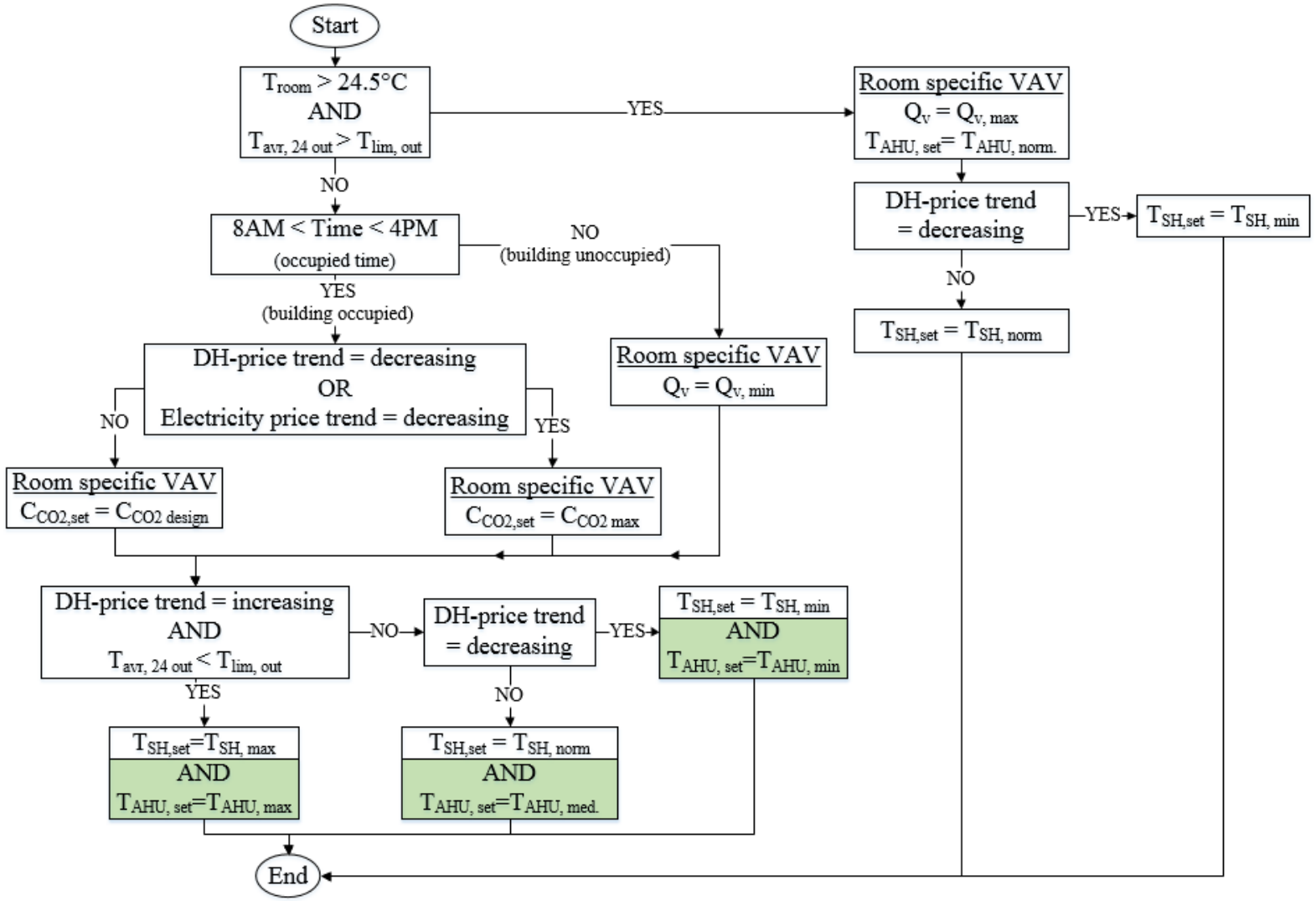

Figure 40. Algorithm C3 for ventilation airflow, space heating and supply air temperature.

Figure 41 presents control algorithm C4 which in addition to DR-controlled airflow, space heating and supply air temperature includes night time set-back mode (green boxes).

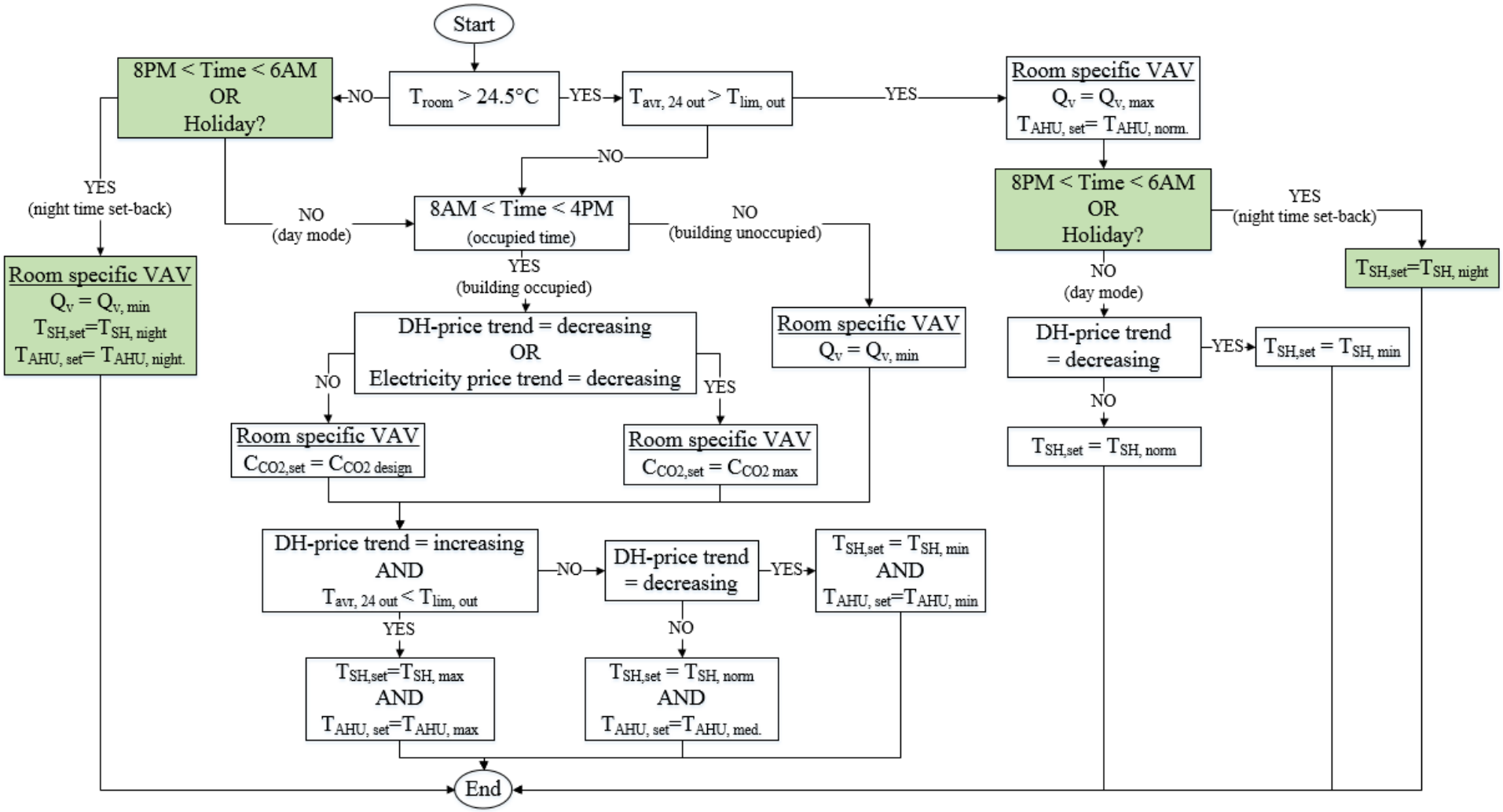

Figure 41. Control algorithm C4 for airflow, space heating, supply air temperature and night time set-back mode.

5.3.5 Centralized space heating and supply air temperature

Figure 42 presents the centralized DR control algorithm (D1) of space heating. The control logic follows the one of algorithm A1 (Figure 33), but instead of adjusting room temperature set-points it adjusts water radiator inlet temperatures. During loading or conservation, the inlet water temperature is increased or decreased to e.g. a value equaling 20% more or 10% less heat output respectively (Figure 43). The inlet temperatures corresponding to the adjusted heat output are calculated according to the verified method presented by Stephan (Stephan, 1986). The room air temperature set-point is regardless of the situation kept at 21°C. The reason is that the control of centralized heat output is handled by the thermostatic radiator valves, and their set-point (physical adjustment) is constant. As a result, during loading the valves will reduce the water mass flow rate as the room air temperature increases. Likewise, the mass flow rate will be increased during conservation. This property of the mechanical thermostats will be in conflict with the actual control algorithm.

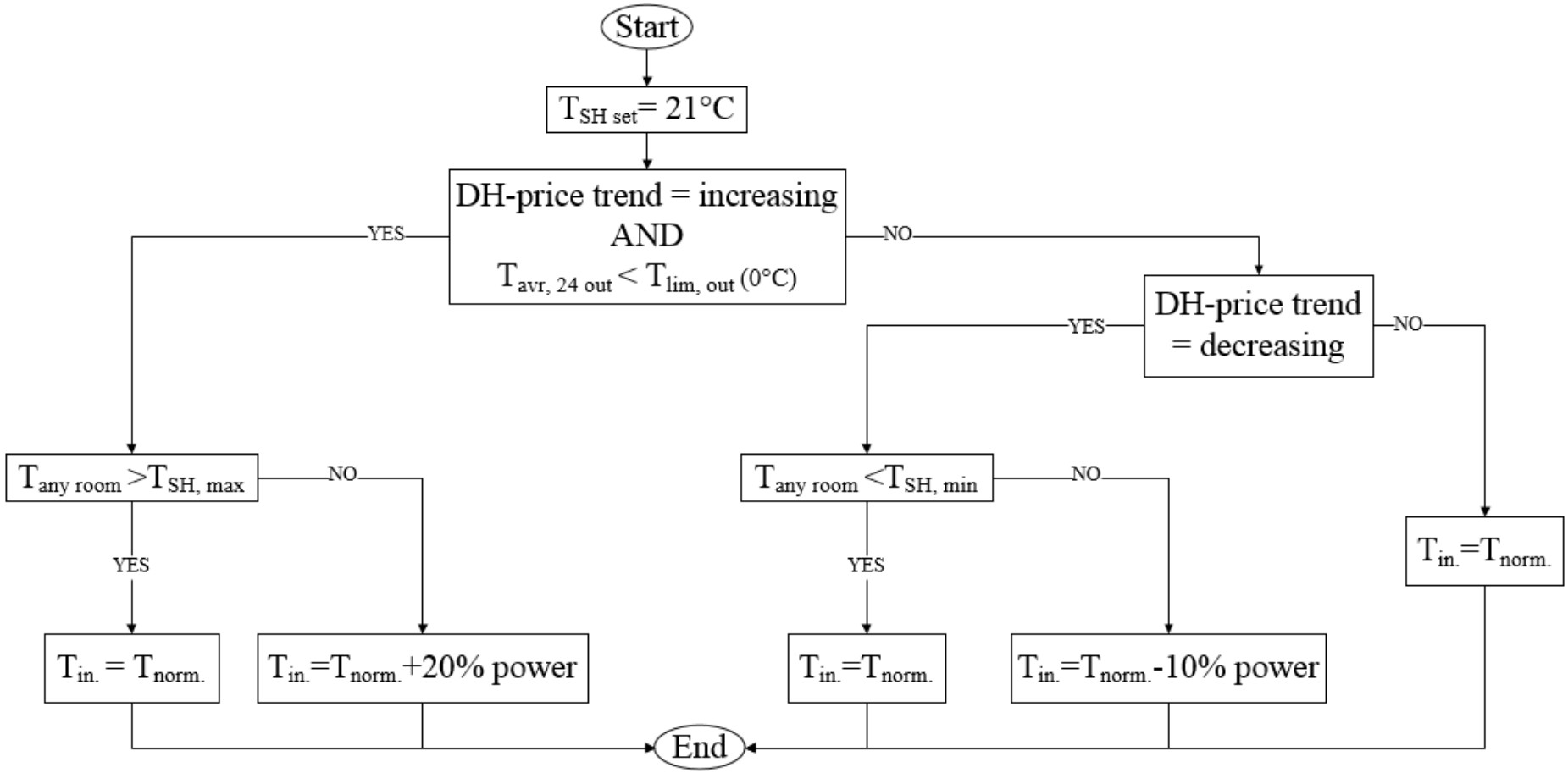

Figure 42. Control algorithm D1 for centralized DR control of space heating.

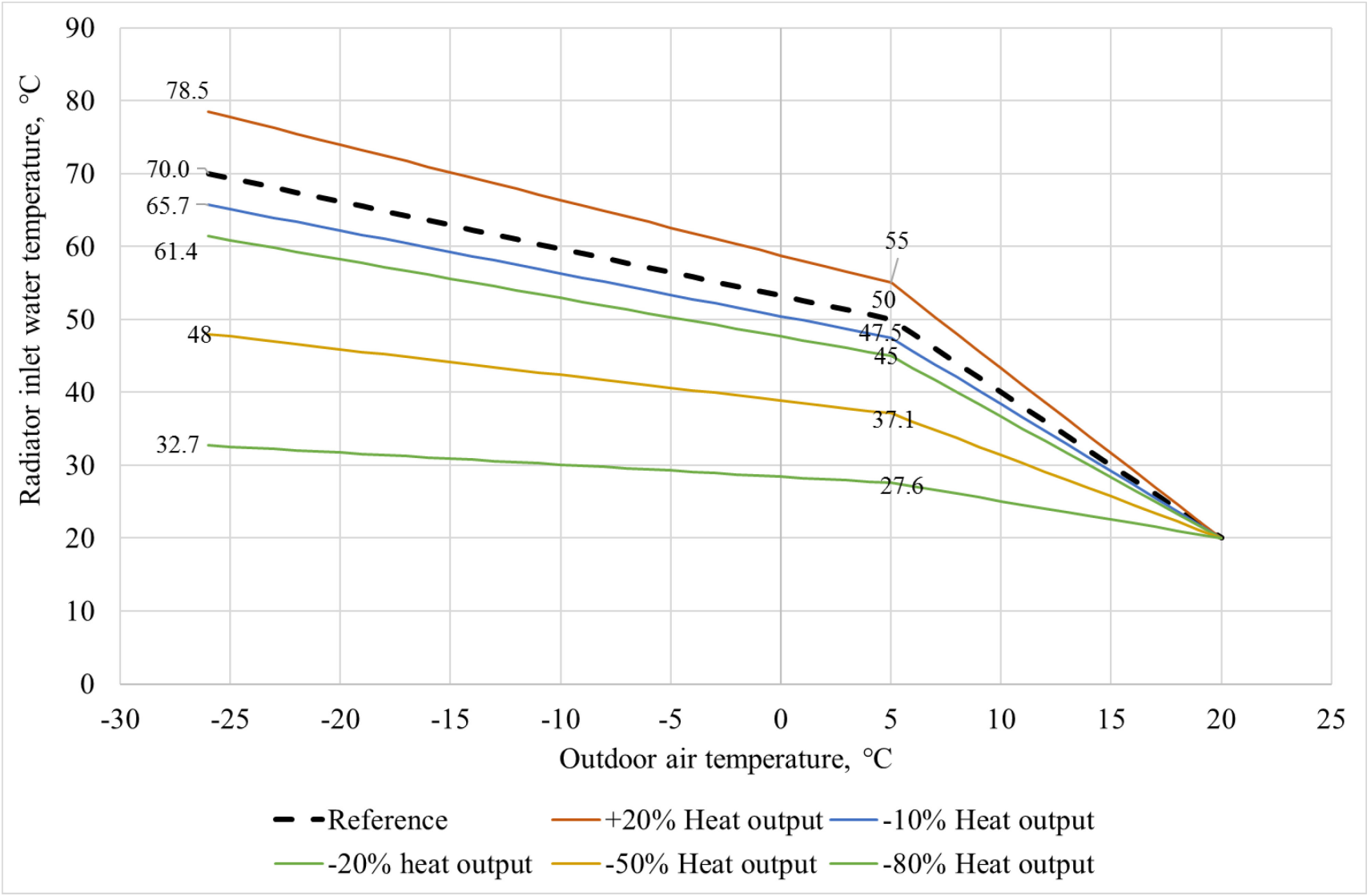

Figure 43. Water radiator inlet temperature curves as a function of outdoor temperature.

Figure 44 presents the centralized DR control algorithm (D2) which controls both space heating and supply air temperature. When $T_{avr,\ 24\ out} > T_{lim,\ out}$ (0 °C), the supply air temperature is defined according to the normal curve (Figure 29) but water radiator inlet temperature is either $T_{,norm.}$ or $T_{norm.}$ − 10% power depending on price trend.

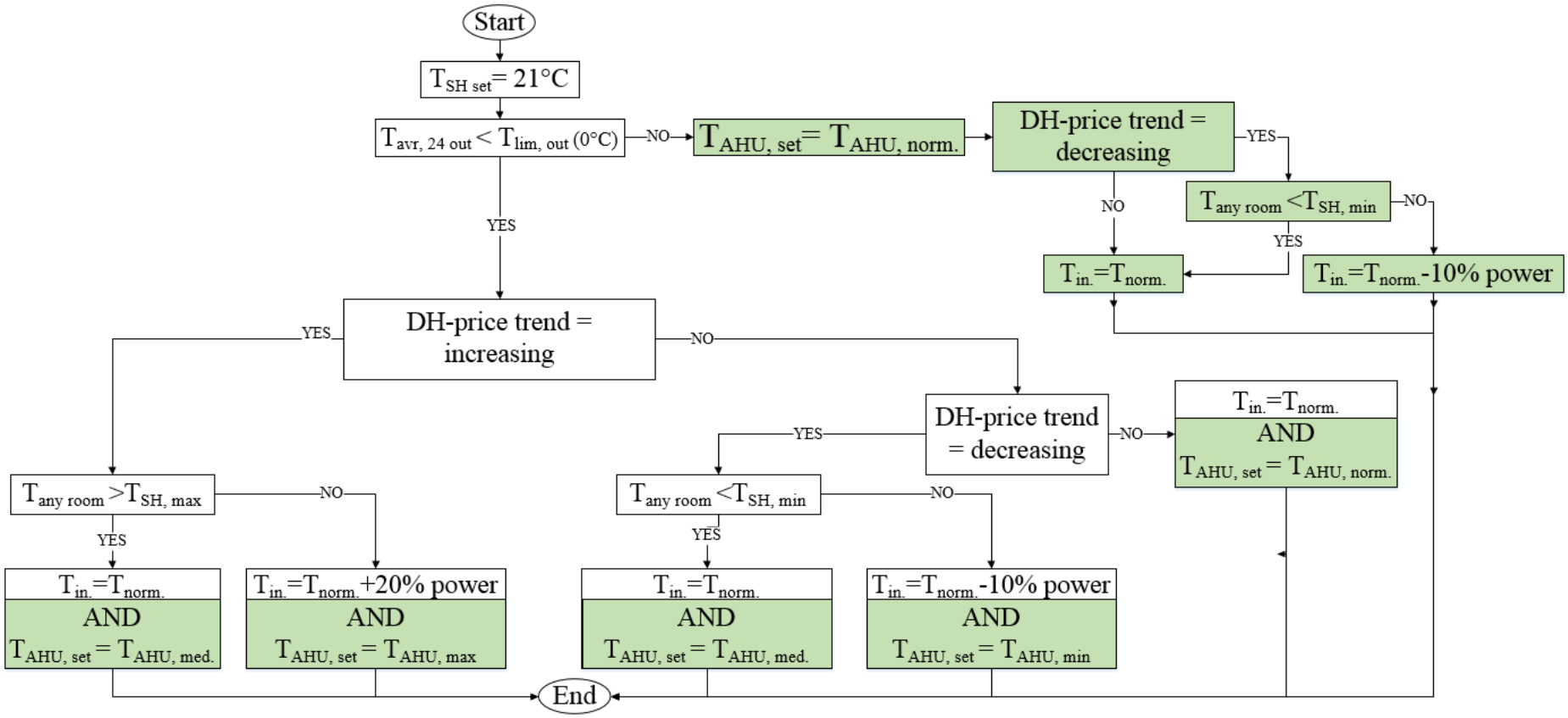

Figure 44. Control algorithm D2 for centralized DR control of space heating and supply air temperature.

5.4 Simulation cases

The simulation cases include both reference cases (no DR-control) and DR-controlled cases. Three initial reference cases were chosen with constant temperature set-point of 21°C but different occupancy or ventilation design. Additionally, three more references were added with constant temperature set-point of 20°C. This enables the comparison of the DR controlled cases with a normal constant room temperature case (21°C) and a reduced room temperature case (20°C). The lower temperature of 20°C was chosen since that is the minimum allowed room air temperature of the DR cases. Table 15 shows the chosen reference simulation cases.

Table 15. Reference cases without DR-control.

REFERENCE CASES (NO DR-CONTROL)						
Case	**DR-algorithm**	**Occupancy**	**Indoor air temperature set-point [°C]**		**$T_{sup.}$ control**	**Ventilation design**
			Heating	**Cooling**		
1	No DR-control	*70 %*	*21*	-	*1)*	*CAV*
1.1	No DR-control	*70 %*	*20*	-	*1)*	*CAV*
2	No DR-control	*40 %*	*21*	-	*1)*	*CAV*
2.1	No DR-control	*40 %*	*20*	-	*1)*	*CAV*
3	No DR-control	40 %	*21*	24.5 *4)*	*1)*	*VAV*
3.1	No DR-control	40 %	*20*	24.5 *4)*	*1)*	*VAV*

Table 16 shows the decentralized DR-controlled simulation cases. The following abbreviations are used: SH is space heating, NT is night time set-back mode, $T_{sup.}$ is supply air temperature and Q_{air} is airflow control. The cases were divided into sub-groups according to control signal method used. Case 18.1 and 19.1 belong to the Dréau-Heiselberg control signal group, but the signal of these two cases considers only conservation (CS=-1 → $T_{SH, set.}$= 20°C), meaning that all the hours considering loading (CS=+1 → $T_{SH, set.}$= 24.5°C) have been manually changed into "normal set-point hours" (CS=0 → $T_{SH, set.}$= 21°C) . This was done to evaluate the effect of heat loading versus conservation.

Only two cases have the occupancy of 70%. The reason is that initial test simulations showed a negligible difference in final results depending on occupancy alternatives. The occupancy of 40% was chosen as the main interest since it is more in line with the real occupancy in the building floor.

Table 16. DR-controlled decentralized simulation cases.

Case	DR-algorithm	Occupancy	Indoor air temperature set-point [°C]		$T_{sup.}$ control	Ventilation design
			Heating	Cooling		
DECENTRALIZED DR-CONTROL						
Control signal definition: Behrang-Sirén, marginal value: ±75 €/MWh (DH & electricity)						
4	A1 (SH, see Figure 33)	70 %	20-24.5	-	1)	CAV
5		40 %	20-24.5	-	1)	CAV
6	A2 (SH+NT, see Figure 34)	40 %	20-24.5	-	1)	CAV
7	B1 ($T_{sup.}$, see Figure 35)	40 %	21	-	2)	CAV
8	B2 (SH+$T_{sup.}$, see Figure 36)	40 %	20-24.5	-	2)	CAV
9	B3 (SH+$T_{sup.}$+NT, see Figure 37)	40 %	20-24.5	-	3)	CAV
10	C1 (Q_{air}, see Figure 38)	40 %	21	24.5 4)	1)	**VAV**
11	C2 (Q_{air}+SH, see Figure 39)	40 %	20-24.5	24.5 4)	1)	**VAV**
12	C3 (Q_{air}+SH+$T_{sup.}$, see Figure 40)	40 %	20-24.5	24.5 4)	2)	**VAV**
13	C4 (Q_{air}+SH+$T_{sup.}$+NT, see Figure 41)	40 %	20-24.5	24.5 4)	3)	**VAV**
Control signal definition: Behrang-Sirén, marginal value: District heat ±15 €/MWh						
14	A1 (SH, see Figure 33)	70 %	20-24.5	-	1)	CAV
15		40 %	20-24.5	-	1)	CAV
16	B2 (SH+$T_{sup.}$, see Figure 36)	40 %	20-24.5	-	2)	CAV
Control signal definition: Dreaú-Heiselberg, generated for two weeks of historical price data						
17	A1 (SH, see Figure 33)	70 %	20-24.5	-	1)	CAV
18		40 %	20-24.5	-	1)	CAV
18.1	A1 (SH, see Figure 33) 5)	40%	20-21	-	1)	CAV
19	B2 (SH+$T_{sup.}$, see Figure 36.)	40 %	20-24.5	-	2)	CAV
19.1	B2 (SH+$T_{sup.}$, see Figure 36) 5)	40%	20-21	-	2)	CAV
1) According to supply air temperature compensation curve						
2) Constant set-points (17, 20 or 22°C) when $T_{24\ avr} < T_{lim}$. Otherwise according to supply air temperature compensation curve (see algorithm description)						
3) As for 2) but during night-time T_{sup}= 18°C						
4) Applies for cases involving VAV ventilation						
5) Dréau-Heiselberg control where only conservation is considered						

Table 17 show the centralized DR-controlled scenarios. Cases 20 – 21.1 deals with peak demand limiting. There is no control algorithm used, but the maximum DH water mass flow through the substation was reduced with 35%, 43% or 50% compared to the nominal flow. In cases 22 – 23.1 the control signal definition Behrang-Sirén with marginal value ±75 €/MWh was used, which effectively resulted in only conservation and no heat loading (the matter is presented in more detail in chapter 6.2). P_{heat} is the normal heat output of a radiator at a certain outdoor temperature based on the reference radiator inlet temperature curve (Figure 43). The negative percentage describes how much the normal heat output was decreased by adjusting the inlet water temperature during DR-control.

Table 17. DR-controlled centralized simulation cases.

CENTRALIZED DR-CONTROL						
Case	**DR-algorithm**	**Occupancy**	**Indoor air temperature set-point [°C]**		**$T_{sup.}$ control**	**Ventilation design**
			Heating	**Cooling**		
20	Peak demand limiting -35%	40 %	21	-	1)	CAV
21	Peak demand limiting -43%	40 %	21	-	1)	CAV
21.1	Peak demand limiting -50%	40 %	21	-	1)	CAV
Control signal: Behrang-Sirén method - Marginal value: ±75 €/MWh (DH & electricity)						
22	D1 (SH, P_{heat}-10%, see Figure 42)	40 %	20-24.5	-	1)	CAV
22.1	D1 (SH, P_{heat}-20%, see Figure 42)	40 %	20-24.5	-	1)	CAV
22.2	D1 (SH, P_{heat}-50%, see Figure 42)	40 %	20-24.5	-	1)	CAV
22.3	D1 (SH, P_{heat}-80%, see Figure 42)	40 %	20-24.5	-	1)	CAV
23	D2 (SH, P_{heat}-10% + $T_{sup.}$, see Figure 44)	40 %	20-24.5	-	2)	CAV
23.1	D2 (SH, P_{heat}-80% + $T_{sup.}$, see Figure 44)	40 %	20-24.5	-	2)	CAV
1) According to supply air temperature compensation curve						

The room specific and total airflows, the calculated CO_2 concentration and the calculated fan power are shown in Table 18 for both design conditions and 40% occupancy respectively. $Q_{fan\ nominal}$ and $P_{fan\ nominal}$ indicate respectively the ratio of airflow and fan power to their nominal values. The values are shown for different ventilation designs and room air CO_2 set-points. The partial load fan powers were calculated according to equation 8 in chapter 4.2.2, on the assumption that the whole AHU is behaving in the same way as the 4th floor area. The efficiency of the variable frequency drive (VFD) used in the VAV systems is neglected. In practice the VFD efficiency is around 98 – 95 % at nominal flow and 70 – 90 % at 25% of nominal flow (Brelih, 2012).

Table 18. Airflow, CO_2 concentration (at steady-state) and fan power in different occupancy schemes.

Ventilation design			**CAV**	**CAV**	**VAV, CO_2 set-point = 800 PPM**	**VAV, CO_2 set-point = 1200 PPM**	**VAV**
Occupancy			100%	40 %	40 %	40 %	Night
Room	**Area [m^2]**	**Q_v [l/(s m^2)]**	**PPM_{CO2}**	**PPM_{CO2}**	**Q_v [l/(s m^2)]**	**Q_v [l/(s m^2)]**	**Q_v [l/(s m^2)]**
1 Conference	25.3	2.57	798	798	2.55	1.27	0.15
2 Kitchen	27.4	2.19	400	400	0.15	0.15	0.15
3 Office	29.2	2.05	831	615	1.10	0.55	0.15
4 Office	28.3	2.12	831	615	1.14	0.57	0.15
5 Office	28.4	2.12	508	508	0.57	0.28	0.15
6 Office	28.6	2.10	831	615	1.13	0.57	0.15
7 Office	19.0	2.10	885	723	1.70	0.85	0.15
8 Office	20.3	1.97	885	400	0.15	0.15	0.15
9 Office	18.7	2.14	885	562	0.86	0.43	0.15
10 Office	17.2	2.32	723	562	0.94	0.47	0.15
11 Office	18.4	2.18	723	400	0.15	0.15	0.15
12 Office	18.5	2.16	723	562	0.87	0.44	0.15
13 Office	18.5	2.17	723	400	0.15	0.15	0.15
14 Office	18.2	2.20	723	562	0.89	0.44	0.15
15 Office	18.1	2.21	723	400	0.15	0.15	0.15
16 Office	16.9	2.37	723	562	0.96	0.48	0.15
17 Corridor	108.2	1.02	400	400	0.15	0.15	0.15
18 Corridor	126.5	1.90	400	400	0.15	0.15	0.15
Q_{fan} [l/s]		**1115**			**341**	**196**	**88**
$Q_{fan\ nominal}$ %		100 %			30.6 %	17.6 %	7.9 %
P_{fan} [W]	Supply	9619			4404	3648	3195
	Exhaust	6682			4725	4448	4203
$P_{fan\ nominal}$ %	Supply	100 %			46 %	38 %	33 %
	Exhaust	100 %			71 %	67 %	63 %

6 Simulation results

6.1 Reference cases without DR-control

In the following the energy consumption and cost are presented for the 6 reference cases without DR-control (presented in Table 15).

Table 19 presents the annual energy consumption, cost and their allocations for the reference cases per heated net floor area. The total heated net floor area for the 4th floor of the building is 586 m^2.

Table 19. Energy consumption and cost for the non-DR reference cases.

	Case	Total delivered district heating	Zone heating	AHU heating	Total delivered electricity	Electric cooling	Equip-ment	HVAC aux.	Light-ing
Energy, kWh/m^2,a	1	124.9	62.5	58.7	59.3	1.1	5.7	38.7	13.9
	1.1	117.7	47.4	66.8	59.6	1.1	5.7	39.0	13.9
	2	128.7	65.8	59.1	57.3	1.0	3.8	38.7	13.9
	2.1	121.3	50.3	67.4	57.6	1.0	3.8	39.0	13.9
	3	72.0	62.6	7.4	41.1	1.0	3.8	22.5	13.9
	3.1	75.8	53.7	19.9	43.1	1.0	3.8	24.5	13.9
Cost, €/m^2,a	1	8.0	4.0	3.7	8.2	0.1	0.9	5.0	2.2
	1.1	7.6	3.1	4.2	8.2	0.1	0.9	5.1	2.2
	2	8.2	4.2	3.8	7.9	0.1	0.6	5.0	2.2
	2.1	7.8	4.2	3.3	7.9	0.1	0.6	5.1	2.2
	3	4.7	4.0	0.5	5.8	0.1	0.6	2.9	2.2
	3.1	5.0	3.5	1.4	6.1	0.1	0.6	3.2	2.2

The total annual delivered DH energy consumption is lower in case 1.1 compared to case 1 due to the 1°C lower room temperature set-point (20°C). The same goes for case 2 and case 2.1 respectively. Case 3 has a substantially lower DH consumption than cases 1 – 2.1, due to the VAV ventilation system. Case 3.1 however has bigger DH and electricity consumption than case 3 which is a result of the supply air temperature being 20°C and the VAV system trying to heat the rooms with an increased airflow whenever the room temperature slips below the set-point of 20°C. This does seldom happen for case 3 since the room temperature set-point is higher (21°C).

The total annual delivered district heat is divided into two sub-categories: zone heating and AHU heating. The zone heating and AHU heating fractions ranges from 41% – 50% and 47% – 57% respectively for the CAV cases. For the VAV cases the zone heating fraction is bigger (71% – 87%) due to the lower airflow rate.

The total annual delivered electricity consumption stays on the same level with little change in magnitude for case 1 – 2.1 but is lower for the VAV cases (3 & 3.1) due to the lower airflow rate. However, as for the DH consumption, case 3.1 has a higher electricity consumption than case 3 due to the VAV system's efforts to aid the space heating whenever the room temperature slips below the set-point level (20°C).

The total annual delivered electricity divides into 4 sub-categories where HVAC auxiliary and lighting constitute the biggest shares, ranging from 54.7% – 67.7% and 23% – 32 % respectively. The electricity used for the chiller and equipment is in the range of 1.7% – 2.3% and 6.5% – 9.6% respectively. The electricity used for equipment and lighting stays rather constant for all simulation cases and is not analyzed further. The electrical cooling vary depending on ventilation design and DR-control, but constitute only a small fraction of the total electricity usage. The biggest alone electricity consumer in the building is the auxiliary HVAC equipment such as fans and pumps of which fans constitute about 99.5% of the share.

6.2 Determination of marginal value and limiting outdoor temperature

Within the Behrang-Sirén method of generating the control signal a marginal value had to be chosen (see chapter 5.3.1). Marginal values of different magnitude generate different control signals (-1, 0 or 1). A high marginal value (relative to the actual price level of energy) decreases the number of positive ones in the control signal output. Within heating DR this results in a lower number of potential heat loading hours. The relationship between DH or electricity control signal output values and marginal value is shown in Figure 45 and Figure 46 respectively.

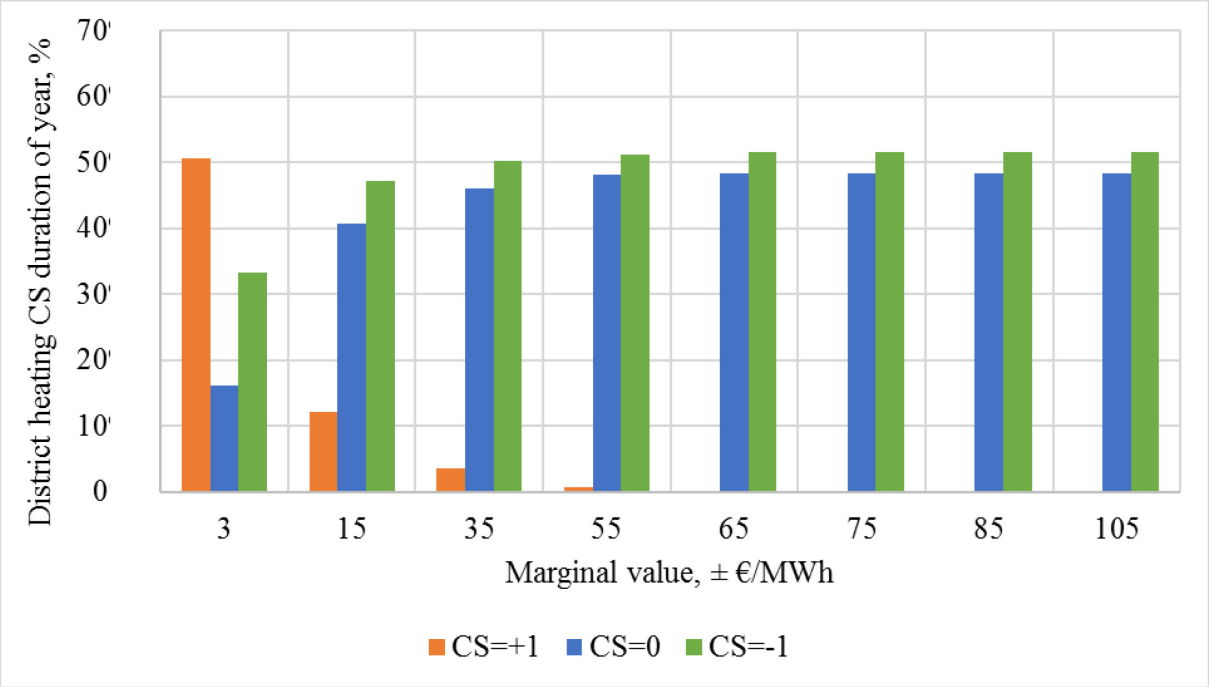

Figure 45. District heating, control signal output values depending on marginal value (Behrang-Sirén method).

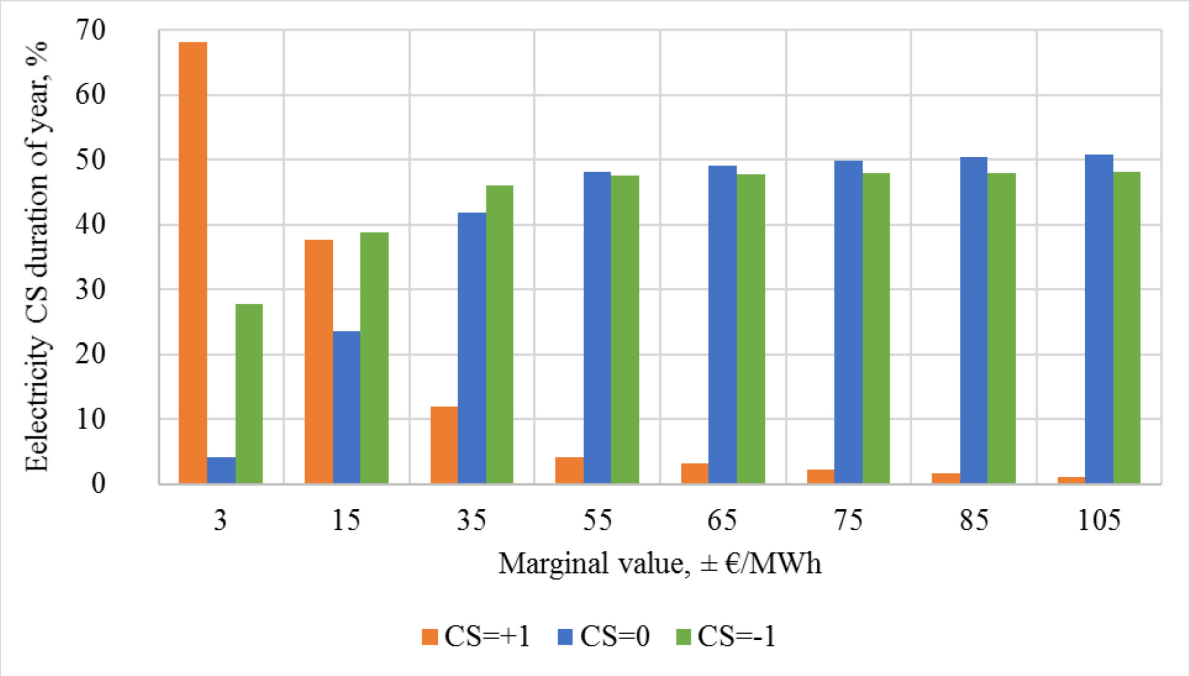

Figure 46. Electricity, control signal output values depending on marginal value (Behrang-Sirén method).

Both figures show the similar trend in control signal output values, but for electricity the number of positive ones is not decreasing as fast as for DH. The reason is that the electricity price is fluctuating more in magnitude compared to DH (see chapter 5.1.5, Figure 26 and Figure 27).

The impact of marginal value was studied by simulating DR-case 5 (see Table 16) with a range of values from ±3 – ±105 €/MWh. The optimal 24-hour average limiting outdoor temperature ($T_{lim, out}$) for allowing heat loading was also determined during the simulations.

Table 20 shows the annual district heating consumption and cost for non-DR cases (2 & 2.1) and marginal value simulation cases. Control algorithm A1 for space heating (see Figure 33) was used in the simulations and case 2 is the reference case for comparison. DR-control of space heating does not affect the electricity consumption or cost and therefore they are not included in the result summary.

Table 20. The effect of marginal value and limiting outdoor temperature ($T_{lim,\ out}$) on heat energy consumption and cost in a space heating DR-controlled case with 40% occupancy.

	Marginal value, ± €/MWh	District heating			
		kWh/m²,a	Δ-%	€/m²,a	Δ-%
Case 2, No DR, reference $T_{SH\ set}$ = 21 °C	-	128.7	-	8.2	-
Case 2.1 No DR $T_{SH\ set}$ = 20 °C	-	121.3	-5.7	7.8	-5.0
$T_{lim,\ out}$, °C					
0	3	130.4	1.3	8.5	3.6
0	15	127.4	-1.0	8.2	-0.5
0	35	125.9	-2.1	7.9	-3.6
0	55	125.4	-2.5	7.8	-4.8
0	65	125.3	-2.6	7.8	-5.1
0	75	125.3	-2.7	7.8	-5.2
0	85	125.2	-2.7	7.8	-5.2
0	105	125.2	-2.7	7.8	-5.2
5	3	133.8	4.0	8.6	4.8
5	15	127.9	-0.6	8.2	-0.4
5	35	126.1	-2.0	7.9	-3.7
5	75	125.3	-2.7	7.8	-5.2
10	3	136.4	6.0	8.7	6.1
10	15	128.0	-0.6	8.2	-0.4
10	35	126.1	-2.0	7.9	-3.7
10	75	125.2	-2.7	7.8	-5.2

Regardless of $T_{lim,\ out}$ value, a high marginal value (≥ ±75) gives at most 2.7% heating energy savings in the DR-controlled cases. The non-DR case 2.1 ($T_{SH,\ set}$=20°C) gives 5.7% heating energy savings. Despite this difference in heating energy, the annual heating cost savings are of the same magnitude (about 5%).

Figure 47 and Figure 48 respectively show the heat energy consumption and cost as a function of marginal value for different $T_{lim.\ out}$ values.

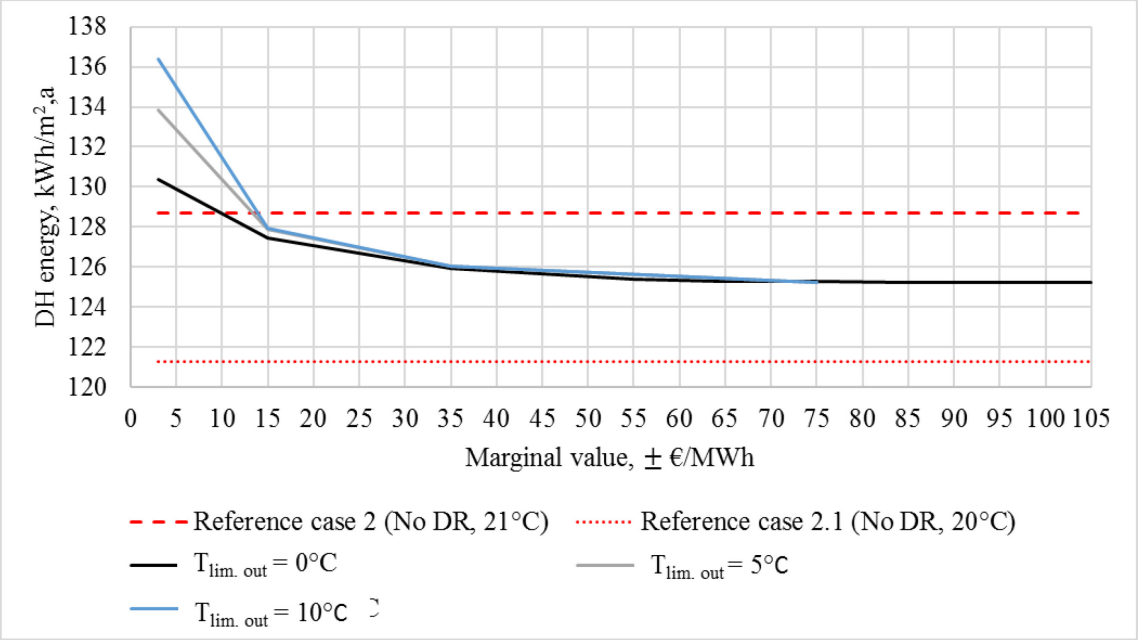

Figure 47. Annual district heating consumption as a function of control signal marginal value.

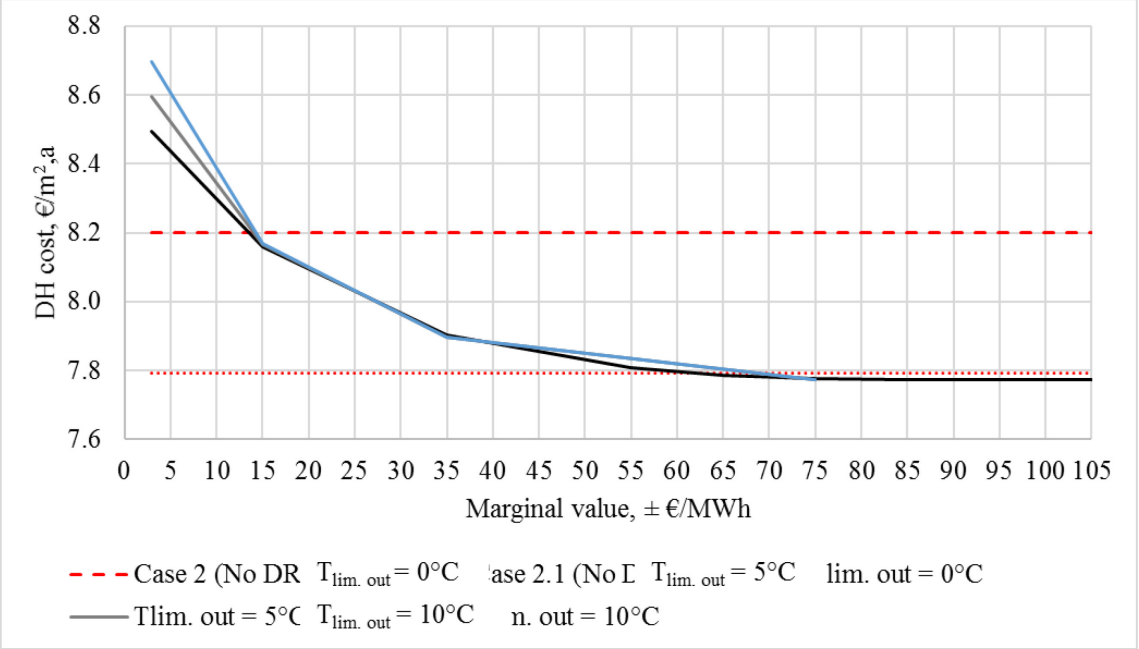

Figure 48. Annual district heating cost as a function of control signal marginal value.

In this building cost savings of the DR-controlled cases are directly connected to less energy usage and therefore the highest marginal values gives the highest benefit. Since heat loading is not favorable, the value of $T_{lim, out}$ is not of importance at all. $T_{lim, out}$ = 0 °C was chosen for the DR-controlled simulations.

Figure 49 shows the annual room air temperature duration for room 4 at $T_{lim, out}$ =0 °C and different marginal values. Only the two lowest marginal values (±15 & 35) show a difference in temperature duration. All the higher marginal values have the same effect on the room air temperature due to the minimum hours of heat loading.

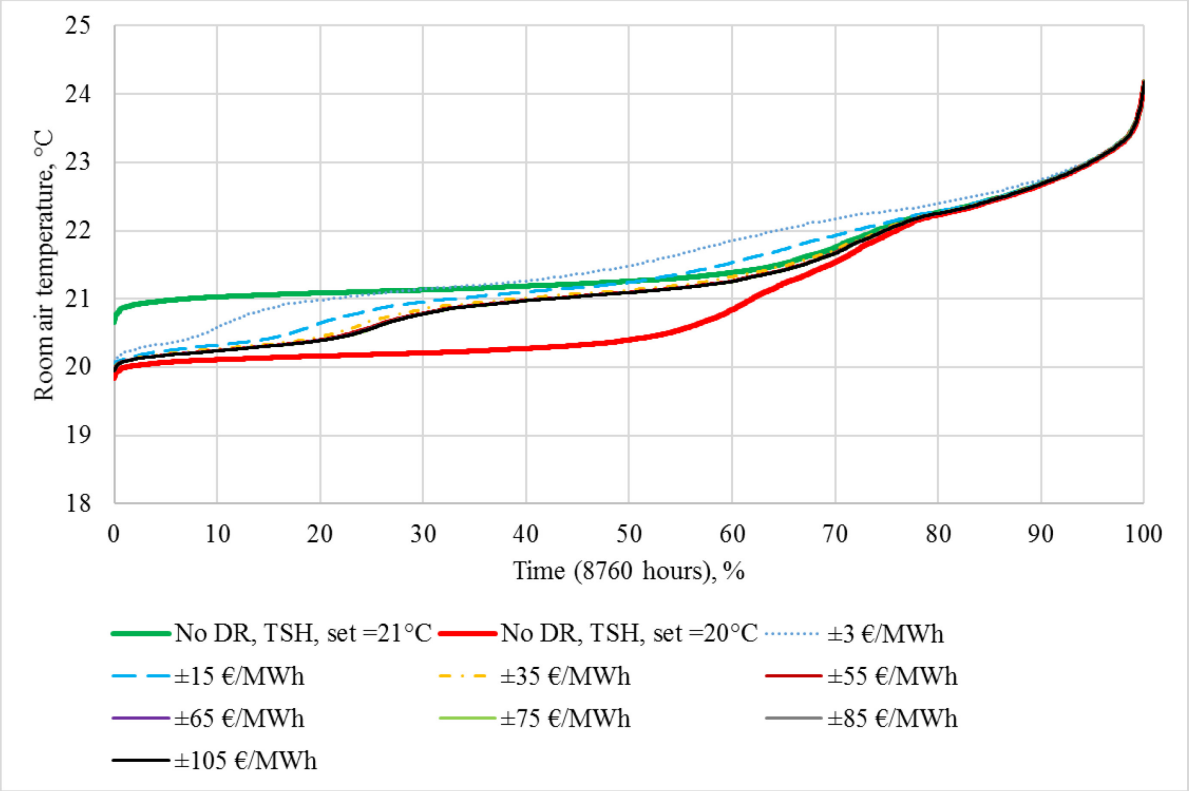

Figure 49. Annual temperature duration of room 4 for different marginal values and constant $T_{lim.\ out.}$ = 0°C.

The results from the marginal value simulations show that with DR the preferred temperature (21°C) is achieved for a majority of the heating season while the cost saving is of the same magnitude as for a constant set-point reduction (Case 2.1).

The optimal marginal value ±75 €/MWh was chosen for most DR-controlled simulations and the $T_{lim.\ out}$ value of 0°C was chosen as a default value. After some initial test simulations including DR-control of space heating and supply air temperature (algorithm B2, see Figure 36) it was decided to assign a $T_{lim,\ out}$ value of +10°C for the AHU. Otherwise the annual hours of DR-control would had remained quite low. Additionally, a positive impact was noticed from increasing the $T_{lim,\ out}$ value for the AHU. For space heating the $T_{lim,\ out}$ value remained as 0°C in all cases.

Summary of chosen control signals for simulation cases

As presented in chapter 5.4, Table 16 & Table 17, four different control signal definitions were chosen for the simulations (see chapter 5.3.1 for the definition of each control signal):

- Behrang-Sirén ±75 €/MWh
- Behrang-Sirén ±15€/MWh
- Dréau-Heiselberg loading + conservation
- Dréau-Heiselberg conservation only

The output values of the four control signal definitions are presented in Figure 50. The Behrang-Sirén ±15 signal includes heat loading (CS=+1) but the Behrang-Sirén ±75 regards

only conservation since there are no positive ones as output value. Also the Dréau-Heiselberg signal definitions include both loading + conservation and conservation only.

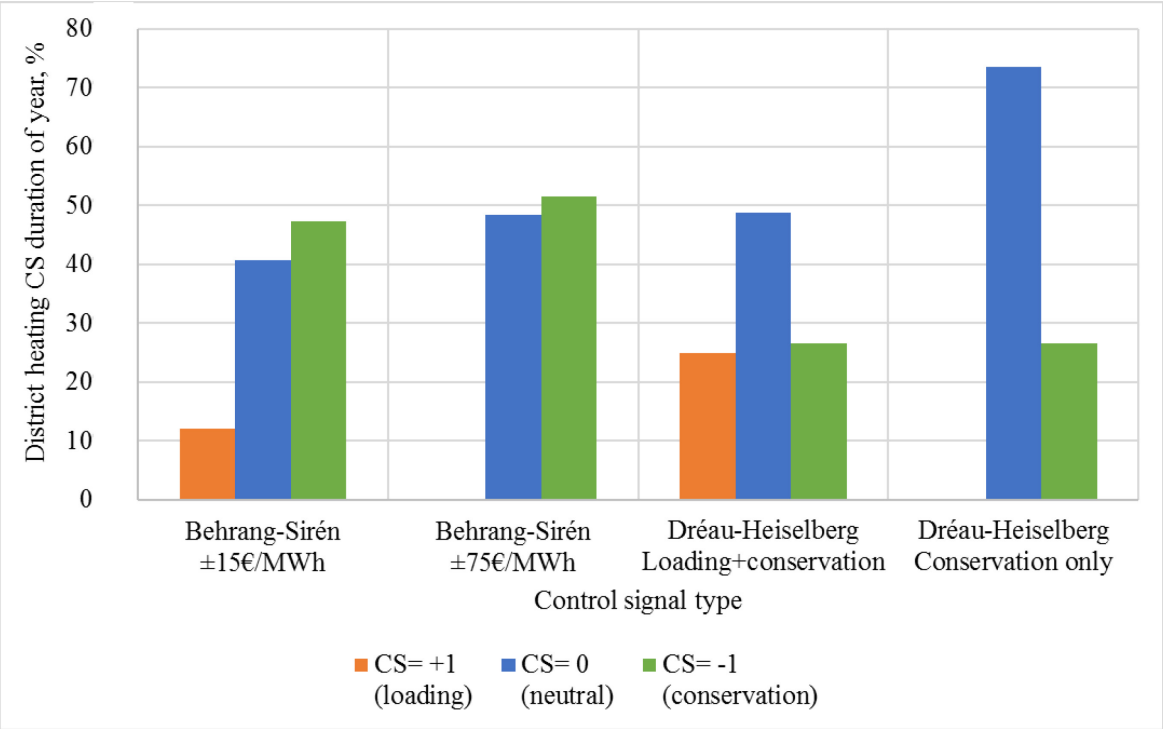

Figure 50. Chosen control signal definitions and their distribution of output values.

6.3 Decentralized DR-controlled cases

6.3.1 Energy consumption and cost

In the following the annual energy consumption and cost are presented for all the decentralized DR-control cases (defined in Table 16) and their respective reference case (defined in Table 15). Figure 51 presents the relative change in energy consumption and cost of all cases. Results of the same cases are shown in Table 21 and Table 22.

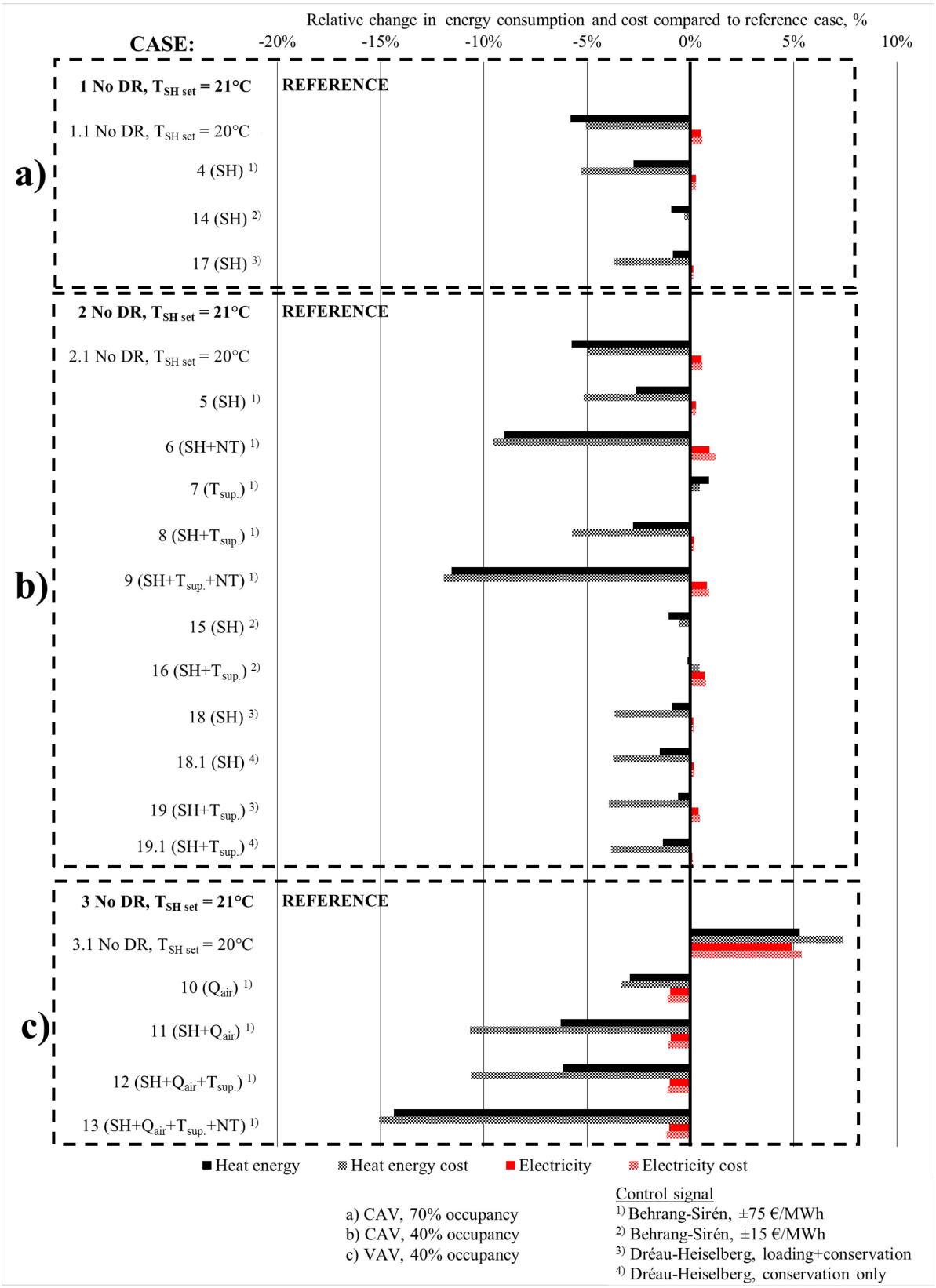

Figure 51. Control algorithm effect on annual energy consumption and cost of the decentralized DR cases with different occupancy and airflow rate control.

Table 21. Main features, annual energy consumption, cost and relative change for DR-controlled decentralized CAV cases.

	Case	DR-control				CS	$T_{SH\ set}$ Range	DH consumption		DH cost		Electricity consumption		Electricity cost	
		SH	$T_{sup.}$	Q_{air}	NT			kWh/m²,a	Δ, %	€/m²,a	Δ, %	kWh/m²,a	Δ, %	€/m²,a	Δ, %
70% occupancy, CAV	1 No DR $T_{SH\ set}$ = 21°C	No DR-control				-	21	124.9	0.0	8.0	0.0	59.3	0	8.2	0
	1.1 No DR $T_{SH\ set}$ = 20°C	No DR-control				-	20	117.7	-5.8	7.6	-5.1	59.6	0.5	8.2	0.6
	4 (SH)	x				[1]	20-24.5	121.4	-2.8	7.6	-5.3	59.4	0.3	8.2	0.3
	14 SH)	x				[2]	20-24.5	123.7	-0.9	8.0	-0.3	59.3	0.1	8.2	0.1
	17 (SH)	x				[3]	20-24.5	123.8	-0.9	7.7	-3.7	59.4	0.1	8.2	0.1
40% occupancy, CAV	2 No DR TSH set = 21 °C	No DR-control				-	21	128.7	0.0	8.2	0.0	57.3	0	7.9	0
	2.1 No DR TSH set = 20 °C	No DR-control				-	20	121.3	-5.7	7.8	-5.0	57.6	0.5	7.9	0.6
	5 (SH)	x				[1]	20-24.5	125.3	-2.7	7.8	-5.2	57.5	0.3	7.9	0.3
	6 (SH)	x			x	[1]	20-24.5	117.1	-9.0	7.4	-9.6	57.8	0.9	8.0	1.2
	7 ($T_{sup.}$)		x			[1]	21	129.8	0.9	8.2	0.4	57.3	0	7.9	0
	8 (SH+ $T_{sup.}$)	x	x			[1]	20-24.5	125.1	-2.8	7.7	-5.7	57.4	0.2	7.9	0.2
	9 (SH+ $T_{sup.}$+NT)	x	x		x	[1]	20-24.5	113.8	-11.6	7.2	-11.9	57.8	0.8	8.0	0.9
	15 (SH)	x				[2]	20-24.5	127.3	-1.0	8.2	-0.5	57.3	0.1	7.9	0.1
	16(SH+ $T_{sup.}$)	x	x			[2]	20-24.5	128.5	-0.1	8.2	0.4	57.7	0.7	7.9	0.7
	18 (SH)	x				[3]	20-24.5	127.5	-0.9	7.9	-3.7	57.4	0.2	7.9	0.2
	18.1 (SH)	x				[4]	20-24.5	126.8	-1.5	7.9	-3.7	57.4	0.2	7.9	0.2
	19 (SH)+ $T_{sup.}$)	x	x			[3]	20-24.5	127.9	-0.6	7.9	-3.9	57.5	0.4	7.9	0.5
	19.1 (SH+ $T_{sup.}$)	x	x			[4]	20-24.5	126.9	-1.3	7.9	-3.9	57.4	0.1	7.9	0.1

[1] Behrang-Sirén, marginal value: ±75€/MWh

[2] Behrang-Sirén, marginal value: ±15€/MWh

[3] Dréau-Heiselberg, time period for determining CS: 2 weeks

[4] Dréau-Heiselberg, conservation only, time period for determining CS: 2 weeks

Table 22. Main features, annual energy consumption, cost and relative change for DR-controlled decentralized VAV cases.

	Case	DR-control				CS	$T_{SH\ set}$ Range	DH consumption		DH cost		Electricity consumption		Electricity cost	
		SH	$T_{sup.}$	Q_{air}	NT			kWh/m²,a	Δ, %	€/m²,a	Δ, %	kWh/m²,a	Δ, %	€/m²,a	Δ, %
40% occupancy, VAV	3 No DR $T_{SH\ set}$ = 21 °C	No DR-control				-	21	72.0	0.0	4.7	0.0	41.1	0	5.8	0
	3.1 No DR $T_{SH\ set}$ = 20 °C	No DR-control				-	20	75.8	5.3	5.0	7.4	43.1	4.9	6.1	5.4
	10 (Q_{air})			x		[1)]	21	69.9	-2.9	4.5	-3.3	40.7	-1	5.7	-1.1
	11 (Q_{air}+SH)	x		x		[1)]	20-24.5	67.5	-6.3	4.2	-10.7	40.7	-1	5.7	-1.1
	12 (Q_{air}+SH+ $T_{sup.}$)	x	x	x		[1)]	20-24.5	67.6	-6.2	4.2	-10.6	40.6	-1	5.7	-1.1
	13 (Q_{air}+SH+ $T_{sup.}$+NT)	x	x	x	x	[1)]	20-24.5	61.7	-14.4	4.0	-15.1	40.6	-1	5.7	-1.2

[1)] Behrang-Sirén, marginal value: ±75€/MWh

Decentralized CAV cases

Table 21 show that both annual heat energy consumption and cost are varying with DR-control, but annual electricity consumption and cost are quite unchanged. The occupancy does not impact on the simulation results. The relative change in energy consumption and cost (Δ%) are of the same magnitude for both occupancy schemes (see case 4 vs. case 5, case 14 vs. case 15 and case 17 vs. case 18).

The highest heat energy cost saving achieved for the CAV cases is 11.9% and 9.6% respectively by case 9 and case 6. Both cases include night time set-back control. When considering purely DR-controlled cases the highest cost savings are 5.7%, 5.3% and 5.2% respectively for case 8, 4 and 5. Case 4 & 5 consider DR-control of space heating and case 8 space heating + supply air temperature. The control signal definition used in these cases was the Behrang-Sirén ±75 €/MWh, which results in conservation and not any heat loading.

The cases utilizing control signal definition Behrang-Sirén ±15 €/MWh (cases 14, 15 and 16) are both loading and conserving during DR-control. However, the cost savings are negligible. Case 15 (SH) has a cost saving of 0.5% and case 16 (SH+$T_{sup.}$) has an increased cost of 0.4%.

The Dréau-Heiselberg control signal definition cases for both loading and conservation (cases 17, 18 and 19) reaches a cost saving of 3.7% – 3.9%. The same cost saving is achieved by cases 18.1 (SH) and 19.1 (SH+$T_{sup.}$) which are utilizing the Dréau-Heiselberg signal definition for conservation only.

There are some small differences in the electricity consumption resulting from the conference room which is VAV-controlled in every case. The VAV of the conference room is trying to aid the space heating system whenever the room temperature decreases below 20°C by increasing the airflow. This increased consumption can be neglected since it is a result of poor control possibilities in the simulation software. In a real building such a condition could be avoided easily by correct programming of the building automation. Eliminating this phenomenon would give slightly higher cost savings.

Figure 52 shows the effect on annual heat energy consumption and cost when adding different DR-control elements to the CAV cases. All cases have a 40% occupancy and utilizes the Behrang-Sirén control signal definition with ±75 €/MWh marginal value.

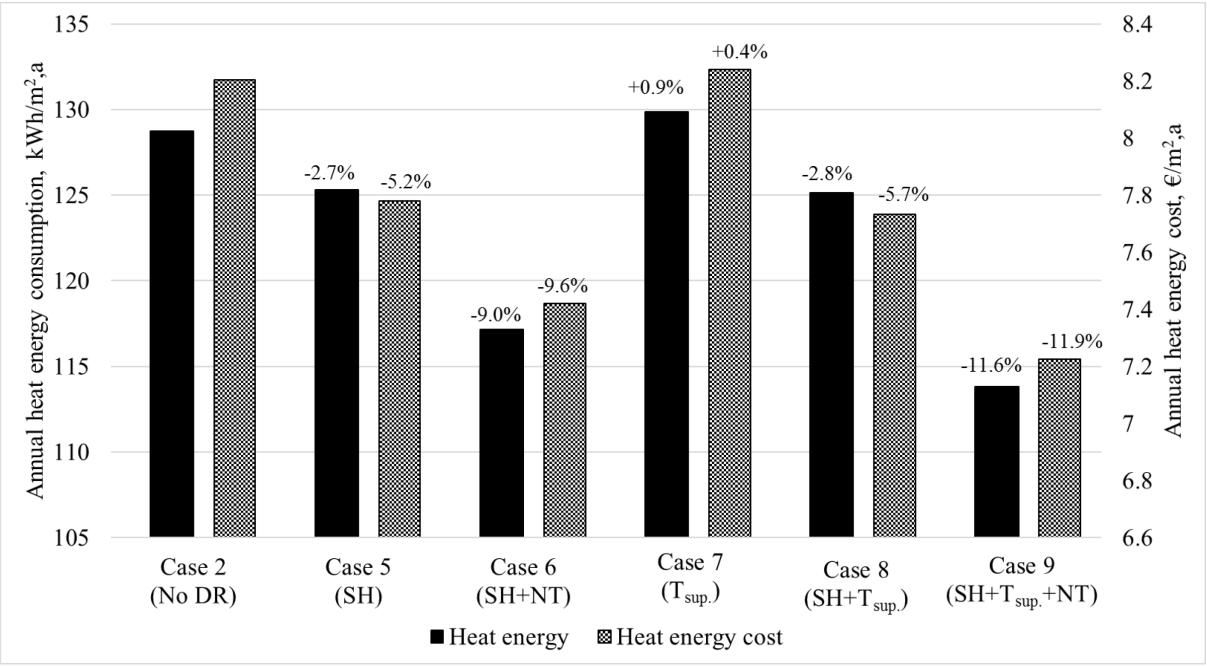

Figure 52. Annual heat energy consumption, cost and relative change from DR-control in the decentralized CAV cases with 40% occupancy and Behrang-Sirén ±75 €/MWh control signal definition.

Figure 52 show that space heating control (case 5) and space heating + night time set-back (case 6) decreases both the energy consumption and cost. DR-control of only supply air temperature (case 7) does not give any benefit, instead the energy consumption and cost increase a bit. The reason is that room temperature set-point is constantly 21 °C which increases the heat output from the radiators when the supply air temperature is reduced. Combining space heating and supply air temperature control (case 8) gives a slight improvement (0.5%-units) in the cost savings compared to only space heating control. The same trend can be seen in case 9 compared to case 6, where night time set-back mode is included along with space heating and supply air temperature control.

The reason for why supply air temperature control gives additional benefit when combined with space heating control but don't give any benefit when solely controlled is due to the room temperature set-points. For case 8 (SH+$T_{sup.}$), whenever the supply air temperature is decreased, the room temperature set-point is also decreased. This means that the radiators do not have to compensate for the cooling effect of the supply air until the room temperature has reached its new reduced set-point (20°C).

The change in AHU heating energy as a function of change in space heating energy is presented in Figure 53. Additionally, the fitted linear regression curve of the results is plotted.

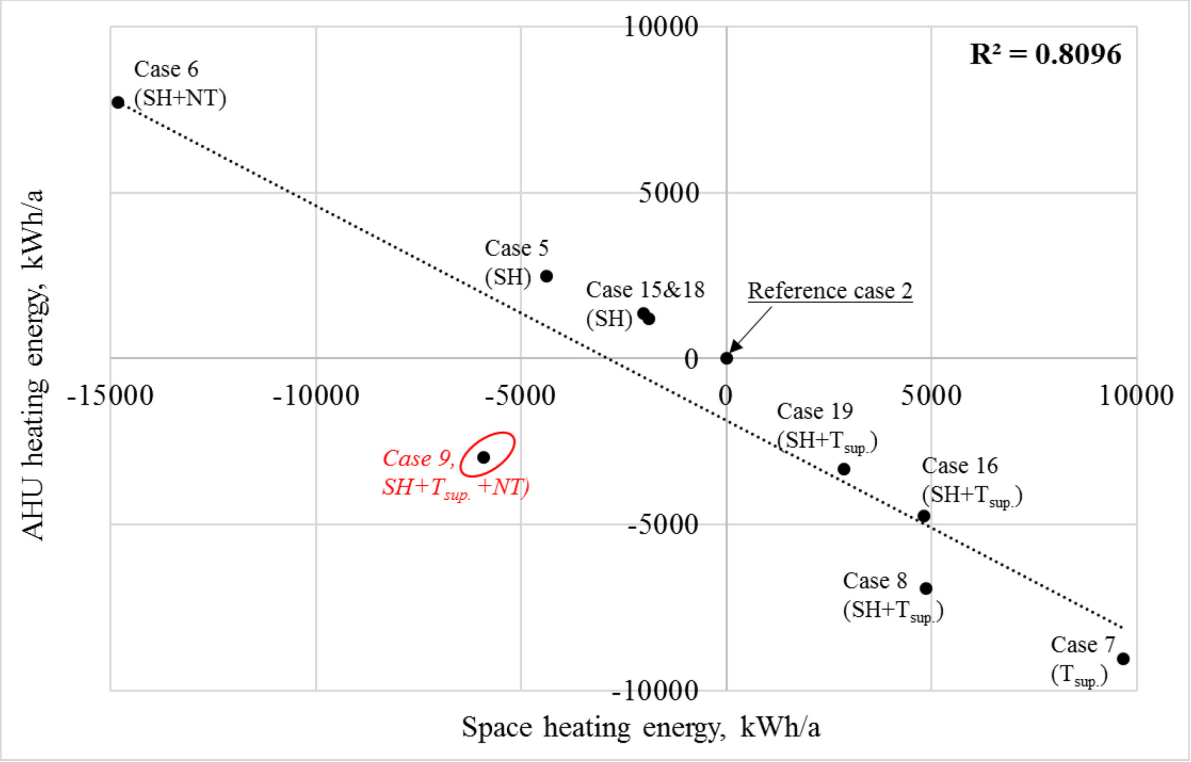

Figure 53. Change in annual AHU heating energy as a function of change in annual SH energy.

In Figure 53, the case specific change in either AHU or space heating energy is defined as the difference in energy consumption of a DR-controlled case and the reference case 2. A decrease in space heating energy results in an increase in AHU heating energy and vice versa. Case 7 ($T_{sup.}$) has about a 10 000 kWh decrease in AHU heating energy due to the DR-control, but instead the space heating energy is increased by nearly the same amount. Case 5 (SH) on the other hand has a reduction of around 4 500 kWh in space heating energy which yields an increase of about 3 000 kWh in AHU heating energy due to the colder return temperature arriving at the AHU heat recovery. Case 9 (SH+$T_{sup.}$+NT) is however an exception, since both room air and supply air temperature are decreased during night time, the AHU needs less heating after the heat recovery. The regression line in the figure has a high correlation coefficient (R^2=0.8) which indicates a strong correlation in how the changes in space heating and AHU energy consumption are connected.

Decentralized VAV cases compared to CAV case

When looking at the VAV cases in Table 22 it can be seen that both annual heating and electricity energies and costs are much lower than for the CAV cases (Table 21). Figure 54 and Figure 55 show the energy, cost and relative change for the VAV cases compared to CAV reference case 2. All VAV cases have the occupancy 40% and utilizes the Behrang-Sirén control signal definition with ±75 €/MWh marginal value.

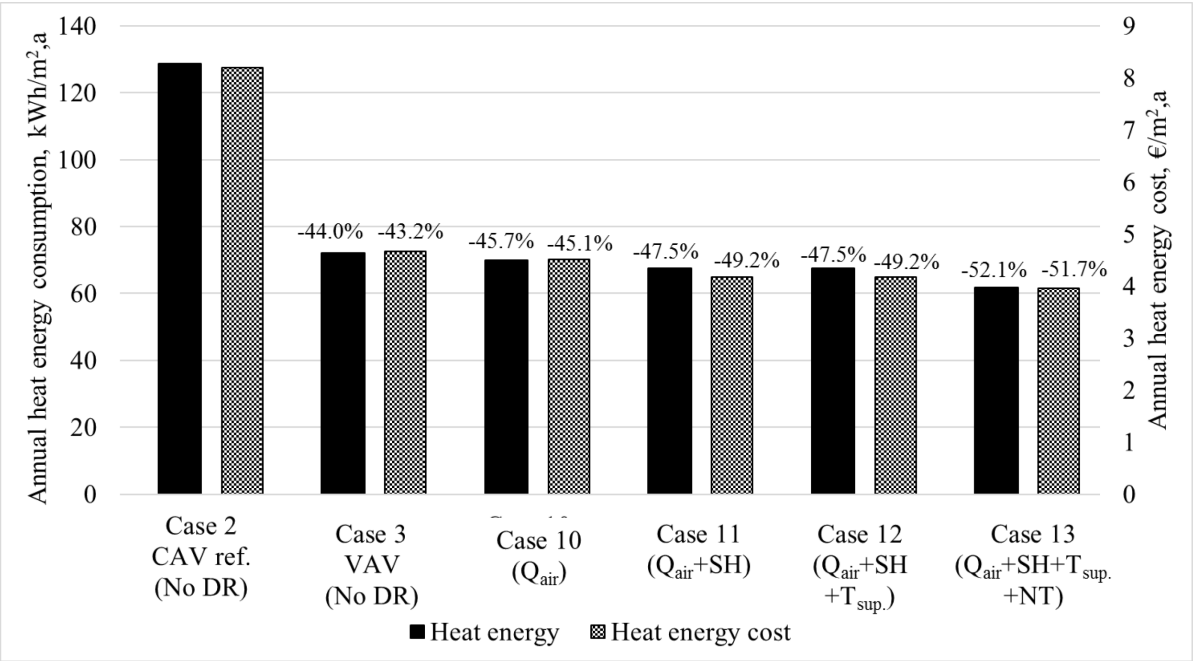

Figure 54. Annual heat energy consumption, cost and relative change for DR-controlled VAV cases compared to CAV case (40% occupancy, Behrang-Sirén ±75 €/MWh control signal definition).

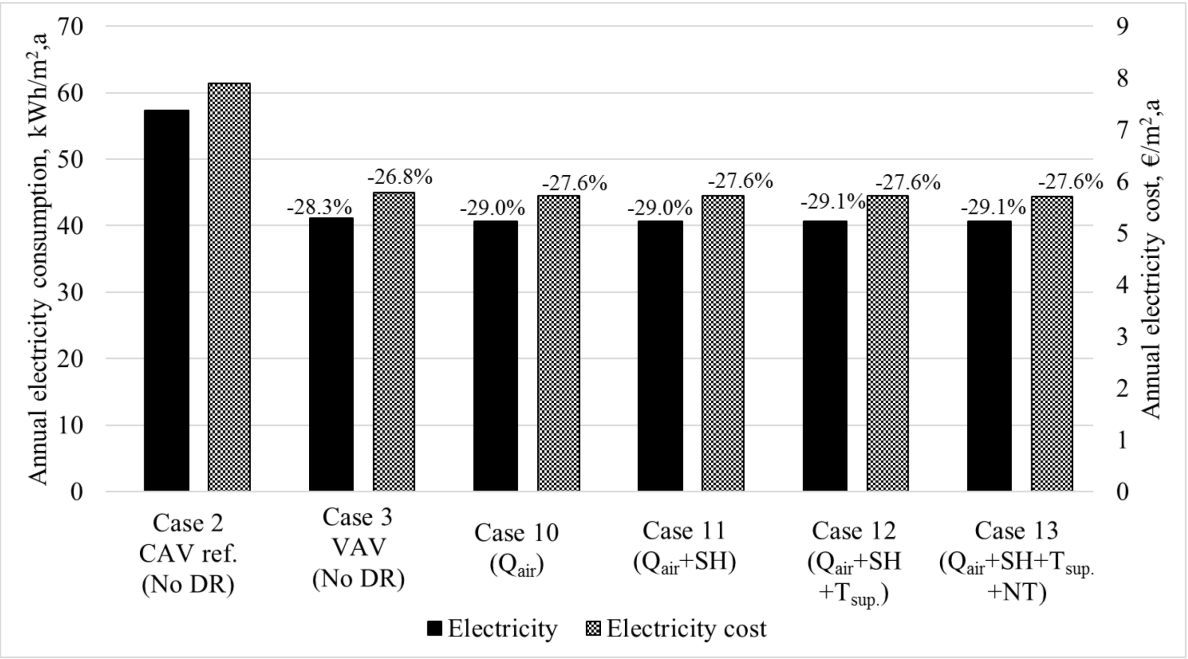

Figure 55. Annual electricity consumption, cost and relative change for DR-controlled VAV cases compared to CAV case (40% occupancy, Behrang-Sirén ±75 €/MWh control signal definition).

Figure 54 and Figure 55 show that by changing the design of the current ventilation system from CAV to VAV (case 2 → case 3) annual cost savings of 43.2% and 26.8% are achieved for heat and electricity respectively. Introducing DR-control of airflow (case 10) gives an additional cost saving of 1.9%-unit and 0.8%-unit respectively for heat and electricity. Including space heating in the DR-control (case 11) adds 4.1%-units of heat energy cost saving while the addition of supply air temperature control does not give any additional benefit. The

last VAV case which includes night time set-back (case 13) has the most heat energy cost saving of 51.7% compared to the reference case.

The results in Figure 54 suggests that DR-control of airflow based on measured CO_2-concentration does not give any substantial benefit. The specific airflow rate duration of the whole 4th floor for the occupied time in both case 3 (VAV, no DR) and case 10 (Q_{air}) are presented in Figure 56.

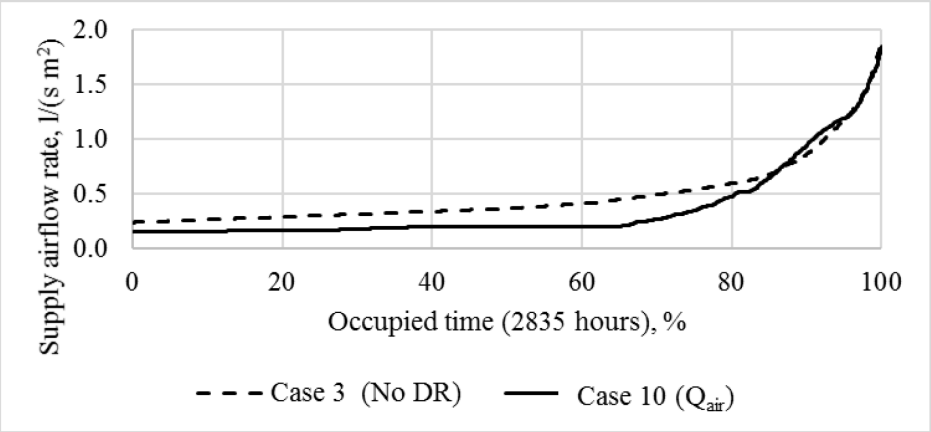

Figure 56. Duration curve for specific supply airflow rate of 4th floor for VAV reference case 3 and DR-controlled airflow case 10 during occupied hours.

For the VAV reference case 3 (No DR) shown in Figure 56 an airflow rate below 0.5 l/(s m^2) is for the majority of the occupied hours enough to keep the CO_2 concentration on the set-point level (800 PPM). Hence the ventilation demand for the VAV reference case (3) is already very low and therefore the DR-control of airflow does not have a significant impact, since the minimum allowed airflow rate is 0.15 l/(s m^2). The reason for the low ventilation demand is partly due to the low occupancy of the building floor and big air volumes of the rooms. Additionally, the office rooms are simulated with open doors during occupied time which dilutes the CO_2-load into the corridor air. This increases the time period of achieving CO_2 set-point level.

Figure 57 shows the duration curve of specific airflow rate for the 4th floor during occupied hours for both open and closed office door alternatives.

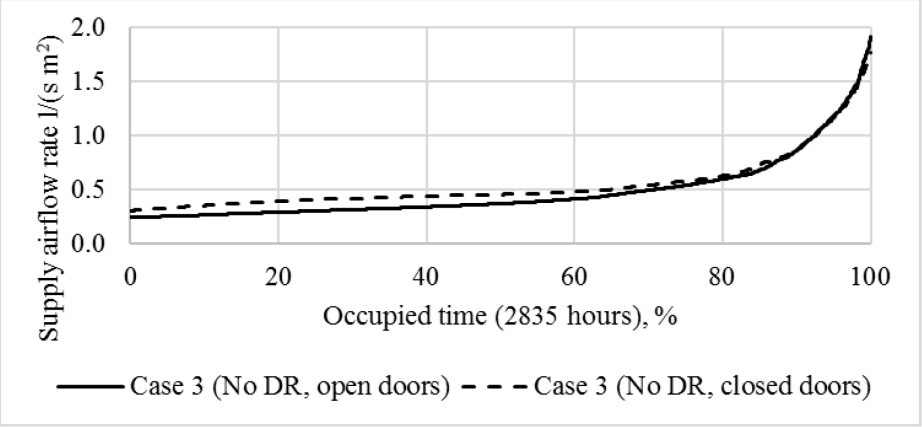

Figure 57. Duration curve for specific supply airflow rate of 4th floor for VAV reference case with open or closed office doors during occupied hours.

The closed-door case demands a slightly higher airflow rate since the diluting effect from the corridor is removed, as showed in Figure 57. The saving potential would be bigger if the office doors were to be kept closed. This also implies that a higher occupancy scheme would have higher savings potential. Higher occupancy results in higher CO_2 load which results in a higher ventilation demand to keep the normal CO_2 set-point. Additionally, during an increased CO_2 set-point situation the airflow reduction would be bigger. However, to be sure about these hypotheses additional simulations are needed.

Decentralized VAV cases compared to VAV reference case

Figure 58 and Figure 59 show the energy, cost and relative saving of the DR-controlled VAV cases compared to the VAV reference case 2. All cases have 40% occupancy and utilizes the Behrang-Sirén control signal definition with ±75 €/MWh marginal value.

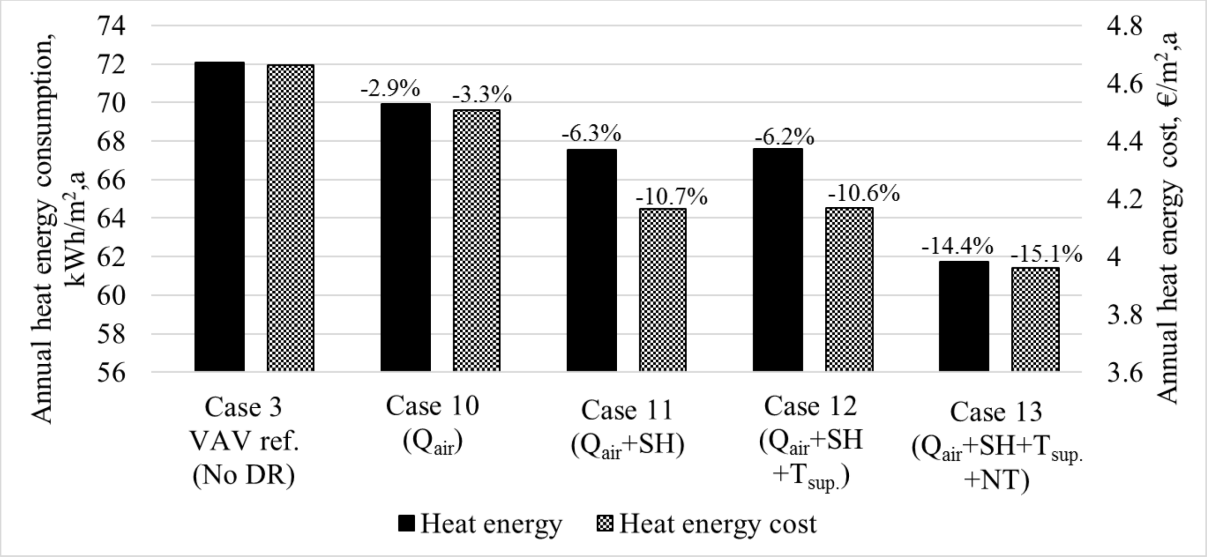

Figure 58. Annual heat energy consumption, cost and relative change for DR-controlled VAV cases compared to VAV reference (40% occupancy, Behrang-Sirén ±75 €/MWh control signal definition).

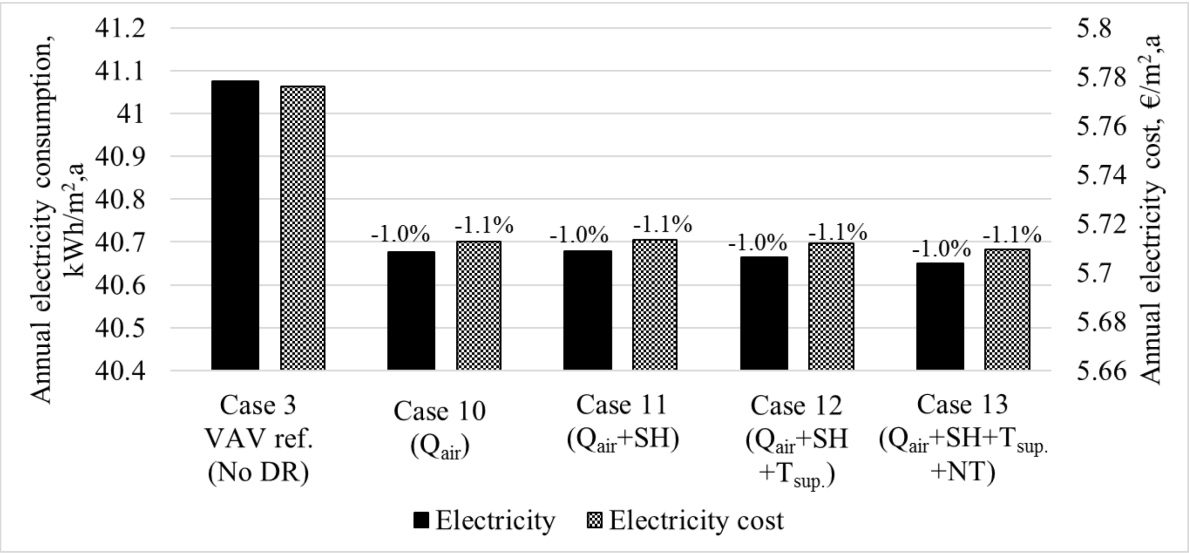

Figure 59. Annual electricity consumption, cost and relative change for DR-controlled VAV cases compared to VAV reference (40% occupancy, Behrang-Sirén ±75 €/MWh control signal definition).

As shown in Figure 58 and Figure 59, DR-control of airflow only (case 10) gives 3.3% and 1.1% cost saving for heating and electricity respectively. Again, the already low need of airflow in the reference case 3 results in a low savings potential by DR-control of airflow. Adding on space heating control (case 11) increases the heat energy cost saving to 10.7%. Space heating + supply air temperature control (case 12) does not give any additional benefit. Including night time set-back mode (case 13) gives the biggest heat energy cost saving of 15.1%.

Figure 60 shows the relative change in heat energy cost by different DR-control elements for CAV and VAV cases respectively. Notice that the VAV reference case includes DR-control of airflow for this comparison to be possible.

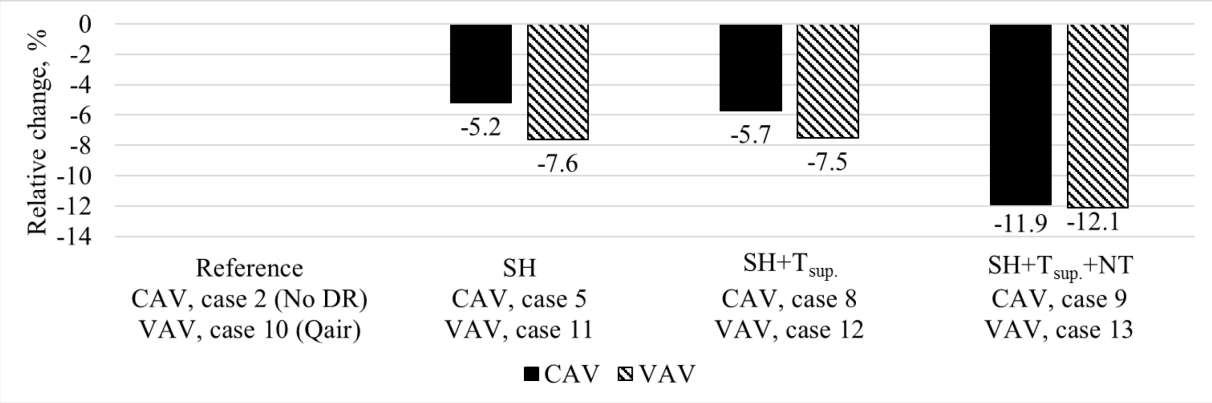

Figure 60. Heat energy and cost savings of DR-controlled CAV and VAV cases (40% occupancy, Behrang-Sirén ±75 €/MWh control signal definition).

The relative cost savings are higher for the VAV cases including space heating and space heating + supply air temperature control. This is due to that the annual heat energy demand and cost of the AHU is smaller in the VAV cases, which then increases the relative importance of the space heating savings. In the night time set-back cases (cases 9 and 13) the relative savings are of the same magnitude, since the CAV case's AHU heat energy cost savings are bigger due to the higher airflow rate.

Effect of control signal definition method

Figure 61 and Figure 62 respectively show the impact on heat energy consumption and cost of algorithms A1 (SH) and B2 (SH+$T_{sup.}$) in the CAV cases depending on control signal definition method.

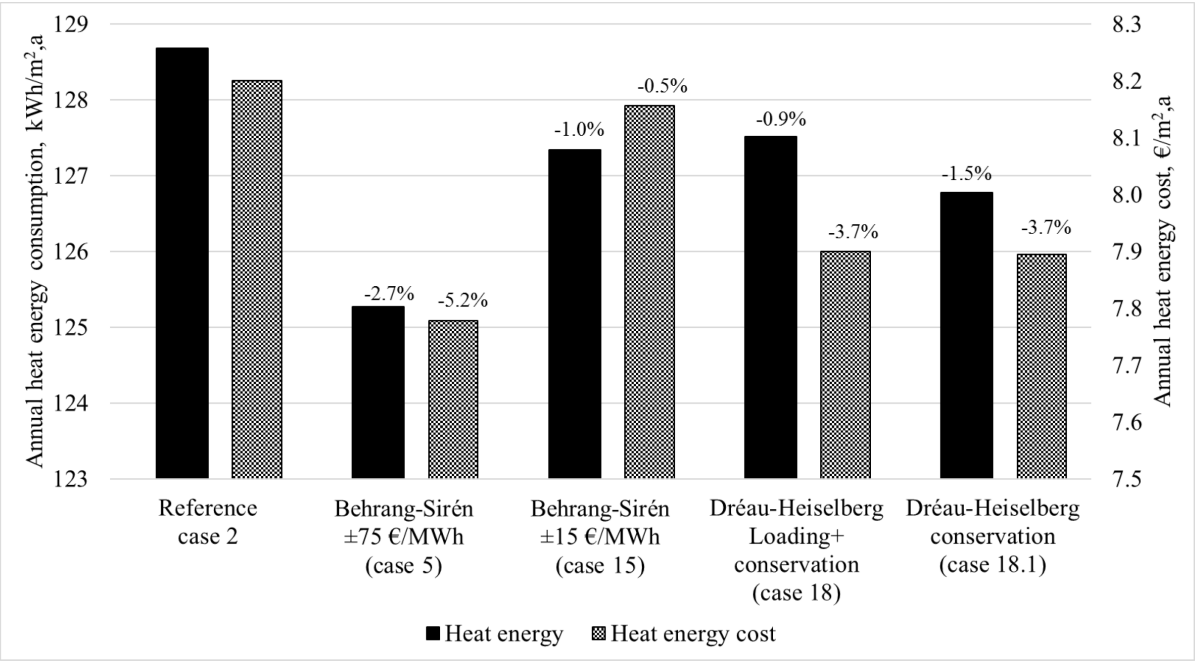

Figure 61. Annual heat energy consumption and cost of DR-controlled CAV cases (SH) depending on control signal definition (40% occupancy).

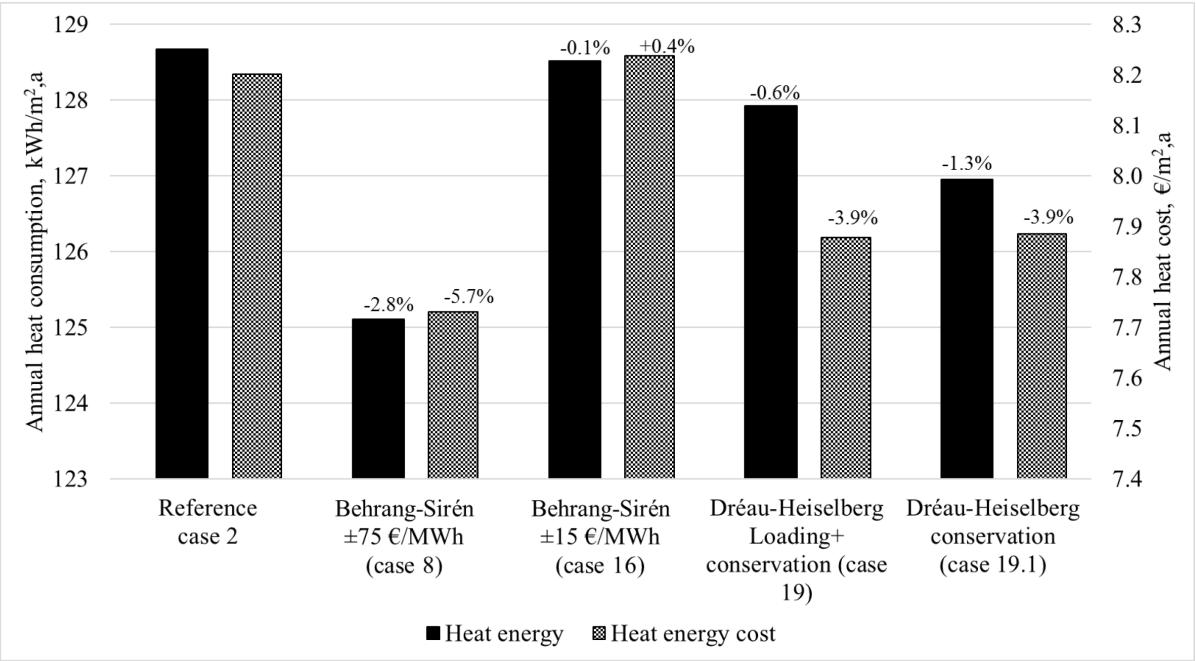

Figure 62 Annual heat energy consumption and cost DR-controlled CAV cases (SH+$T_{sup.}$) depending on control signal definition (40% occupancy).

Figure 61 show that the utilization of the Behrang-Sirén control signal directly connects the reduction of heat energy consumption and cost with a higher marginal value (e.g. case 5, 5.2% vs. case 15, 0.5%) which results in mostly heating conservation. This implies the building does not achieve any benefit from heat loading, which was also the result of the marginal value determination in chapter 6.2. However, when utilizing the control signal defined by the Dréau-Heiselberg method the same trend cannot be seen. Case 18 (includes loading and conservation)

achieves equally much cost savings (3.7%) as case 18.1 (includes only conservation), although the energy savings are lower (0.9% and 1.5% respectively). The same trends in change on heat energy consumption and cost can be seen when including DR-control of both space heating and supply air temperature (Figure 62).

Cost distribution within price ranges

Figure 63 shows the realized heat energy cost at different price ranges for different control signal definitions combined with space heating algorithm A1 (see Figure 33). Additionally, the annual average and median value of the hourly district heat price (HDHP) is shown.

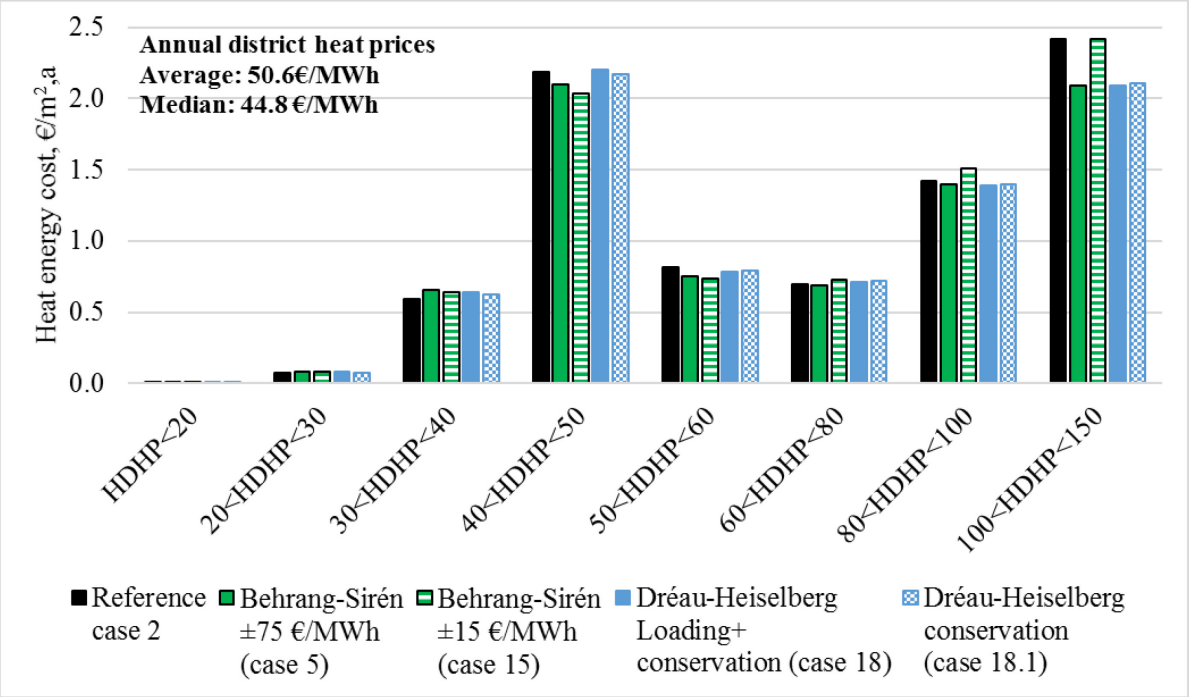

Figure 63. Realized heating cost according to hourly district heating price (HDHP) ranges for reference case and four different control signal definition cases combined with space heating algorithm A1 and 40% occupancy.

The annual maximum and minimum district heating price is 145.4 €/MWH and 9 €/MWh respectively. The heating energy bought at the cheapest price range (HDHP<20€/MWh) constitute only 0.001% of the annual heating energy costs.

The price within the range 20€/MWh < HDHP < 40 €/MWh is more utilized by all control signal definitions than the reference case.

The price range 40€/MWh <HDHP < 50€/MWh constitutes a big share of total annual costs (25% – 28%), which is expectable since both the annual average and median district heat price lays within that range. In this range the Behrang-Sirén control signal definitions (case 5 & 15) manage to cut the costs by 4% – 7% compared to the reference. The Dréau-Heiselberg control signal definitions (case 18 & 18.1) have a much similar heat energy cost share with the reference case, which also is expectable since the median price level is found in this range. A median price is classified as neutral in the Dréau-Heiselberg control signal definition and results in normal heating control according to need. The classification of low, high and neutral

prices was explained more in detail in chapter 4.1.2. The control signal definitions show the same trend in behavior for the following price range (50€/MWh < HDHP < 60 €/MWh) since this range is close to the annual average and median prices.

For the three most expensive price ranges the general trend is that case 5, 18 and 18.1 cuts energy costs and case 15 increases costs, compared to the reference case. The biggest difference is seen in the most expensive energy price range (100€/MWh <HDHP< 150€/MWh) where (case 5, 18 and 18.1) manage to cut energy cost about 14% compared to the reference case. Case 15 does not have any impact at all in this price range.

As presented in chapter 6.2, Figure 50, the Behrang-Sirén ±15 €/MWh control signal definition results in about 12% loading hours (1062 hours) on an annual basis and the Dréau-Heiselberg control signal definition including both loading and conservation results in about 26% (2177 hours). However, the amount of these hours that occur at times when heat loading is allowed by the algorithms ($T_{avr,\ 24\ out} < T_{lim,\ out}$) is only 8.9% (777 hours) and 3.9% (341 hours) respectively for the Behrang-Sirén ±15 and Dréau-Heiselberg control signal definitions. In other words, the Behrang-Sirén signal has more than twice as much loading hours which are applicable. This does however not explain why the loading effect does not have a positive impact for the Behrang-Sirén signal. The reason lays in within how the two different signal definitions determine when to load. Table 23 presents the average, median, maximum and minimum price for which the two control signal definitions has used heat energy during loading.

Table 23. District heat prices during loading.

		District heat price during loading [€]			
Control signal definition	**Characteristic**	**Average**	**Median**	**Max**	**Min**
Behrang-Sirén ±15 €/MWh	Loading + conservation	85	87	145	24
Dréau-Heiselberg	Loading + conservation	40	42	50	22

As shown in Table 23, the Behrang-Sirén ±15 control signal definition results in heat loading with an average district heat price 125% more expensive than for the Dréau-Heiselberg control signal definition. As shown in chapter 5.3.1, the Behrang-Sirén signal initiates loading if the 24-hour future price trend increase sufficiently much relative to the actual hourly energy price. The Dréau-Heiselberg signal initiate loading if the hourly price is low compared to 2 weeks of history data (below 1st quartile of the historical prices). There seem to be room of improvement in the way the control signal is generated. A mixed version of the Behrang-Sirén and Dréau-Heiselberg method of determining heat energy loading could be more effective. However, it seems in general that this building does not really benefit from heat loading and one significant reason is the high ventilation air flow rate with its cooling impact on room air temperature.

6.3.2 Flexibility factor

The flexibility factor concept and its determination were presented in chapter 4.1.2, equation 3. The possible range of the flexibility factor is -100% – +100%. With a flexibility of -100%, the building is only able to buy heating energy during high price periods. The opposite would be a building able to buy heating energy only during cheap price periods, resulting in a flexibility factor of +100%.

Decentralized CAV cases

Figure 64 summarizes the total heating flexibility (delivered district heat) for all the decentralized CAV cases.

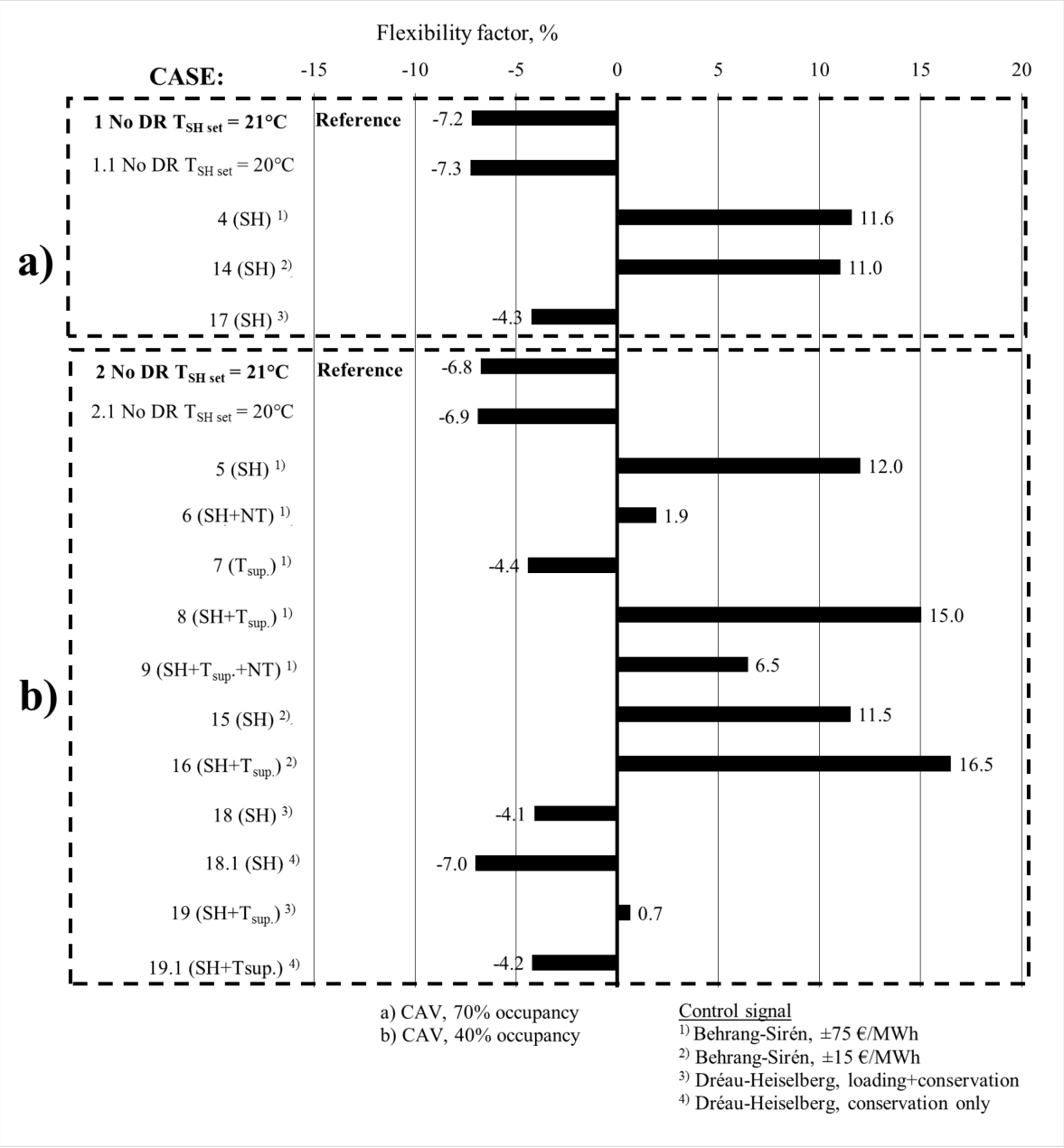

Figure 64. Total district heating flexibility factors for decentralized CAV cases.

For the reference cases without DR, the flexibility factor is about -7%. In general, it can be expected that a building without demand response has a flexibility factor around 0%, since it continuously buys heat according to demand regardless of price fluctuations.

Most of the combinations of DR-control elements and control signal type results in a positive flexibility factor. The occupancy does not seem to have an effect on the flexibility factor (case 4 vs. case 5, case 14 vs. case 15 and case 17 vs. case 18). The magnitude of the flexibility is quite the same regardless of occupancy.

The highest flexibility factor achieved is 16.5% by case 16, which controls both space heating and supply air temperature based on a control signal definition including loading and conservation (Behrang-Sirén ±15 €/MWh). Case 8 achieves 15% flexibility by controlling the same elements but with a control signal definition regarding conservation only (Behrang-Sirén ±75 €/MWh).

Night time set-back mode seems to have a negative effect on the flexibility since both case 6 and 9 have much lower flexibility respectively to case 5 and 8 (same control without night time set-back).

The flexibility of the cases involving control signal definition according to Behrang-Sirén method are better than the cases utilizing Dréau-Heiselberg control signal definitions. One main factor affecting the result is the time period used when defining the limits of low and high price for the flexibility factor (discussed in chapter 4.1.2 and shown in Figure 20). The time period used for categorizing prices also defines the time frame of which the flexibility factor is describing the buildings ability to cooperate with the dynamic price signals of the energy producer. The price limits for cases with Dréau-Heiselberg control signal definition are determined according to the moving 2 weeks historical prices, since that is the time period base for the control signal itself. The Behrang-Sirén control signal is based on moving 24-hour future price information and therefore the flexibility price limits are defined in the same interval.

In other words, the results of cases 17, 18, 18.1, 19 and 19.1 describes the long-term flexibility on a two-week level (Dréau-Heiselberg control signal definition). The rest of the cases describe the short-term flexibility on a daily level (Behrang-Sirén control signal definition). In this sense the flexibility result of cases with different control signal definition is not necessarily comparable with each other.

Figure 65 present the flexibility of total district heating, space heating and AHU for the decentralized DR-controlled CAV cases. The control signal definition used is Behrang-Sirén with a marginal value of ±75 €/MWh.

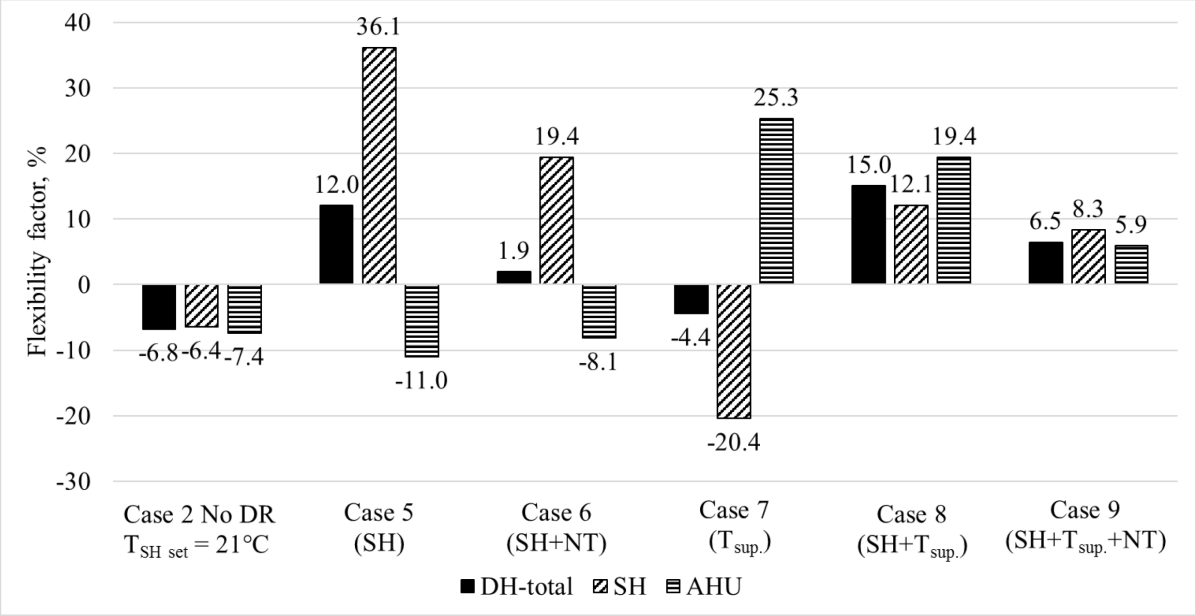

Figure 65.The impact of DR-control on flexibility factors for space heating, AHU and total district heating in the decentralized CAV cases.

DR-control of space heating only (case 5) increases the space heating flexibility from -6.4% to 36.1% but the total flexibility increases only from -6.8% to 12%. The reason is the increased power demand of the AHU due to lower return air temperature to the heat recovery. This increased power demand takes place during high price periods, when the space heating energy usage is decreased.

Addition of night time set-back mode (case 6) decreases the total flexibility quite much compared to case 5. The reason is likely connected to the lesser amount of bought energy at night time. The night time heat is in general more often classified as low-priced. A reduced heating need during night in combination with a normal heating need during day increases the fraction of high-price energy on annual level, which decreases the flexibility factor. The same phenomenon can be seen in case 9 (SH+$T_{sup.}$+NT) compared to case 8 (SH+$T_{sup.}$).

DR-control of supply air temperature only (case 7) increases the AHU flexibility much, but decreases the space heating flexibility resulting in an overall low total flexibility. When combining DR-control of both space heating and supply air temperature (case 8) the best total flexibility (15%) is achieved.

As was shown in Figure 53 the heating demand of space heating and AHU are strongly connected to each other. If one of them is decreased due to DR-control, the other one is increased. The conclusion is that in order to achieve a very good total flexibility, the DR-control has to include both space heating and AHU in an optimized way.

Decentralized VAV cases

Figure 66 present the flexibility of total district heating, space heating and AHU for the decentralized DR-controlled VAV cases. The control signal definition used is Behrang-Sirén with a marginal value of ±75 €/MWh.

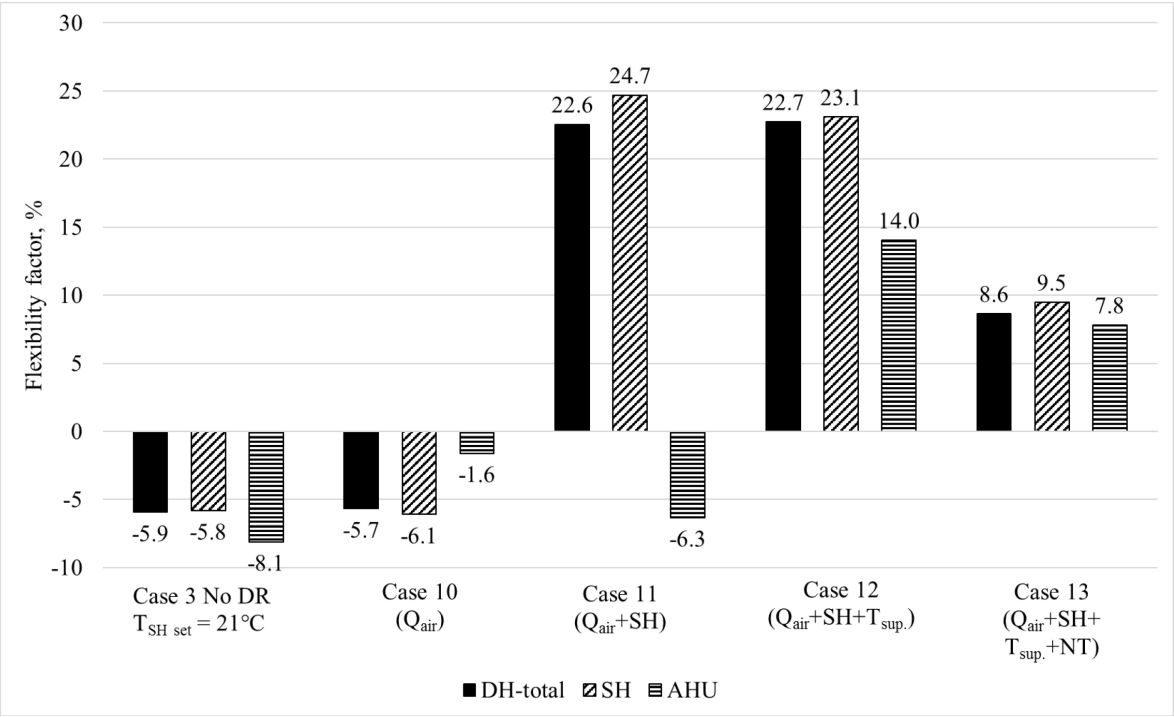

Figure 66. The impact of DR-control on flexibility factors for space heating, AHU and total district heating in the decentralized VAV cases.

Including DR-control of airflow (case 10) increases the AHU heating flexibility from reference case 3 -8.1% to -1.6%, but the total district heating flexibility still stays low. The total flexibility is significantly affected when including space heating control (case 11) even while the AHU flexibility decreases compared to case 10 (Q_{air}). By additionally including DR-control of supply air temperature (case 12) no increased benefit in total flexibility is gained even though the AHU flexibility increases to 14% and the space heating flexibility decreases only 1.6%-units. By including night time set-back mode in addition to all DR-control elements (case 13) the flexibility decreases compared to case 12. Again, the reason is due to the lower amount of cheap heat bought during night time.

It seems that DR-control related to the AHU does not have a significant impact on the total flexibility for the VAV cases. The reason is due to the low need of ventilation (presented in chapter 6.3.1, Figure 56), which in turn results in a low heating need within the AHU.

The AHU heat need for the VAV cases constitute only a small fraction of the total district heat need (as was shown in Table 19) and therefore DR-control of airflow or supply air temperature in a VAV system with low ventilation need does not have an impact on total flexibility. The situation could be different with a higher occupancy or in a different kind of building.

Figure 67 present the flexibility of fans and total electricity consumption for the decentralized DR-controlled VAV cases.

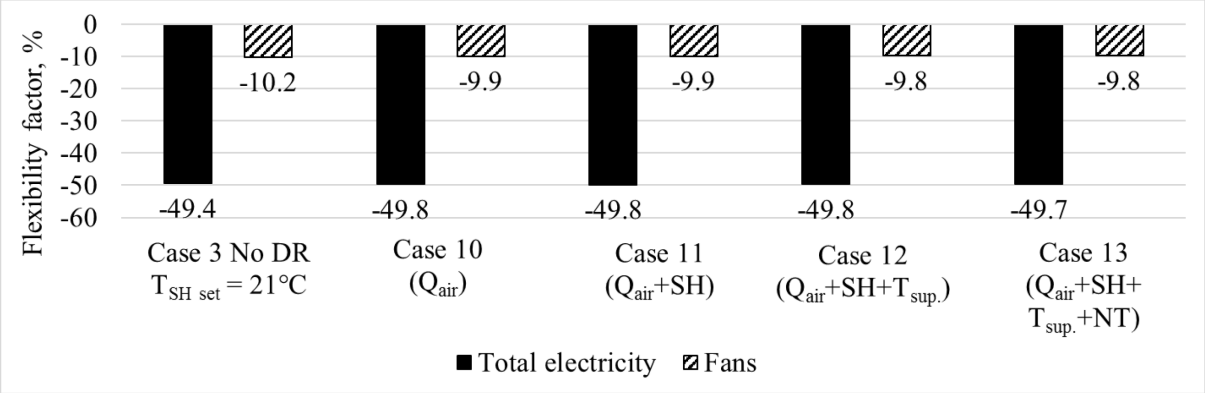

Figure 67. Flexibility of fan electricity and total electricity consumption for decentralized VAV cases.

The flexibility of electricity does not really change at all due to the same reasons as mentioned earlier, namely there is no potential of reducing the airflow compared to the reference VAV case 3 which makes it impossible to increase the flexibility of neither fan nor total electricity consumption. Another factor impacting on the total electricity flexibility is the other electricity consumers in the building such as lighting and equipment. These consumers are not bound to any DR-control.

One conclusion regarding flexibility of the VAV cases is that a lower airflow substantially increases the impact of space heating on total heating flexibility. Therefore, it could be desirable to decrease the total airflow of a CAV system or even turn the AHU off for a while during the most expensive heating hours.

6.3.3 Thermal comfort and indoor air quality

The result from the thermal comfort analysis is presented in form of temperature and PMV duration curves for the coldest zone in the building and for occupied hours only. The indoor air quality (CO_2 concentration) is analyzed for the simulation cases regarding VAV.

Decentralized CAV cases

Figure 68 compare the impact of occupancy on temperature duration of the coldest zone (room 10) for cases controlled by algorithm A1 (SH) and different control signal definitions.

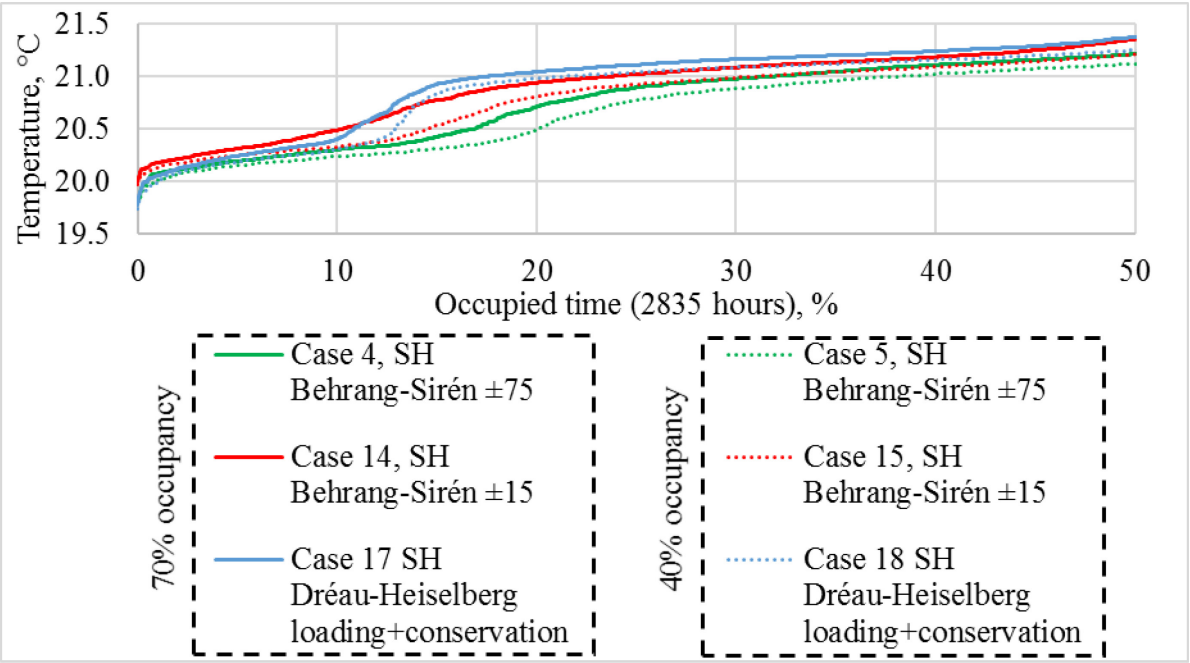

Figure 68. Occupancy impact on room temperature duration for cases with same DR-control and control signal.

The occupancy has no significant impact on temperature duration.

Figure 69 presents the effect on room temperature (room 10) for the different control algorithms in a 40% occupancy scenario. Additionally, the heat energy cost saving of each case is mentioned.

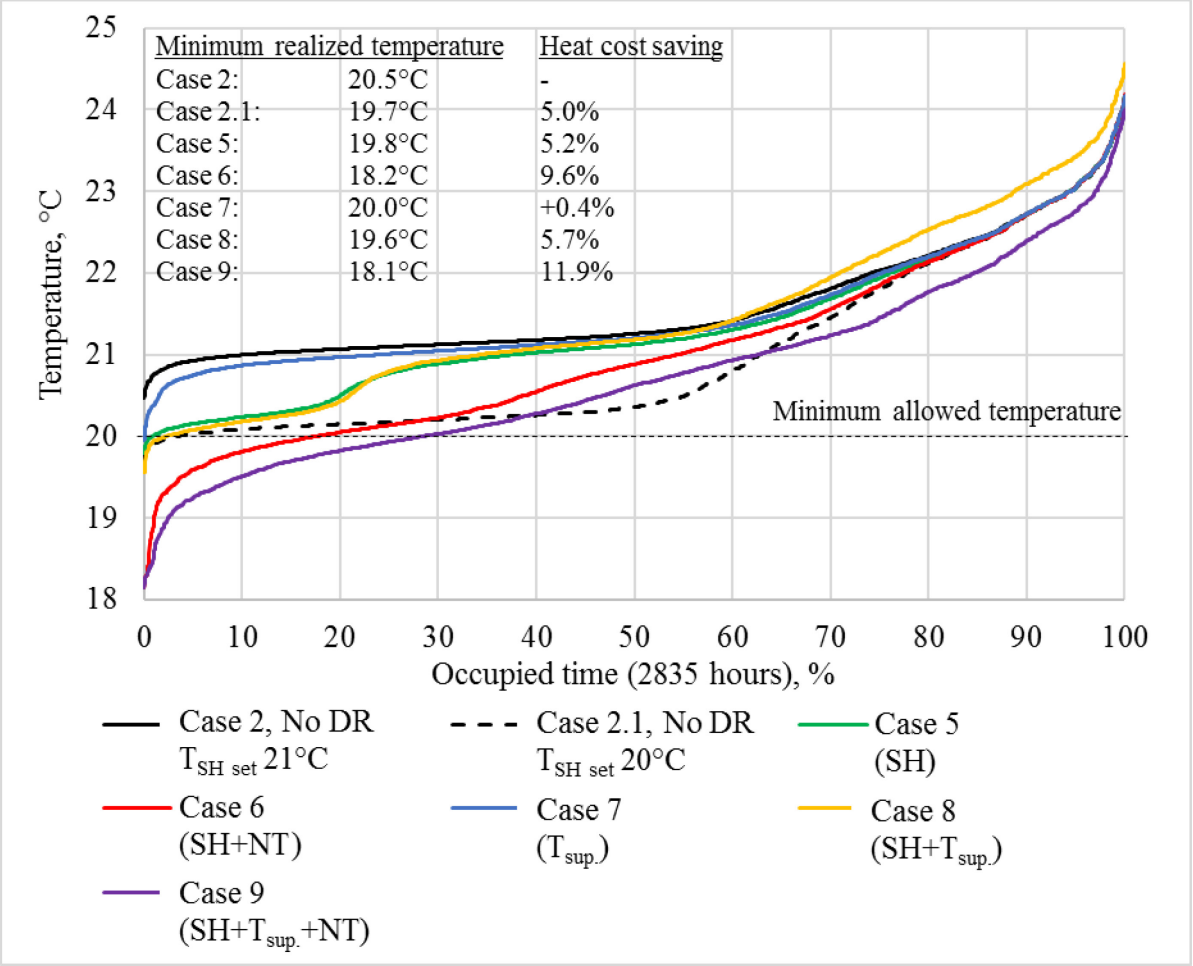

Figure 69. Effect of DR-control elements on room temperature (room 10) in the decentralized CAV cases with 40% occupancy.

Case 5 (algorithm A1, SH) and case 8 (algorithm B2, SH+$T_{sup.}$) has quite identical effect on the room temperature. The minimum temperature does not deviate much from the minimum acceptable value (20°C). Compared to case 2.1 (no DR), case 5 and 8 manages to maintain quite a comfortable temperature for major part of the occupied hours and still achieve a slightly higher heat energy cost saving.

Case 7 (algorithm B1,$T_{sup.}$) has insignificant impact on the temperature compared to reference case 2. The reason is due to the heat output compensation from the radiators whenever the supply air temperature is reduced. The heat energy costs are actually increasing by 0.4% in this case.

Case 6 (algorithm A2, SH+NT) and case 9 (algorithm B3, SH+$T_{sup.}$+NT) includes night time set-back mode. 20% – 30% of the occupied hours are below 20°C even though the temperature recovery is started two hours before the first occupant arrives at 8AM. The reason is due to that the setting "schedule smoothing" was used in the simulation software. This makes the occupancy schedule to be slowly increasing/decreasing and not discrete (Figure 70).

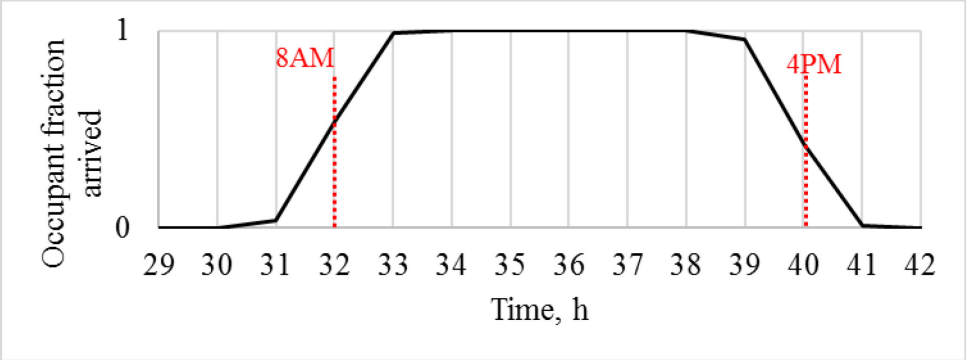

Figure 70. Schedule smoothing effect on occupancy.

Some occupants arrive already at 6AM when the temperature recovery is started. If the schedule smoothing would be deleted the temperature duration curves for case 6 and 9 would be improved. However, since the occupants of a real building cannot be assumed to arrive at the same time it is more realistic to use the schedule smoothing. This indicate that the temperature recovery should be started a bit earlier in the morning to prevent a decrease in performance of the early arriving occupants.

Figure 71 presents the effect on PMV-value (room 10) for the different control algorithms in a 40% occupancy scenario.

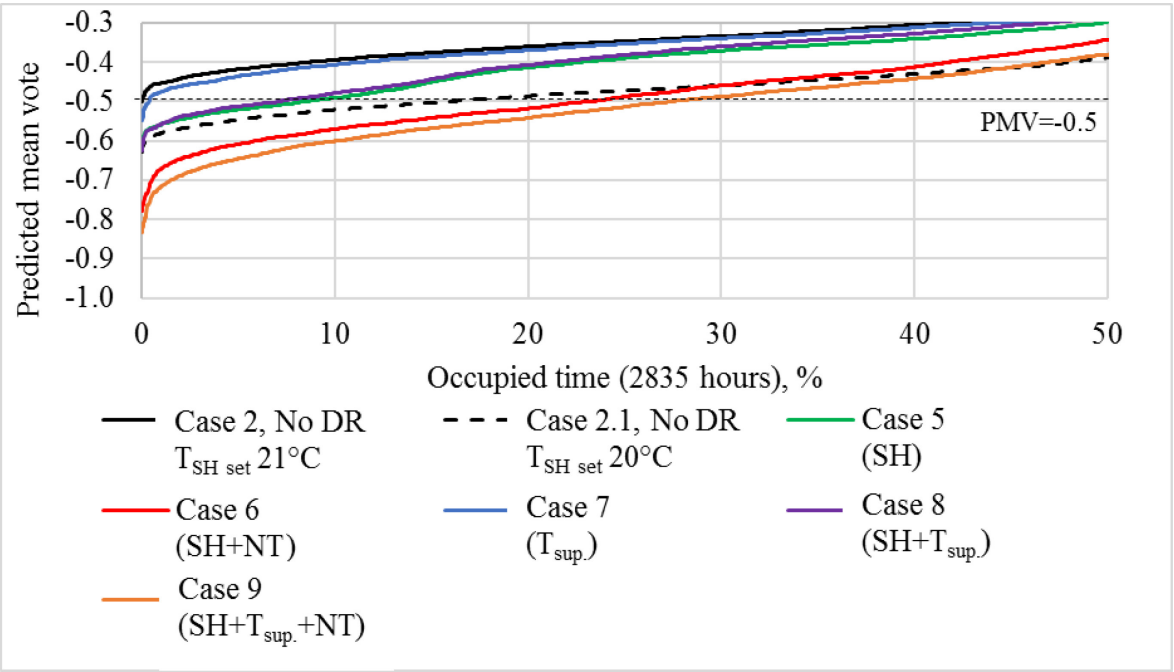

Figure 71. Effect of DR-control elements on PMV-value (room 10) in the decentralized CAV cases with 40% occupancy.

The cases including night time set-back (6 & 9) has a PMV value below -0.5 for over 25% of the occupied time. This is not acceptable and the reason is the late initiation of temperature recovery as explained earlier. All other DR-control cases PMV value durations are acceptable since they stay above -0.5 for over 90% of the occupied time. Additionally, the minimum PMV-value achieved is about -0.6 (case 5 & 8) which is not far from the minimum level.

Figure 72 show the temperature duration of room 10 (40% occupancy) for two non-DR cases and four cases controlled by algorithm B2 (SH+$T_{sup.}$) and different control signal definitions. Additionally, the lowest realized temperature and relative heat energy cost saving for each case is presented.

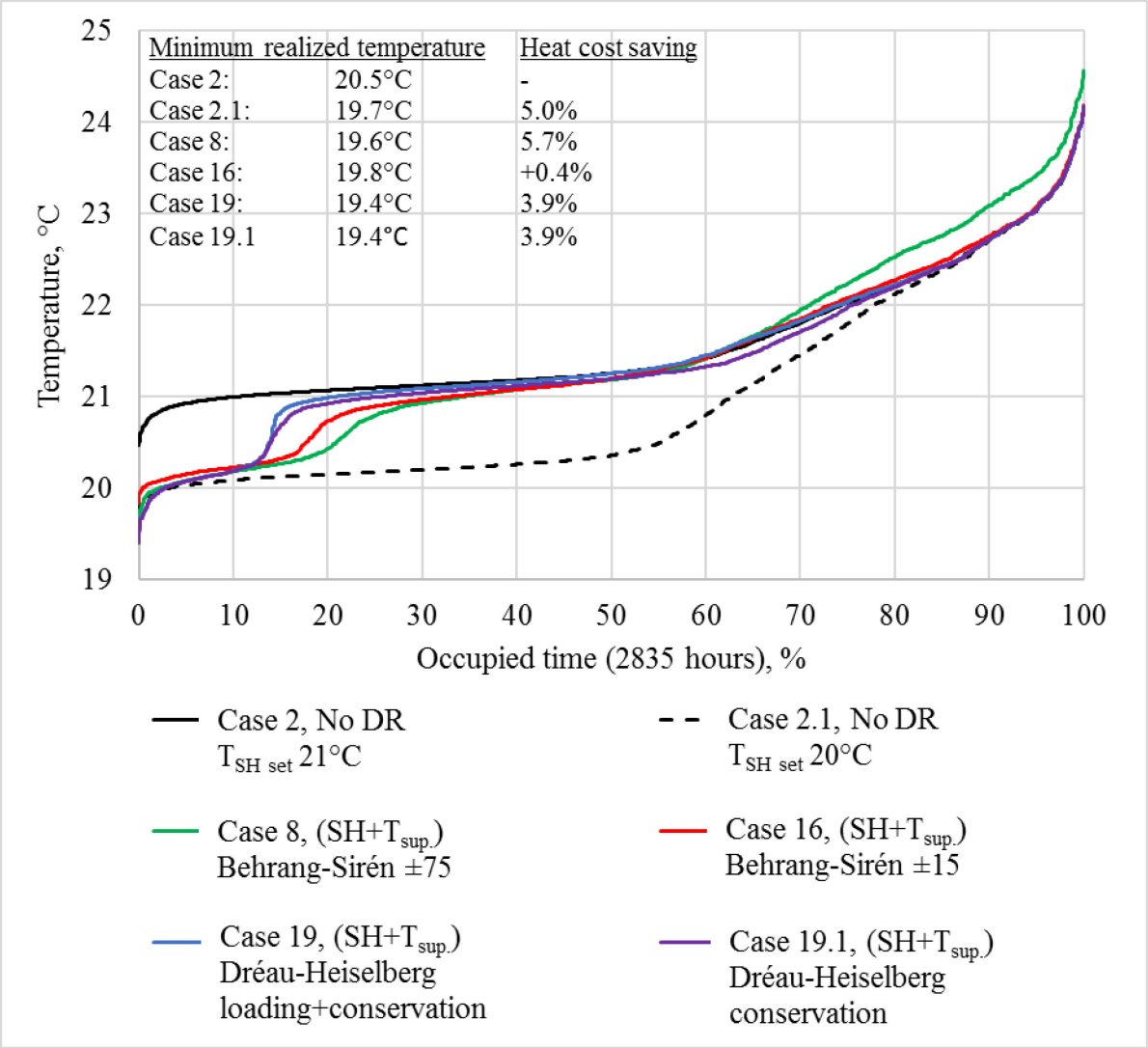

Figure 72. Temperature duration curves of room 10 for cases controlled by algorithm B2 (SH+$T_{sup.}$) and different control signal definitions (40% occupancy).

All DR-controlled cases manage to maintain the desired indoor temperature of 21°C for quite long.

The room temperatures are below 20°C for about 3% of the year with minimum temperatures of about 19.5°C. Case 8 has the overall lowest temperature of the 4 DR-controlled cases and additionally the biggest cost saving (5.7%). Case 19 and 19.1 maintains the best thermal comfort and still achieves a cost saving of 3.9% each. The realized temperatures of each case can be said to be within the acceptable range since the temperature goes below 20°C for just a fraction of the occupied time.

Figure 73 presents the PMV duration curves for the same cases as above.

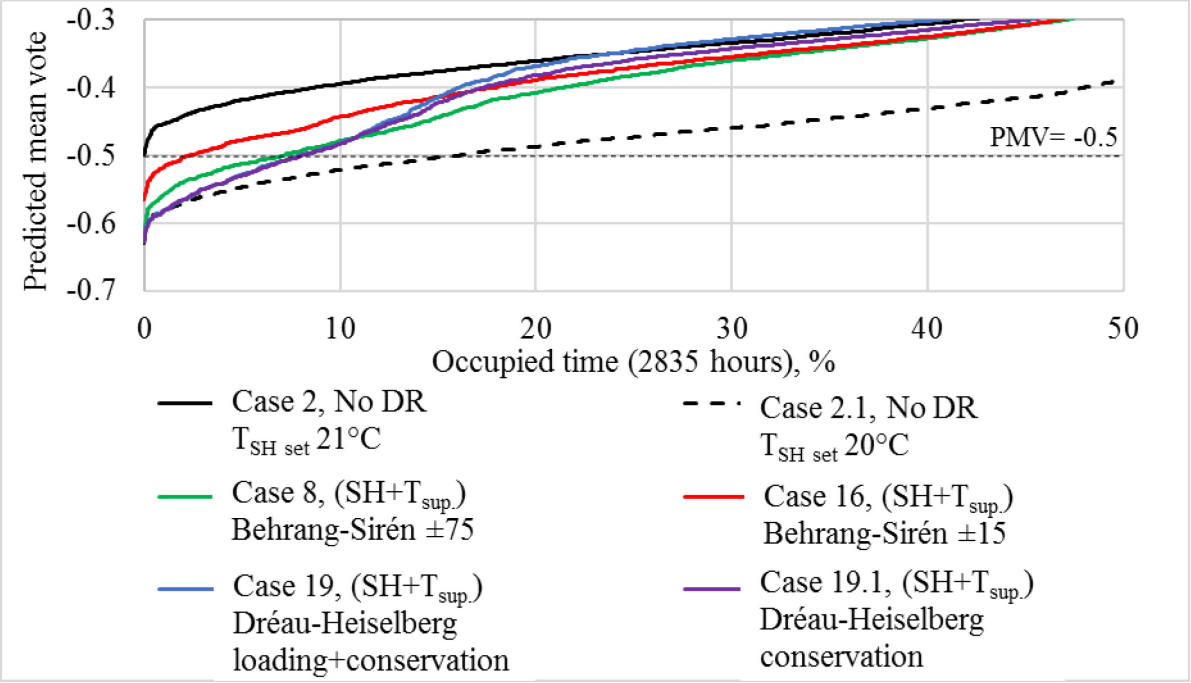

Figure 73. PMV duration curves of room 10 for cases controlled by algorithm B2 (SH+$T_{sup.}$) and different control signal definitions (40% occupancy).

The PMV value of all cases stay above -0.5 for about 92% of the occupied time. This is seen as acceptable.

Decentralized VAV cases, thermal comfort

Figure 74 show the effect on room temperature (room 10) for the different control algorithms in a 40% occupancy scenario. Additionally, the heat energy cost saving of each case is mentioned.

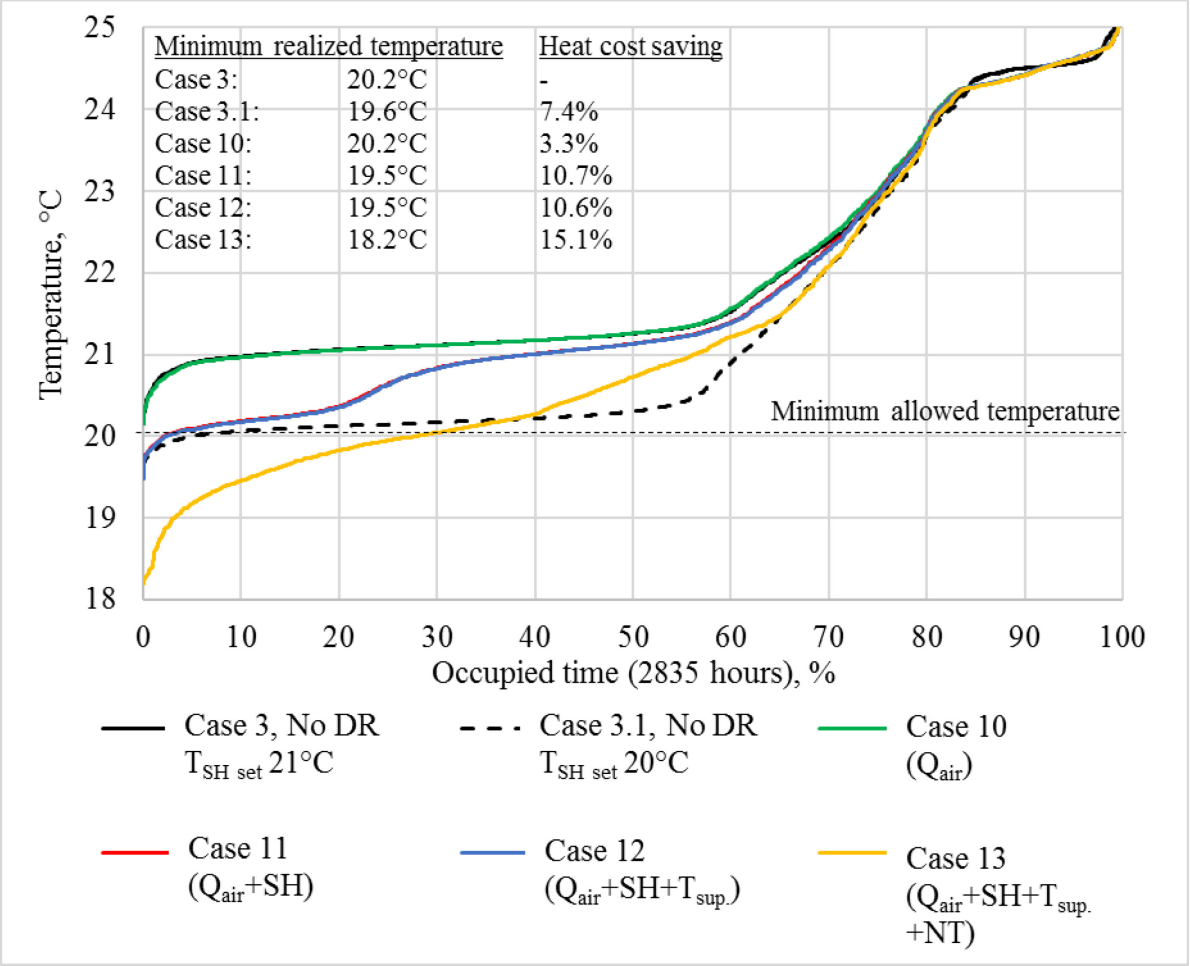

Figure 74. Effect of DR-control elements on room temperature (room 10) in the decentralized VAV cases with 40% occupancy.

DR-control of airflow in case 10 (algorithm C1, Q_{air}) does not have an impact at all on the room temperature. Hence the thermal comfort is the same as in the reference case 2, but a heat energy cost saving of 3.3% is achieved.

Case 11 (algorithm C2, Q_{air}+SH) and case 12 (algorithm C3, Q_{air}+SH+$T_{sup.}$) has exactly the same impact on room temperature. Both cases stay above 20°C for more than 95% of the occupied time. The supply air temperature control of case 12 does not have a decreasing impact on room temperature due to the compensation from the radiators and the overall low airflow rate in the VAV cases (presented in Figure 56). A heat energy cost saving of about 10.7% is achieved for both cases.

Case 13 (algorithm C4, Q_{air}+SH+$T_{sup.}$+NT) achieves a heat energy cost saving of 15.1% but the thermal comfort suffers quite much due to the late temperature recovery discussed about in connection to Figure 69.

The impact on room temperature from different DR-control elements is much similar to the temperature duration curves of Figure 69. Hence, the impact on thermal comfort from DR does not seem to be dependent on ventilation design.

Decentralized VAV cases, indoor air quality

Figure 75 present the impact on room air CO_2 concentration from DR-control of airflow based on CO_2 set-point adjustment (algorithm C1).

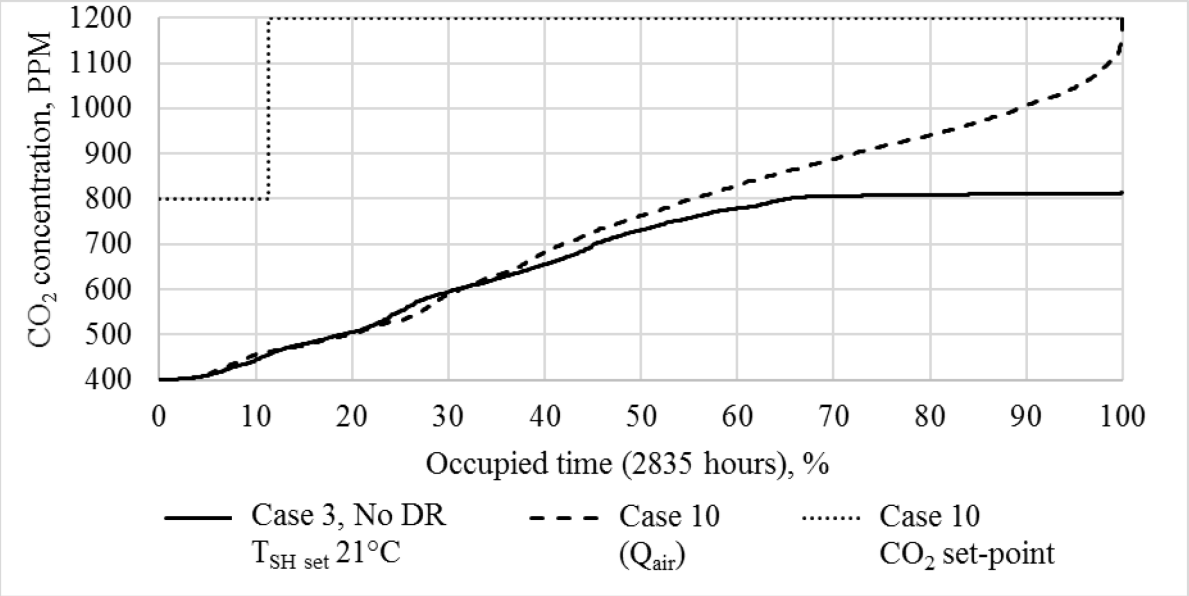

Figure 75. Effect of DR-control elements on CO_2 concentration in room 10 in the decentralized VAV cases with 40% occupancy.

The CO_2 set-point is 1200 PPM for 89% of the occupied time. This is a result from the control signal definition used (Behrang-Sirén ±75 €/MWh) and the dynamic heat and electricity prices used. The maximum DR set-point of 1200 PPM is however achieved only for 0.1% of the occupied time. For over 90% of the time the CO_2 concentration is below 1000 PPM. The reason for the low number of hours achieving the set-point is due to the low ventilation need (presented in Figure 56) of the reference case 3, which results in a low potential of reducing airflows during DR-control.

The high fraction of CO_2 set-points of 1200 PPM is not a problem in this particular case, but with a higher occupancy scheme or another building it might result in a constantly high CO_2 concentration whenever the building is occupied. This cannot be seen as an objective and therefore it would be good to add a condition which sets a time limit for how many hours per day the CO_2 set-point can be 1200 PPM (e.g. 4 hours/day). Those 4 hours could then be concentrated to the most expensive hours during the day. In this way cost savings could be achieved without sacrificing the indoor air quality too much.

6.4 Centralized DR-controlled cases

6.4.1 Energy consumption and cost

Figure 76 presents the change in heat energy consumption and cost for all the centralized DR-control cases. More detailed numbers can be retrieved from Table 24. The electricity consumption and cost are not included in the result analysis since the centralized control algorithms do not affect them.

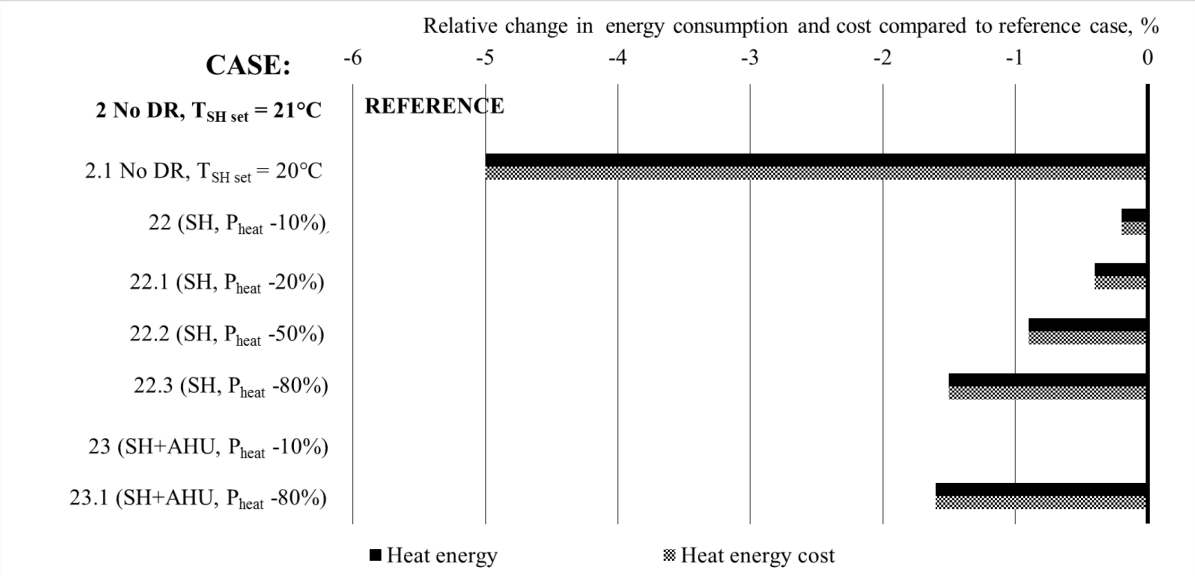

Figure 76. Control algorithm effect on energy consumption and cost of the centralized DR cases.

Table 24. Main features, annual energy consumption, cost and relative change for DR-controlled centralized cases.

	Case	DR-control				CS	$T_{SH\ set}$ Range	DH consumption		DH cost	
		SH	$T_{sup.}$	Q_{air}	NT			kWh/ m^2,a	Δ, %	€/m^2,a	Δ, %
40% occupancy, CAV	2 No DR $T_{SH\ set}$ = 21 °C	No DR-control				-	21	128.7	0	8.2	0
	2.1 No DR $T_{SH\ set}$ = 20 °C	No DR-control				-	20	121.3	-5	7.8	-5
	22 (SH, P_{heat}-10%)	x				1)	20-24.5	128.6	-0.2	8.2	-0.2
	22.1 (SH, P_{heat} -20%)	x				1)	20-24.5	128.6	-0.4	8.2	-0.4
	22.2 (SH, P_{heat} -50%)	x				1)	20-24.5	128.8	-0.9	8.1	-0.9
	22.3 (SH, P_{heat} -80%)	x				1)	20-24.5	128.9	-1.5	8.1	-1.5
	23 (SH, P_{heat} -10% & $T_{sup.}$)	x	x			1)	20-24.5	129.6	0	8.2	0
	23.1 (SH, P_{heat} -80% & $T_{sup.}$)	x	x			1)	20-24.5	128.5	-1.6	8.1	-1.6

1) Behrang-Sirén, marginal value: ±75€/MWh

The centralized DR-control of space heating (algorithm D1, Figure 42) is conducted by a decrease/increase in inlet water temperature to the radiator. The control signal definition used

for the centralized cases is Behrang-Sirén ±75 €/MWh, which results in conservation only. The abbreviation P_{heat} stands for the normal heat output at normal inlet water temperature. P_{heat}-10% (case 22) mean that the inlet water temperature has been decreased to correspond to a 10% less heat output than outside of DR-control.

The heat energy cost savings potential remains small for all the centralized cases. The highest cost saving is 1.6% and 1.5% for case 23.1 (SH+$T_{sup.}$) and 22.3 (SH) respectively. The room air temperature set-point remain unchanged (21°C) in the centralized cases and the savings are trying to be achieved by reduction of radiator inlet water temperature. It takes however quite a big modification to inlet water temperature to achieve any cost saving at all. The reason is that in the reference case the radiator thermostat valves are not near their nominal flows and when decreasing inlet water temperature in the DR-cases the thermostat simply increases mass flow through the radiator to compensate for the reduced inlet water temperature.

Figure 77 shows the duration curve of radiator mass flow rate in room 3 for the space heating DR-controlled centralized cases.

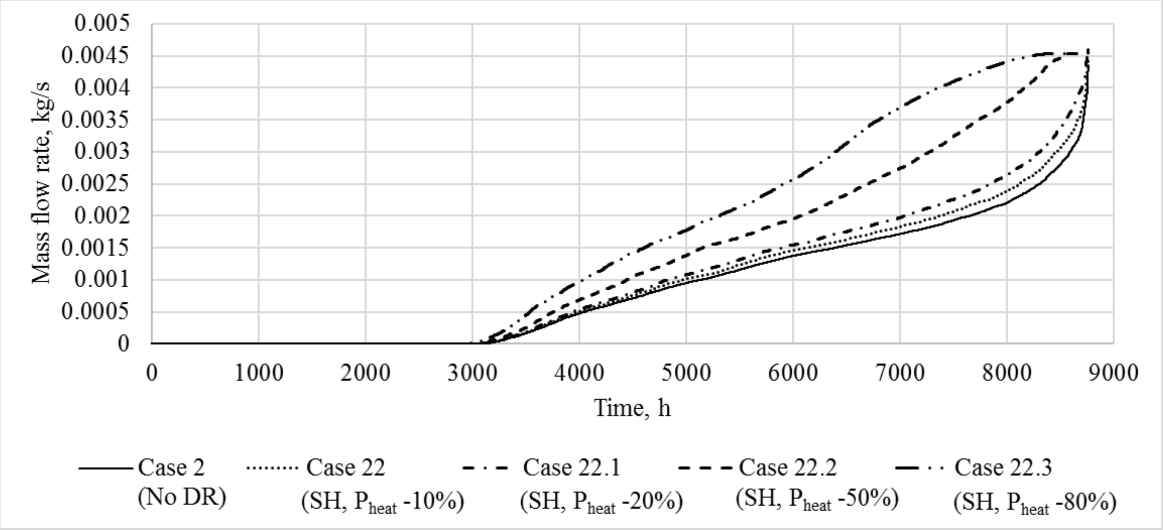

Figure 77. Duration curves of radiator mass flow rate in centralized DR-cases.

The mass flow rate of rooms 3's radiators rarely achieves the nominal flow, meaning that the inlet water temperature is almost all the time high enough to provide sufficient heat output to the room. The P-band of the radiator thermostat is set to 1 C, meaning that when the mass flow rate is at nominal flow, the room air temperature should be about 20.5 C.

Hence, with a big modification of inlet water temperature it is possible to achieve some savings. However, since the DR-control is controlled by the coldest room in the building, the inlet water temperature reduction is not present for very long time periods. There is neither any substantial benefit from including the supply air temperature in the DR-control since the radiators are compensating for the cooling effect of a reduced supply air temperature.

The results propose that instead of using centralized DR-control of heating, more savings would be achieved by simply reducing the indoor air temperature set-point by one degree (case 2.1, 5% cost savings). Another issue affecting the results is that IDA cannot account for the

thermal inertia of the heat distribution system. The set-point of the DH-substation outlet water is instantly reaching the radiators, but in a practical application there would be some delay.

6.4.2 Flexibility factor

Figure 78 present the flexibility of total district heating, space heating and AHU for the centralized DR-controlled CAV cases. The control signal used is Behrang-Sirén ±75 €/MWh.

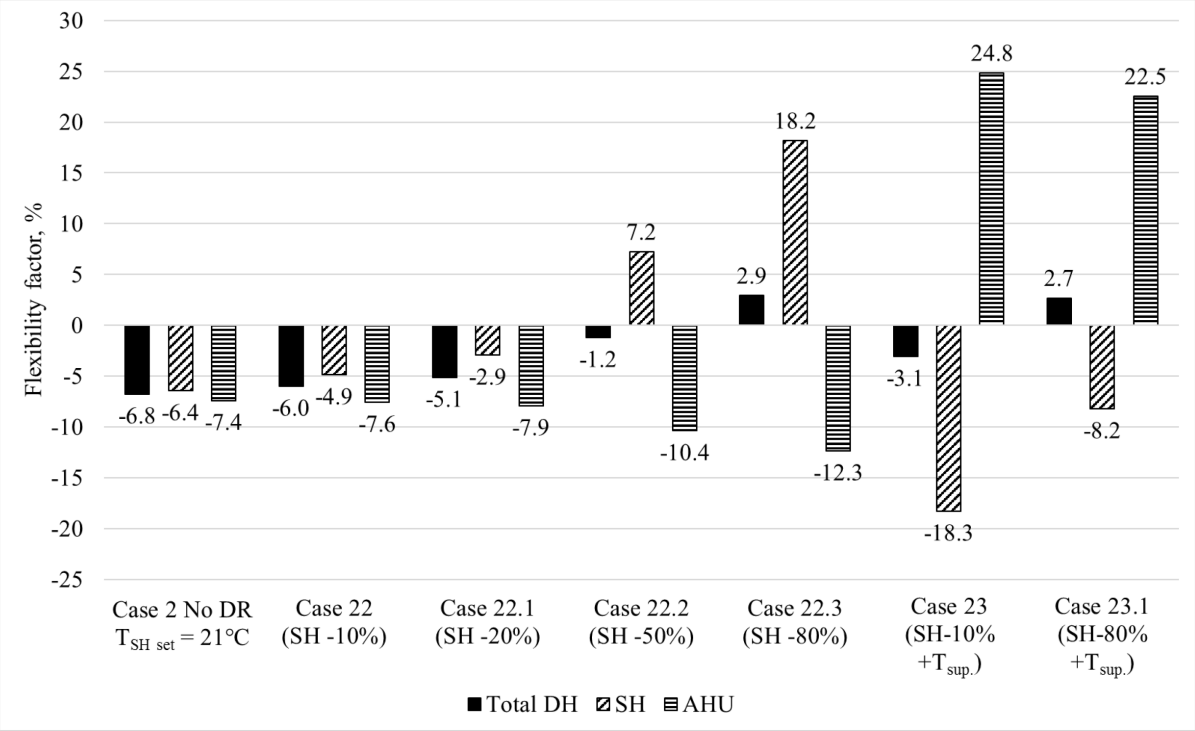

Figure 78. The impact of DR-control on flexibility factors for space heating, AHU and total district heating in the centralized DR-cases.

As for the cost savings, the total flexibility of the centralized cases remains quite low. The best flexibilities achieved are 2.9% and 2.7% for case 22.3 (SH) and 23.1 (SH+$T_{sup.}$) respectively. The separate flexibilities of space heating or AHU does in some cases increase quite much, but at the same time the other part increases and keeps the total flexibility low.

There is needed a big drop in inlet water temperature curve before the flexibility of space heating increases. A temperature curve modification equaling in power drop of 50% or more is needed to achieve a positive flexibility factor for space heating. This is, as for the cost savings, connected to the water mass flow rate through the radiator valves. A small temperature decrease only increases the mass flow rate, but a big enough reduction makes the valves work at nominal mass flow more often which makes temperature decrease in rooms possible and reduced heat energy usage during high price periods.

In general, it can be stated that the heating flexibility of a centralized DR-controlled heating system is poor regardless of DR-control element utilized.

6.4.3 Thermal comfort

Figure 79 presents the centralized control algorithms impact on room temperature duration during occupied hours.

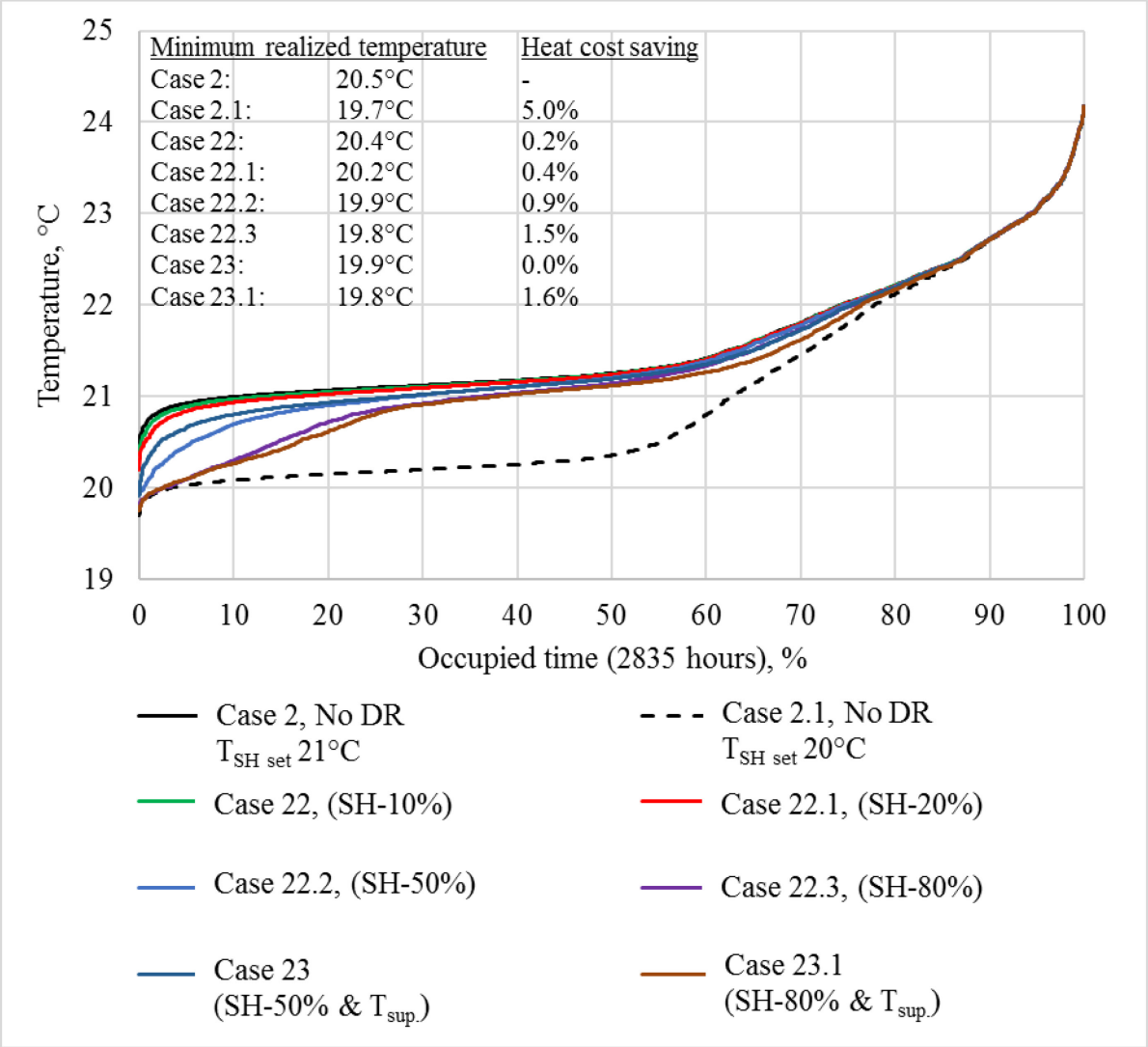

Figure 79. Effect of DR-control elements on room temperature (room 10) in the centralized CAV cases with 40% occupancy.

The bigger adjustment to inlet water temperature curve, the bigger decrease in room temperature (case 22, 22.1 and 22.2). However, the temperature does still not decrease very much compared to the reference case. When including supply air temperature control (case 23 and 23.1) the room temperature is in general a bit lower. It can be concluded that a centralized DR-control approach does not have any severe impact on the thermal comfort, but neither does it cut much energy costs.

6.5 Peak demand limiting

As presented in chapter 5.2.2 and Table 9 the available heat power for the 4th floor was calculated based on square-meter ratio and the buildings DH-substation's total heating power.

The calculated power was 57.7 kW. During simulations for determining time of temperature recovery after night time set-back, the dimensioning outdoor temperature (-26°C) was used. During these conditions the average total district heat power demand of the 4th floor was 40 kW. In order to fully investigate the potential of peak power limiting the whole building should have been simulated. Three peak power demand limiting cases regarding district heating were simulated (Table 25).

Table 25. Peak demand limiting simulation cases.

	Case	Dimensioning power, kW	Peak demand limiting	Available power, kW
40% occupancy, CAV	2 (reference)	40	-	40
	20		-35 %	26
	21		-43 %	23
	21.1		-50 %	20

The occupancy in all cases were 40% and the peak power was cut by 36%, 43% and 50%. The power limiting concerns only space heating, hence the AHU heating of supply air was never restricted. The total district heat power duration curves for the annual hours with heating demand are presented in Figure 80

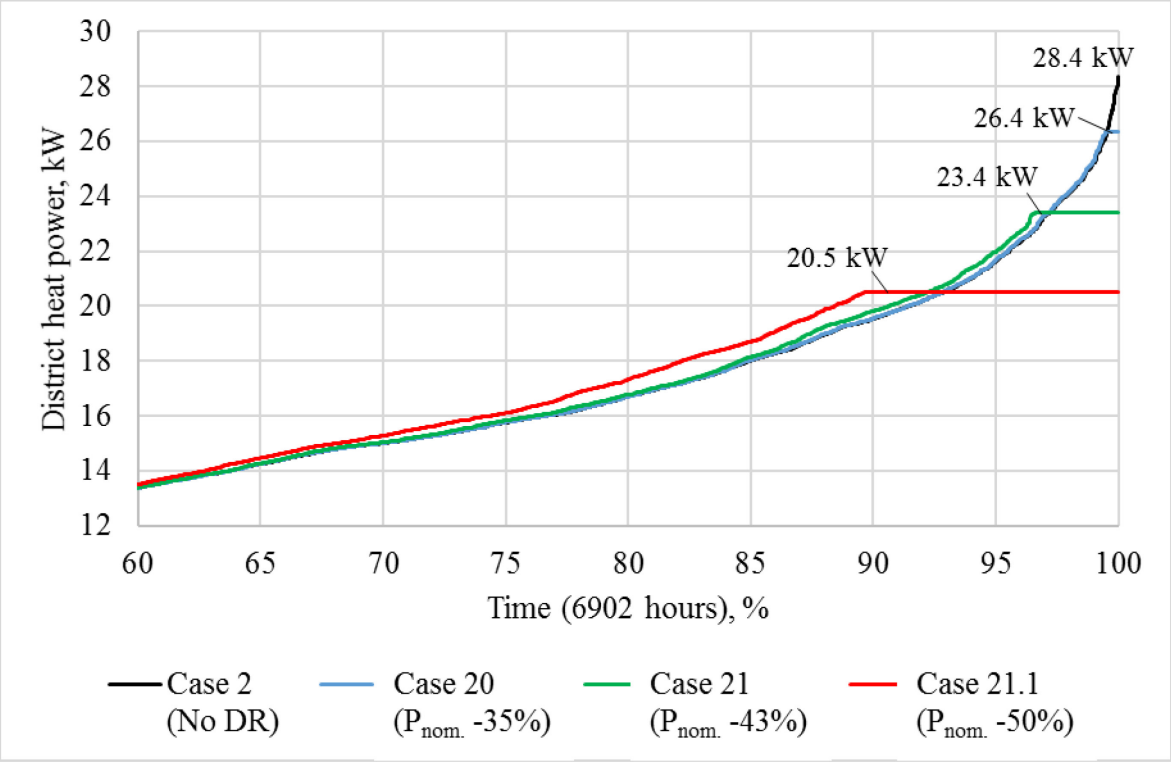

Figure 80. District heat power duration for hours with heating demand in the reference case and peak demand limiting cases (40% occupancy).

This simulation analysis utilizes Finnish test reference year weather data (Finnish Meteorological institute, 2012), which does not include colder outdoor temperatures than about -20°C. The maximum district heat power demand of the reference (case 2) during these conditions was 28.4 kW. For some reason the maximum DH-power used in the peak demand

cases is slightly bigger than what the DH-substation restrictions are set to. By cutting the nominal power with 35% (case 20) only 0.5% of the annual heating hours are affected. Case 21 involves a 43% cut of peak power which affects 3.4% of the annual heating hours. Case 21.1 with 50% peak power limiting affects 10.4% of the annual heating hours.

Compared to the reference case, there was a slightly increased power demand for hours out of nominal power demand in case 21. The reason is the so called rebound effect (presented in chapter 3.2.1, Figure 10). When the nominal power is restricted, the temperature in the zones are decreasing, which in turn increases the heat power need compared to the reference when recovering the room temperatures to the set-point level. The same phenomena can be seen for case 21.1 which involves as peak power limit of 30%. In this case the hours affected by rebound are about 20% of the annual heating hours.

The peak power demand limiting effect on indoor temperature, power usage and the related rebound effect is presented in Figure 81.

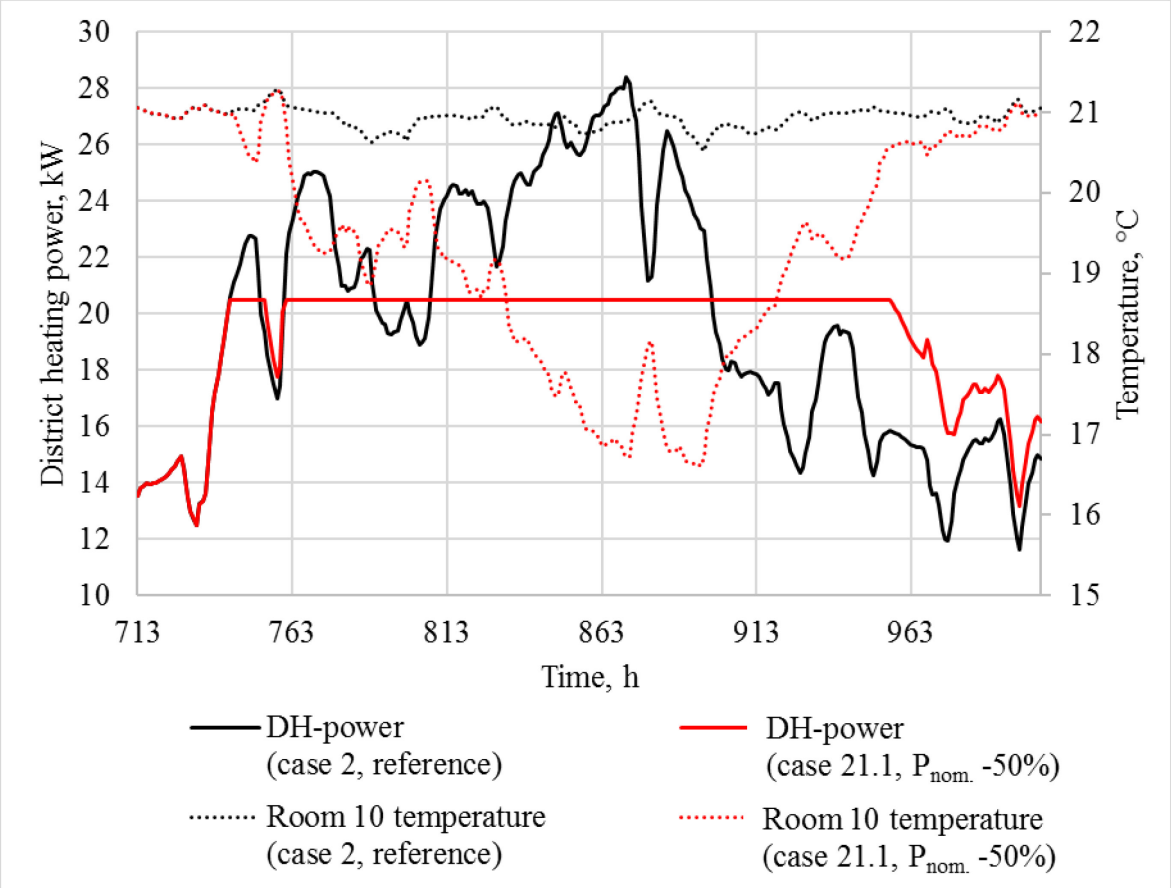

Figure 81. Peak power demand limiting effect on indoor temperature, power usage and the related rebound effect in case 21.1 compared to reference case 2.

Every time after power limiting the power demand of case 21.1 is higher than for case 2 due to the decreased room temperature that has to be recovered.

6.5.1 Thermal comfort

The coldest room in the building during peak demand limiting is room 10, which lies in the south-west corner of the building. The power limiting effect on room air temperature is presented in Figure 82 as temperature duration curves for occupied hours only.

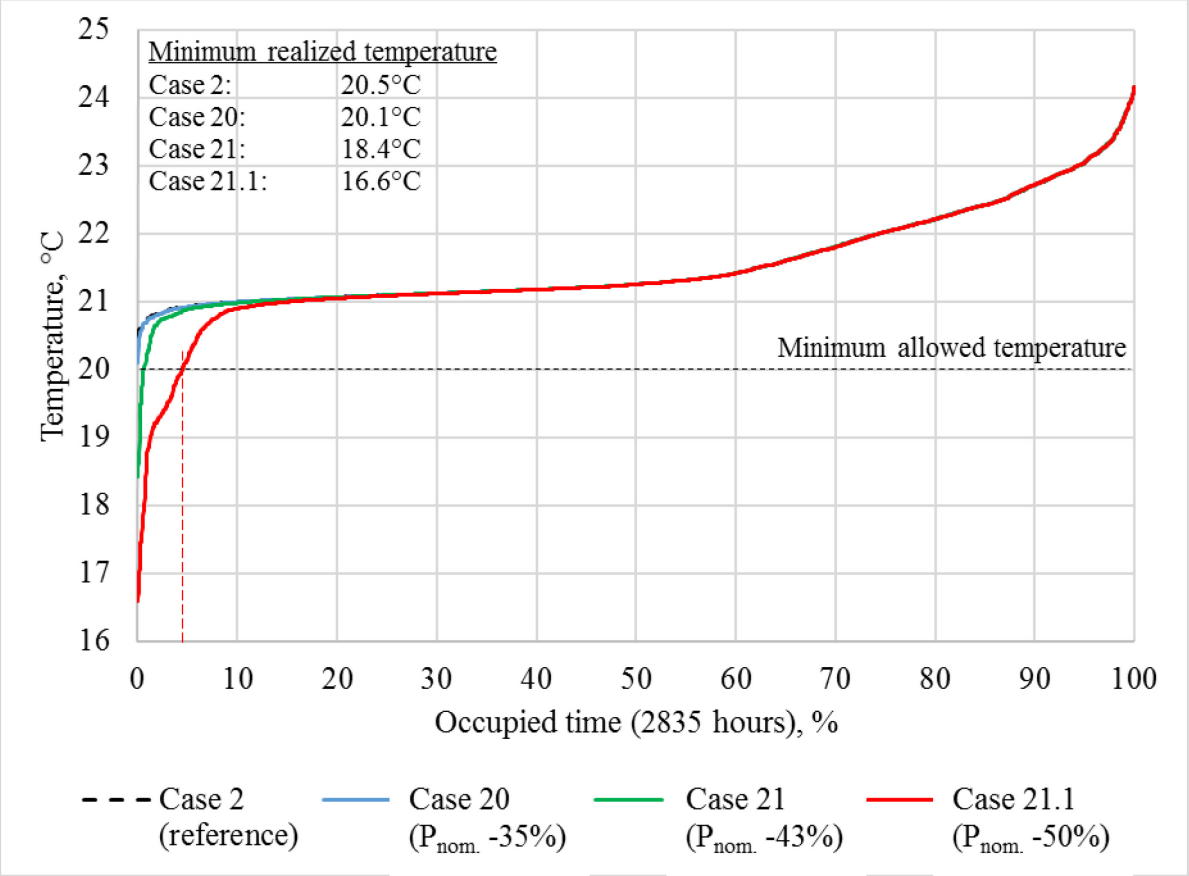

Figure 82. Temperature duration curve of coldest occupied room in building (room 10) for different peak demand limiting cases.

A peak demand limit of 35% does not have an impact on the room air temperature. Limiting power by 43% gives a minimum room temperature of 18.4°C, but the temperature is below 20°C for only 0.6% of the occupied hours (about 17 hours) and below 19°C for 0.2% of the time (about 6 hours). A power limiting of 50% results in a minimum temperature of 16.6°C with 4.4% of the occupied time (about 124 hours) being below 20°C. However, the temperature is below 19°C for only 1.2% of the occupied time (about 34 hours).

A peak demand limiting of 50% may seem tolerable due to the low amount of hours with temperatures below 19°C. If the cold room temperature would be present only for a moment per day it may be acceptable to use a high peak power limit. However, the coldest temperatures are likely to be present for many hours in a row during cold weather periods. This would greatly sacrifice the indoor thermal comfort and is not acceptable.

Figure 83 presents the duration curve of predicted mean vote values in room 10 for the reference case and the peak demand limiting cases. The duration curve is plotted for occupied hours only.

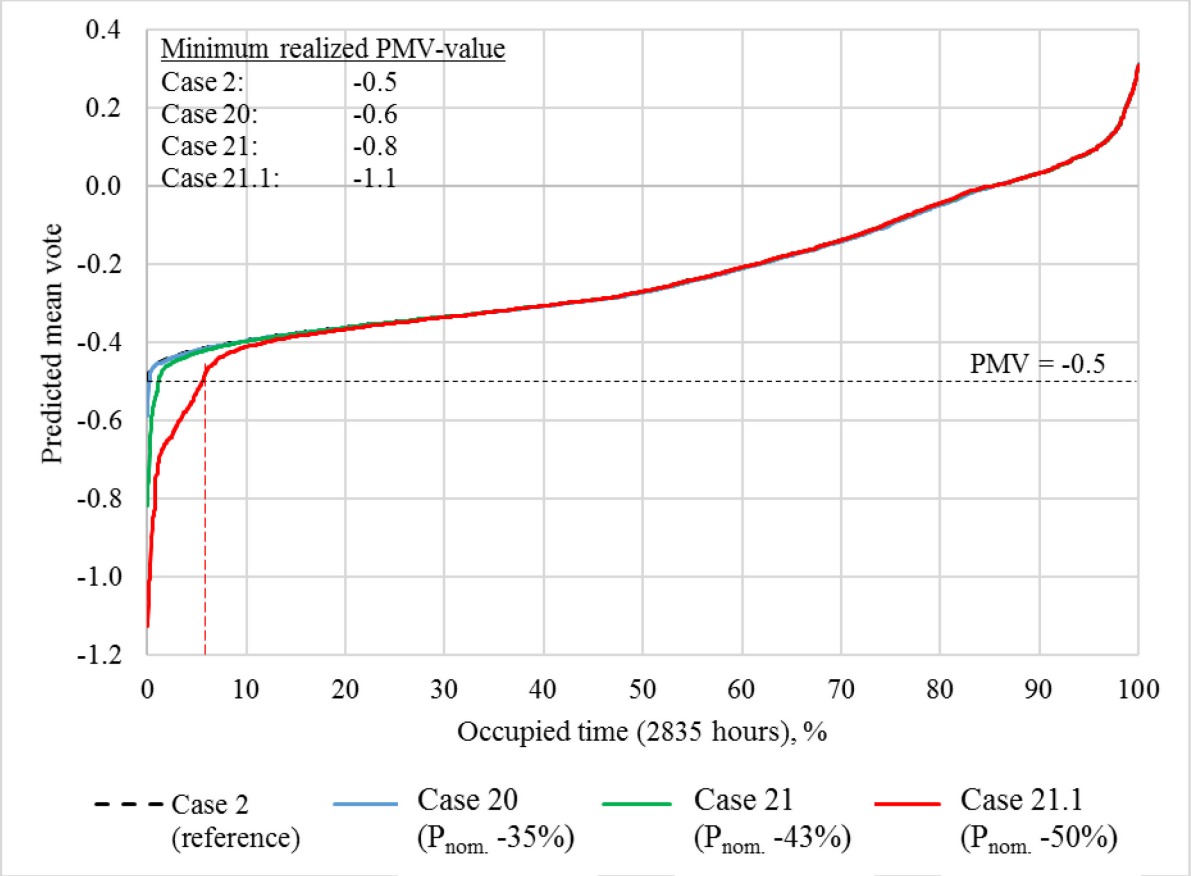

Figure 83. Predicted mean vote duration curve of coldest occupied room in building (room 10) for different peak demand limiting cases.

Case 20 has a minimum PMV of -0.6, case 21 goes down to -0.8 and case 21.1 achieves -1.1. As presented in chapter 5.1.2, the lowest allowable PMV value was chosen to be -0.5, but a lower value can be accepted for a short period of time if for example significant cost saving benefits are achieved. Case 21 goes below the minimum value for 1.1% of the occupied time (about 31 hours) which can be held as acceptable when regarding the realized temperatures presented and discussed in Figure 82.

6.5.2 Cost saving potential

Assuming the relative power demand (kW/m^2) is the same for the rest building as for the 4th floor, the total district heat power demand would be 528 kW equaling a mass flow rate of 1.8 l/s. The actual power demand and mass flow rate according to the design documents are however 760 kW and 2.6 l/s respectively.

The buildings cost saving potential in power charge by peak demand limiting was calculated for two alternatives: nominal power demand according to simulations with dimensioning outdoor temperature, nominal power demand according to design documents.

The simulated building is connected to the energy distributor Fortums network in the Espoo region but additionally to this, the cost saving potential is calculated for a situation where the building is connected to Helens network in the Helsinki region.

Fortum is changing its district heating pricing structure starting from 1.1.2018. There are two main alternatives available: active heat, stable heat. The energy tariff in the Fortum active heat package have monthly variations and are based on the real production costs of the district heat. In the Fortum stable heat alternative the energy tariff is constant throughout the year. The power charge in the two pricing packages are differing from each other. The active heat package has a progressive relative power charge with increasing nominal heat power demand. The stable heat package has a constant relative power charge based on nominal power (Fortum, 2017).

Helen updated its district heat prices 1.10.2017. The energy price is seasonally based and the power charge is based on nominal mass flow rate of the building (m^3/h) with no separate pricing structure alternatives (Helen, 2017).

Fortums "stable heat" power pricing and Helens only available power pricing alternative was used for the cost saving calculations. Table 26 presents the relevant price information used in the calculations.

Table 26. District heating power charge for Fortum and Helen.

FORTUM							
€/(kW year) (VAT 0%)	85.4						
HELEN							
Mass flow rate, m3/h	3.2 - 3.4	3.6 - 3.8	4 - 4.4	4.4 - 4.8	5.2 - 5.6	6.0 - 6.4	9.2 - 9.6
€/year (VAT 0%)	7970	8781	9593	10404	11740	12689	16485

Table 27 presents the nominal power demand (kW & m3/h) and the annual power charges of each case for power demand based on simulation results and power demand based on design documents.

Table 27. Nominal power and mass flow rates for the reference case and demand limiting cases.

POWER DEMAND BASED ON SIMULATIONS

				Annual power charge, €	
Case	Power demand limiting	Nominal power, kW	Nominal mass flow rate, m^3/h	Fortum	Helen
2 (reference)	-	528	6.5	45091	13164
20	-35 %	343	4.2	29309	9593
21	-43 %	301	3.7	25702	8781
21.1	-50 %	264	3.3	22546	7970

POWER DEMAND ACCORDING TO DESIGN DOCUMENTS

				Annual power charge, €	
Case	Power demand limiting	Nominal power, kW	Nominal mass flow rate, m^3/h	Fortum	Helen
2 (reference)	-	760	9.4	64904	16485
20	-35 %	494	6.1	42188	12689
21	-43 %	433	5.3	36995	11740
21.1	-50 %	380	4.7	32452	10404

The annual power charge is differing a lot between Fortum and Helen. Fortums power charges are 280% – 340% and 310% – 400% more expensive for the simulation based and design document based power demand cases respectively. Figure 84 presents the annual power charge and cost saving potential according to peak demand limiting.

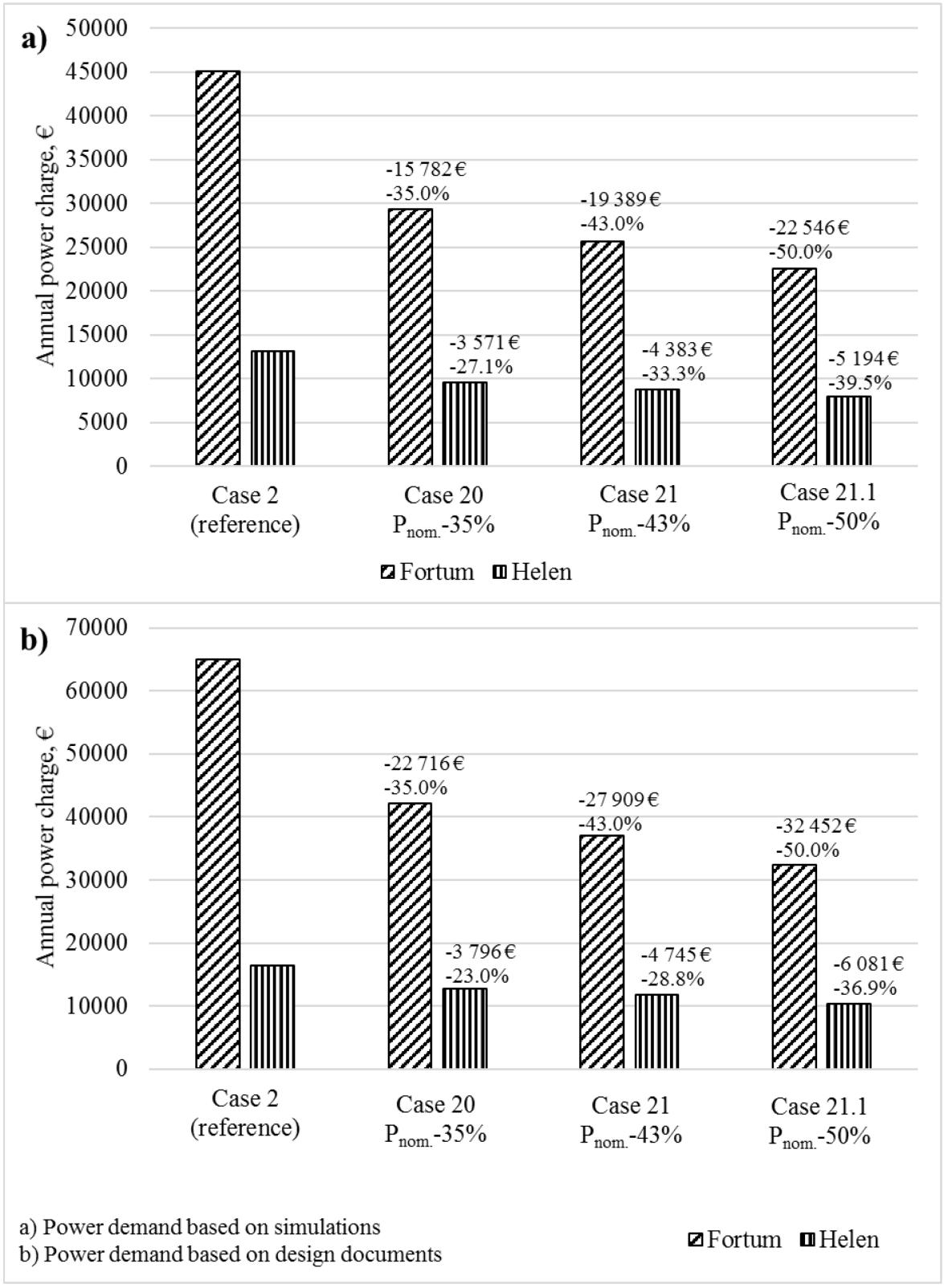

Figure 84. Annual power charge and cost saving depending on magnitude of peak demand limiting.

Due to the fixed kW-based power charge in Fortums "stable heat" price package the annual costs can be cut by 35%, 43% or 50% depending on peak demand limiting case. For Helen, the cost savings ranges from 23% - 39.5% depending on peak demand limiting case and nominal power demand.

The difference in absolute cost savings between the two district heat distributors is quite big due to the different power charge structure of the companies. The results show that if the building were connected to Helens network a maximum cost saving of 6 081 € (10.4 €/m^2) with -50% peak demand limiting is possible. If connected to Fortum, even the smallest peak demand limiting of -10% (case 20) would cut the power charge by 22 716 € (38.8 €/m^2), which is nearly four times more than for a -30% peak demand limit in Helens network (case 21.1).

Based on the thermal comfort analysis in chapter 6.5.1, case 21 with a power demand limiting of 43% would be possible in this building without sacrificing the thermal comfort too much. For alternative a) in Figure 84 this would bring an absolute annual cost saving of 4 383 € – 19 389 € (7.5 – 33.1 €/m^2) for a connection to Helen or Fortums network respectively. For alternative b) the corresponding absolute cost savings would be 4 745 € – 27 909 € (8.1 – 47.6 €/m^2).

Bigger peak demand limiting of 50% or more could also be possible if the building would be equipped with a thermal storage tank as a buffer. A buffer tank and the related piping is quite simple and probably not too expensive. The main problem can be to find enough space for the installation of tank. However, due to the quite significant annual cost saving potential this kind of solution might be attractive in practice.

7 Conclusions

The main objective with this study was to simulate a detailed model of an educational office building to determine the monetary saving potential of demand response combined with dynamic hourly district heating and electricity prices. In addition, the difference in potential between centralized and decentralized control approaches was to be examined. The decentralized simulations included both CAV and VAV cases.

The main conclusions from the study are that demand response within heating is only beneficial with a decentralized control on room level. Occupancy do not have an impact on neither cost savings, flexibility nor thermal comfort. Peak demand limiting within district heating have a big cost saving potential.

Centralized demand response

Regarding centralized DR-control the total heat cost saving potential is negligible according to the simulation results. A cost saving of 1.6% was achieved at best when including both space heating and supply air temperature control. For comparison, a non-DR case with decreased room air temperature set-point (20°C) yielded about 5% total heat cost savings. The space heating DR-control was mainly executed by decreasing the inlet water temperature to the radiators. The main restriction in this alternative was that the coldest zone in the simulation model governed the control. Hence, the inlet water temperature could be decreased only if all zones were above the minimum allowed room temperature (20 °C).

The flexibility factor (total district heat) for centralized DR remained constantly low with the best result of 2.9% compared to the non-DR reference case flexibility of about -7%. The thermal comfort was generally maintained on a good level due to the low potential in reducing room temperatures in the occupied office rooms.

Decentralized demand response

The decentralized DR-control approach had higher potential in saving heat energy costs compared to the centralized approach. In the CAV cases a total heat cost saving of 5% – 6% was achieved by controlling space heating or combining it with supply air temperature control. In the VAV cases the corresponding relative cost saving was a bit higher (about 7.5%) due to lower AHU heat energy demand, which increased the relative importance of space heating. The AHU showed to have a big restrictive impact on the DR-control, since in the CAV cases the constant airflow rate with supply air temperature 20 °C resulted in a cooling effect restricting the time period the rooms would manage without heating.

Demand response control of airflow through CO_2 set-point adjustments in the VAV cases did not have any significant impact in this specific building. The low CO_2 load from the occupants at the 40% occupancy scheme in combination with a diluting effect from the open office doors connected to the big corridor resulted in a low ventilation demand. The total cost savings from airflow control was 3.3% and 1.1% for heat energy and electricity respectively.

The combination of night time set-back mode with DR-control of space heating and supply air temperature was studied for both CAV and VAV cases and the results show a total heat cost saving potential of about 10%.

The best flexibility factor (total district heat) achieved in the CAV DR-controlled cases was 16.5% (reference case, -7%), but none heat cost savings were achieved. The case with secondly highest flexibility factor (15%) had in addition the highest heat cost savings (5.7%). The DR-control included both space heating and supply air temperature. The heat flexibility factor of the VAV cases was a bit higher (about 23%) due to the low ventilation impact on room temperatures. The flexibility factor for electricity remained very low due to the minimal potential in airflow reduction during DR-control.

The thermal comfort could be kept on an acceptable level for all DR-controlled cases except the ones containing night time set-back mode. The reason was the late schedule for temperature recovery which could easily be avoided by starting the recovery a couple of hours earlier.

In this building there could not be seen any positive impact from heat loading during cheap price periods. One main reason seems to be the cooling effect from the ventilation flushing out the additional heat loaded. Another reason is the way the different control signal definitions determines what a cheap heat energy price for loading is. The median price during loading phases was 87 €/MWh and 42 €/MWh for the Behrang-Sirén and Dréau-Heiselberg signal definitions respectively.

Peak demand limiting

The results from peak demand limiting of district heat contract power included the highest cost saving potential of all elements studied in this thesis. A peak demand limiting of 35% could be achieved without any impact on the thermal comfort. This would bring the annual cost saving of 27.1% – 35% (6.1 €/m^2 – 26.9 €/m^2) depending on district heating connection (Helen or Fortum). The peak demand limit of 43% had only minor impact on the thermal comfort and would bring cost savings ranging from 33.3% – 43% (7.5 €/m^2 – 33.1 €/m^2) depending on DH connection.

8 References

Aalto university, (2017) *Arkkitehtuuri (Architecture).* [Online]
Available at: http://www.aalto.fi/fi/about/campus/architecture/
[Accessed 8 September 2017].

Acherman, M. & Zweifel, G. (2003) *RADTEST – Radiant Heating and Cooling Test Cases. A Report of Task 22, Subtask C Building Energy Analysis Tools Comparative Evaluation Tests,* Switzerland: Lucerna School of Engineering and Architecture. 83 p.

Alanne, K. (2016) *Course material: Ventilation and Air Conditioning Systems - Ventilation requirements,* Espoo: Aalto University.

Alimohammadisagvand, B., Alam, S., Ali, M., Degefa, M., Jokisali, J. & Sirén, K. (2015) Influence of energy demand response actions on thermal comfort and energy cost in electrically heated residential houses. *Indoor and Built environment.* [Online journal]. p. 1-19. [Cited 15 Jun. 2017] Available: DOI: 10.1177/1420326X15608514

Alimohammadisagvand, B., Jokisalo, J. & Sirén, K., (2017) Comparison of four rule-based demand response control algorithms in an electrically and heat pump-heated residential building. *Submitted 15.6.2017 to Applied Energy.*

Alimohammadisagvand, B., Jokisalo, J., Kilpeläinen, S., Ali, M. & Sirén, K. (2016a) Cost-optimal thermal energy storage system for a residential building with heat pump heating and demand response control. *Applied Energy.* [Online journal]. Vol. 174. p. 275-287. [Cited 4 Jun. 2017] Available at: https://doi.org/10.1016/j.apenergy.2016.04.013

Alimohammadisagvand, B., Jokisalo, J. & Sirén K. (2016b) The potential of predictive control in minimizing the electricity cost in a heat-pump heated residential house. Conference proceedings of 3rd IBPSA-England Conference BSO 2016, Great North Museum, Newcastle, 12th - 14th September 2016. Available at: http://www.ibpsa.org/proceedings/BSO2016/p1049.pdf

ASHRAE 55-2013, (2013) *Thermal Environmental Conditions for Human Occupancy*. ANSI - American national standards institute & ASHRE - American Society of Heating, Refrigerating, and Air-Conditioning Engineers.

Baumann, F. & McClintock, M. (1993) *A study of occupand comfort and workstation performance in PG&E's advanced office systems testbed, Final report to PG&E Research and development, Center for Envrionmental design research,* Berkeley: University of California. Available at: https://escholarship.org/content/qt4zc1s0sw/qt4zc1s0sw.pdf

Borenstein, S., Jaske, M. & Rosenfeld, A. (2002) *Dynamic pricing, advanced metering and demand response in electricity markets,* Berkeley: UCEI - University of California Energy Institute. Available at: https://escholarship.org/uc/item/11w8d6m4

Brelih, N. (2012) How to improve energy efficiency of fans for air handling units. *Rehva journal*. [Online journal]. Vol. 49:2. p. 5-10. [Cited 3 Jul. 2017]. Available at: http://www.rehva.eu/fileadmin/REHVA_Journal/REHVA_Journal_2012/RJ1202_WEB_v2.pdf.

California energy commission, (2003) *Advanced variable air volume system design guide.* [Online]
Available at: https://newbuildings.org/sites/default/files/A-11_LG_VAV_Guide_3.6.2.pdf
[Accessed 31 August 2017].

Chiller Oy, Co-worker., 2017. *Sales engineer* [Interview] (3 July 2017).

Dréau, J. L. & Heiselberg, P. (2016) Energy flexibility of residential buildings using short term heat storage in the thermal mass. *Energy.* [Online journal] Vol. 111. p. 991-1002. [Cited 3 Jul 2017]. Available at: http://dx.doi.org/10.1016/j.energy.2016.05.076

EN 15251, (2007) *Indoor environmental input parameters for design and assessment of energy performance of buildings addressing indoor air quality, thermal environment, lighting and acoustics. Helsinki*: Finnish standards association SFS. 81 p.

Energy authority, (2015) *Documents.* [Online]
Available at:
https://www.energiavirasto.fi/documents/10191/0/Kertomus+s%C3%A4hk%C3%B6n+toimitusvarmuudesta_2015.pdf/318257ac-ef63-4929-8419-c68d8137fa74
[Accessed 29 June 2017].

Engdahl, F. & Johansson, D. (2004) Optimal supply air temperature with respect to energy use in a variable air volume system. *Energy and buildings.* [Online journal] Vol. 36:3. p. 205-218. [Cited 5 Jul 2017]. Available at: doi:10.1016/j.enbuild.2003.09.007

Engdahl, F. & Svensson, A. (2003) Pressure controlled variable air volume system. *Energy and buildings.* [Online journal] Vol. 35:11, p. 1161-1172. [Cited 5 Jul 2017]. Available at: doi:10.1016/j.enbuild.2003.09.009

EQUA Simulation Ab, (2010) *Validation of IDA Indoor Climate and Energy 4.0 build 4 with respect to ANSI/ASHRAE Standard 140-2004,* Solna: EQUA Simulation Ab.

European commission (2009) *2009/28/EC. The EU directive on* the promotion of the use of energy from renewable sources [Online]
Available at: http://eur-lex.europa.eu/legal-content/EN/ALL/?uri=CELEX:32009L0028
[Accessed 27 June 2017].

European Commission, (2017) *Buildings.* [Online]
Available at: https://ec.europa.eu/energy/en/topics/energy-efficiency/buildings
[Accessed 25 July 2017].

Fanger, P. O., (1970) *Thermal comfort: Analysis and applications in environmental engineering. Copenhagen Danish technical press: 244 p.*

Finnish Meteorological institute, (2012) *Energialaskennan testivuodet nykyilmastossa (Test years for energy calculation in current climate).* [Online]
Available at: http://ilmatieteenlaitos.fi/energialaskennan-testivuodet-nyky
[Accessed 5 May 2017].

Finnish Meteorological institute, (2017) *Lämmitystarveluvut (Heating degree days).* [Online]
Available at: http://ilmatieteenlaitos.fi/lammitystarveluvut
[Accessed 8 May 2017].

FiSIAQ, (2008). *Finnish Society of Indoor Air Quality (FiSIAQ), Classification of indoor environment,* Helsinki: Rakennustieto Oy.

FiSIAQ, (2017) *Finnish Society of Indoor Air Quality (FiSIAQ) Classification of indoor environment,* Helsinki: (will be published in 2017).

Fortum, 2017. *Hinnat taloyhtiöille ja yrityksille (Prices for housing cooperatives and companies).* [Online]
Available at: https://www.fortum.com/countries/fi/lampo/tuotteet-ja-palvelut/hinnat-taloyhtioille-ja-yrityksille/pages/default.aspx
[Accessed 5 November 2017].

Fujitsu, 2011. *Publications.* [Online]
Available at: https://sp.ts.fujitsu.com/dmsp/Publications/public/wp-energy-ESPRIMO-E9900-EStar5.pdf
[Accessed 13 June 2017].

Fujitsu, 2014. *Publications.* [Online]
Available at: https://sp.ts.fujitsu.com/dmsp/publications/public/ds-display-b23t-6-led.pdf
[Accessed 13 June 2017].

Gelazanskas, L. & Gamage, K. A. (2014) Demand side management in smart grid: A review and proposals for future direction. *Sustainable cities and society.* [Online journal]. Vol. 11. p. 22-30. [Cited 15 Jun. 2017]. Available at: http://dx.doi.org/10.1016/j.scs.2013.11.001

Gellings, C. W. (1985) *The concept of demand side management for utilities. Proceedings of the IEE 1985 conference. p.1468-1470. Available at: DOI:*10.1109/PROC.1985.13318

Gyamfi, S., Krumdieck, S. & Urmee, T. (2013) Residential peak electricity demand response - Highlights of some behavioural issues. *Renewable and sustainable energy reviews.* [Online journal]. Vol. 25. p. 71-77. [Cited 15 Jun. 2017]. Available at: http://dx.doi.org/10.1016/j.rser.2013.04.006

Hasan, A., Kurnitskit, J. & Jokiranta, K. (2009) A combined low temperature water heating system consisting of radiators and floor heating. *Energy and buildings.* [Online journal]. Vol. 41:5. p. 470-479. [Cited 15 Jun. 2017]. Available at: doi:10.1016/j.enbuild.2008.11.016

Helen, 2017. *Heat for companies and facilities (Lämpöä yrityksille ja kiinteistöille).* [Online]
Available at: https://www.helen.fi/lampo/yritykset/hinnat/
[Accessed 5 November 2017].

Helsingin Sanomat, 2017. *Kotimaa (Home country).* [Online]
Available at: http://www.hs.fi/kotimaa/art-2000002638034.html
[Accessed 17 September 2017].

Hu, Z., Kim, J.-H., Wang, J. & Byrne, J., (2015) Review of dynamic pricing programs in the U.S. and Europe: Status quo and policy recommendations. *Renewable and sustainable energy reviews.* [Online journal]. Vol. 42. p. 743-751. [Cited 16 Jun 2017]. Available at: http://dx.doi.org/10.1016/j.rser.2014.10.078

IEA, 1999. *Empirical Validation of EDFETNA and GENEC Test-Cell Models. A report of task 22 Building energy analysis tools.*

ISO 8996:2004, (2004) *Ergonomics of the thermal environment - Determination of metabolic heat rate, Helsinki: Finnish standards association*.

Jokinen, E. (2013) *Kysyntäjousto kaukolämmitetyissä kiinteistöissä (Demand response within district heated buildings). Master's thesis.* Aalto University, Department of Mechanical Engineering. Espoo: 78 p.

Kensby, J., Trüschel, A. & Dalenbäck, J.-O. (2015) Potential of residential buildings as thermal energy storage in district heating systems – Results from a pilot test. *Applied Energy.* [Online journal]. Vol. 137. p. 773-781. [Cited 15 Jun. 2017]. Available at: http://dx.doi.org/10.1016/j.apenergy.2014.07.026

Kreith, F. & Goswami, D. Y. (2016) *Energy management and conservation handbook.* Second edition. CRC Press. p. 391-392. ISBN 9781466585171

Kropf, S. & Zweifel, G. (2001) *Validation of the Building Simulation Program IDA-ICE According to CEN 13791 „Thermal Performance ofBuildings - Calculation of Internal Temperatures of aRoom in Summer Without Mechanical Cooling - General Criteria and Validation Procedures"*. HOCHSCHULE FÜR TECHNIK+ARCHITEKTUR LUZERN. 24 p.

Kärkkäinen, S., Sipilä, K., Pirvola, L., Esterinen, J., Eriksson, E., Soikkeli, S., Nuutinen, M., Aarnio, H., Schmitt, F. & Eisgruber, C. (2003) *Demand side management of the district heating systems,* Espoo: VTT Research notes 2247. ISBN 951-38-6472-3

Kärkkäinen, S., Sipilä, K., Ranne, A., Kekkonen, V., Koponen, P., Koskelainen, L. & Heikkinen, J. (1999) *Kysynnän hallinta kaukolämmitysjärjestelmissä. DSM:n perusteet ja tarvittava tekniikka,* Espoo: VTT.

Lombard-Pérez, L., Ortiz, J. & Pout, C. (2008) A review on buildings energy consumption information. *Energy and buildings.* [Online journal]. Vol. 40. p. 394-398. [Cited 20 Jul. 2017]. Available: doi: 10/1016/j.enbuild.2007.03.007

Lund, H., Werner, S., Wiltshire, R., Svendsen, Svend., Thorsen, J-E., Hvelplund, F. & Van Mathiesen, B. (2014) 4th Generation District Heating (4GDH) Integrating smart thermal grids into future sustainable energy systems. *Energy.* [Online journal]. Vol. 68. p. 1-11. [Cited 20 Jul. 2017]. Available: http://dx.doi.org/10.1016/j.energy.2014.02.089

Manicca, D., Rutledge, B., Rea, M. & Morrow, W. (1999) Occupant use of manual lighting controls in private offices. *Journal of the illuminating engineering society.* [Online journal]. Vol. 28. p. 42-56. [Cited 20 Jul. 2017].
Available at: http://dx.doi.org/10.1080/00994480.1999.10748274

Manninen, A.-K. (2014) *Kaukolämmön tuotantoa ja kulutusta tasapainottavat liiketoimintamallit.* Master's thesis. Oulu University. Oulu: 100 p.

Mendell, M. J. & Heath, G. A. (2005) Do indoor pollutants and thermal conditions in schools influence student performance? A critical review of the literature. *Indoor air.* [Online journal]. Vol. 15. p. 27-52. [Cited 5 Jun. 2017]. Available at: doi:10.1111/j.1600-0668.2004.00320.x

Mohagheghi, S., Stoupis, J., Wang, Z. & Li, Z. (2010) *Demand response architecture: Integration into the distribution management system.* IEEE 2010 First IEEE International Conference on Smart Grid Communications.

Motegi, N., Piette, M.A., Watson, D.S., Kiliccote, S. & Xu, P. (2007) *Introduction to commercial building control strategies and techniques for demand response,* Berkeley, California: Demand response research center - Lawrence Berkeley National Laboratory. Available at: https://drrc.lbl.gov/sites/default/files/59975.pdf

National Building Code of Finland D2, 2012. *Part D2, Rakennusten sisäilmasto ja ilmanvaihto, Määräykset ja ohjeet 2012 (Indoor climate and ventilation of buildings, regulations and instructions). Ministry of the Environment.* [Online]
Available at: http://www.finlex.fi/data/normit/37187-D2-2012_Suomi.pdf
[Accessed 15 August 2017].

National building code of Finland, D3, 2012. *Part D3, Rakennusten energiatehokkuus, Määräykset ja ohjeet 2012 (Energyperformance of buildings, regulations and instructions). Ministry of the Environment.* [Online]
Available at: http://www.finlex.fi/data/normit/37188-D3-2012_Suomi.pdf
[Accessed 15 August 2017].

National building code of Finland, D5, 2012. *Part D5, Rakennuksen energiankulutuksen ja lämmitystehontarpeen laskenta, guidelines 2012 (Calculation of energy consumption and heat demand in buildings). Ministry of the Environment.* [Online]
Available at: http://www.ym.fi/download/noname/%7B8C5C3B41-E127-4889-95B0-285E9223DEE6%7D/40468
[Accessed 15 August 2017].

Nord Pool, 2017a. *Nord Pool - History.* [Online]
Available at: http://www.nordpoolspot.com/About-us/History/
[Accessed 27 July 2017].

Nord Pool, 2017b. *Nord Pool - Intraday market.* [Online]
Available at: http://www.nordpoolspot.com/How-does-it-work/Intraday-market/
[Accessed 27 July 2017].

Nord Pool, 2017c. *Nord Pool - The Power Market.* [Online]
Available at: http://www.nordpoolspot.com/How-does-it-work/
[Accessed 27 July 2017].

Nord Pool, 2017d. *Nord Pool - Day ahead market Elspot.* [Online]
Available at: http://www.nordpoolspot.com/the-power-market/Day-ahead-market/
[Accessed 27 July 2017].

Nord Pool, 2017e. *Nord Pool - Bidding areas.* [Online]
Available at: http://www.nordpoolspot.com/How-does-it-work/Bidding-areas/
[Accessed 27 July 2017].

Nord Pool, 2017f. *Nord Pool - Producers.* [Online]
Available at: http://www.nordpoolspot.com/How-does-it-work/The-market-

members/Producers/
[Accessed 27 July 2017].

Page, J., Robinson, D., Morel, N. & Scartezzini, J.-L. (2008) A generalised stochastic model for the simulation of occupang presence. *Energy and Building.* [Online journal]. Vol. 40. p. 83-98. [Cited 15 Aug. 2017]. Available: doi:10.1016/j.enbuild.2007.01.018

Palensky, P. & Dietrich, D. (2011) Demand side management: demand response, intelligent energy systems and smart loads. *Proceedings of IEEE Transactions on industrial informatics,* 7(3), p. 381-388.

Partanen, J., Viljainen, S., Lassila, J., Honkapuro, S., Salovaara, K., Annala, S. & Makkonen, M. (2015) *Electricity markets - Education handout (Sähkömarkkinat - Opetusmoniste),* Lappeenranta: Lappeenrannan Teknillinen Yliopisto - LUT Energia Sähkötekniikka.

Pierluigi, S. (2014) Demand response and smart grids - A survey. *Renewable and sustainable energy reviews.* [Online journal]. Vol. 30, p. 461-478. [Cited 15 Aug 2017]. Available at: https://doi.org/10.1016/j.rser.2013.10.022

Pöyry Management Consulting (2016) *Kaksisuuntaisen kaukolämmön liiketoimintamallit (Business models for bidirectional district heating),* Helsinki: Energiateollisuus ry; Sitra. Available at: https://media.sitra.fi/2017/02/27175247/Kaksisuuntaisen_kaukolammon_liiketoimintamallit-2.pdf

Rinne, S. (2017) *Dynamical pricing of district heating and electricity in Finland* [Interview] (1 June 2017).

Saari, M. & Laine, J. (2009) *Passive energy house from besserblocks (Passiivienergiatalo harkoista),* Espoo: VTT. Available at: http://kivitalo.asiakkaat.sigmatic.fi/core/wp-content/images/2012/06/vtt-r-08496-09_passiivienergiatalo_harkoista_lvi-ohje_2009_rakennesuunnittelu.pdf

Salo, S. (2016) *Predictive Demand-side Management in District Heating and Cooling connected buildings.* Master's thesis. Aalto University, department of mechanical engineering. Espoo: 97 p.

Sarvaranta, A., Jääskeläinen, J., Puolakka, J. & Kouri, P. (2012) *Kaukolämmön hinnoittelun nykytila ja tulevaisuuden mahdollisuudet - Loppuraportti (Current pricing of district heating and the future possibilities - Report).* Espoo: ÅF-Consult. Available at: http://docplayer.fi/1155236-Kaukolammon-hinnoittelun-nykytila-ja-tulevaisuuden-mahdollisuudet.html

Satish, U., Mendell, M., Shekhar, K., Hotchi, T., Sullivan, D., Streufert, S. & Fisk, W. (2012) Is CO2 an Indoor Pollutant? Direct Effects of Low-to-Moderate CO2 Concentrations on Human Decision-Making Performance. *Environmental health perspectives.* [Online journal]. Vol. 120:12. p. 1671-1677. [Cited 2 Jul. 2017]. Available at: doi: 10.1289/ehp.1104789

Schuler, R. E. (2004) *Self-Regulating Markets for electricity: Letting consumers into the game.* Proceedings of IEEE Power Systems Conference and Exposition.

Seppänen, O. (1995) *Heating of Buildings (Rakennusten lämmitys).* Espoo: Suomen LVI-yhdistysten liitto ry. ISBN 951-97233-1-5

Seppänen, O. A., Fisk, W. J. & Mendell, M. J. (1999) Association of Ventilation Rates and CO2 Concentrations with Health and Other Responses in Commercial and Institutional Buildings. *Indoor air.* [Online journal]. Vol. 9. p. 226-252. [Cited 2 Jun. 2017]. Available at: DOI: 10.1111/j.1600-0668.1999.00003.x

Seppänen, O., Fisk, W. J. & Lei, Q. H. (2005) Ventilation and performance in office work. *Indoor air.* [Online journal] Vol. 16. p. 28-36. [Cited 3 Jun. 2017]. Available at: DOI: 10.1111/j.1600-0668.2005.00394.x

Shan, K., Wang, S., Yan, C. & Xiao, F. (2016) Building demand response and control methods for smart grids: A review. *Science and technology for the built environment.* [Online journal]. Vol. 22. p. 692-704. [Cited 13 Jun 2017]. Available at: DOI: 10.1080/23744731.2016.1192878

Statistics Finland (2015). *Energian hankinta ja kulutus 2015 (Energy procurement and consumption 2015).* [Online]
Available at: http://tilastokeskus.fi/til/ehk/2015/04/ehk_2015_04_2016-03-23_fi.pdf
[Accessed 25 July 2017].

Stephan, W. (1986). *IEA Annex 10, System simulation, radiator,* Stuttgart: IEA.

Strbac, G. (2008) Demand side management: Benefits and challenges. *Energy policy.* [Online journal]. Vol. 36. p. 4419-4426. [Cited 10 Aug. 2017]. Available at: doi:10.1016/j.enpol.2008.09.030

Swegon (2014). *Technical indoor climate guide.* [Online]
Available at: https://www.swegon.com/PageFiles/106535/Indoor_climate_guide.pdf
[Accessed 4 September 2017].

Syri, S., Mäkelä, H., Rinne, S. & Wirgentius, N. (2015) *Open district heating for Espoo city with marginal cost based pricing.* International conference on the European energy market (EEM).

Tiptipakorn, S. & Lee, W.-J. (2007) *A residential Consumer-Centered Load Control Strategy in Real-Time Electricity Pricing Environment. Conference proceedings ot the* 39th North American Power Symposium.

Vaillencourt, R. (2005) The correct formula for using the affinity laws when there is a minimum pressure requirement. *Energy Engineering.* [Online journal]. Vol. 102:4. p. 32-46. [Cited 17 Aug. 2017]. Available at: http://dx.doi.org/10.1080/01998590509509435

Valor Partners Oy (2015) *Kaukolämmön kysyntäjousto (Demand response of district heating),* Helsinki: Energiateollisuus. Available at:
https://energia.fi/files/439/Kaukolammon_kysyntajousto_loppuraportti_VALOR.pdf

Wang, S. & Yan, C. (2014) Building power demand response methods toward smart grid. *HVAC & R RESEARCH.* [Online journal] Vol. 20. p. 665-687. [Cited 12 Aug. 2017]. Available at: DOI: 10.1080/10789669.2014.929887

Wargocki, P. & Wyon, D. P. (2017) Ten questions concerning thermal and indoor air quality effects on the performance of office work and schoolwork. *Building and Environment.* [Online journal]. Vol. 112. p. 359-366. [Cited 12 Aug. 2017]. Available at: http://dx.doi.org/10.1016/j.buildenv.2016.11.020

Wargocki, P., Wyon, D., Sundell, J., Clausen, G., Fanger, P-O. (2000) The Effects of Outdoor Air Supply Rate in an Office on Perceived Air Quality, Sick Building Syndrome (SBS) Symptoms and Productivity. *Indoor air.* [Online journal]. Vol. 10:4. p. 222-236. [Cited 12 Aug. 2017]. Available at: DOI: 10.1034/j.1600-0668.2000.010004222.x

Wernstedt, F. & Johansson, C. (2008) *Intelligent distributed load control.* Reykjavik, Iceland, Conference proceedings of the 11th International symposium on district heating and cooling.

Vinha, J., Korpi, M., Kalamees, T., Jokisalo, J., Eskola, L., Palonen, J., Kurnitskit, J., Aho, H., Salminen, M., Salminen & K., Keto, M. (2009). *Residential buildings airtightness, indoor climate and energy economy (Asuinrakennusten ilmanpitävyys, sisäilmasto ja energiatalous),* Tampere: Tampereen teknillinen yliopisto, Rakennustekniikan laitos. ISBN 978-952-15-2105-8

Xu, X., Wang, S. & Sun, Z. X. F. (2009). A model-based optimal ventilation control strategy of multi-zone VAV air-conditioning systems. *Applied Thermal Engineering.* [Online journal]. Vol. 29:1. p. 91-104. [Cited 22 Jun 2017]. Available at: https://doi.org/10.1016/j.applthermaleng.2008.02.017